UNIVERSIDAD NACIONAL AUTÓNOMA DE MÉXICO

PROGRAMA DE DOCTORADO EN CIENCIAS BIOMÉDICAS

FACULTAD DE MEDICINA

ESTUDIO DE LA REACTIVIDAD DE LA MITAD DE LOS SITIOS EN LA ENZIMA ALDEHÍDO DESHIDROGENASA CLASE I HUMANA

TESIS

QUE PARA OPTAR POR EL GRADO DE:

DOCTOR EN CIENCIAS

PRESENTA

Q.F.B. BELEM YOVAL SANCHEZ

TUTOR: DR. JOSÉ SALUD RODRÍGUEZ ZAVALA

PROGRAMA DE DOCTORADO EN CIENCIAS BIOMÉDICAS

IMÉXICO, D.F. **Enero 2014**

Resumen

Las aldehído deshidrogenasas (ALDHs) se encuentran involucradas en la desintoxicación de aldehídos endógenamente generados en varias enfermedades que involucran un incremento en el estrés oxidante. Se ha determinado que las ALDHs tetraméricas utilizan sólo dos de sus cuatro sitios activos (reactividad de la mitad de los sitios), pero la razón mecanística de esta característica en las enzimas tetraméricas permanece aún desconocida. En este trabajo, ALDH1A1 (enzima tetramérica) fue dimerizada con el fin de estudiar la correlación entre la estructura oligomérica de la enzima y la presencia de la reactividad de la mitad de los sitios. Dímeros estables fueron generados a partir de ALDH1A1 mediante la fusión de la proteína GFP en el C-terminal de la proteína. El sitio activo de la enzima fue modificado de manera indirecta por esta mutación y esto se reflejó en el cambio de la especificidad por sus sustratos. Algunas propiedades cinéticas de la enzima mutante (ALDH1A1-HDS-GFP) semejaron a las propiedades de ALDH3 (dímerica), por ejemplo, la enzima mutante no mostró la presencia del *"burst"* y fue menos sensible a la acción de moduladores específicos de la actividad. De manera interesante, esta mutante mostró mejor actividad con malondialdehído y acroleína y fue más resistente a la inactivación por estos compuestos, comparada con la enzima silvestre. Por otro lado, también se observó que el perfil cinético de la mutante presentó dos componentes hiperbólicos cuando se ensayaron los sustratos, revelando dos sitios activos con diferentes afinidades. Esto último indica que la mutante ALDH1A1-HDS-GFP cuenta con reactividad de sitio completo, sugiriendo que la estructura oligomérica es importante para determinar la reactividad de la mitad de los sitios.

Abstract

Aldehyde dehydrogenases (ALDHs) are involved in the detoxification of aldehydes endogenously generated in several diseases involving an increment in oxidative stress. It has been determined that tetrameric ALDHs work only with two of their four active sites (half site reactivity), but the mechanistic reason for this characteristic of tetrameric ALDHs remains unknown. In this work, ALDH1A1 was dimerized in order to study the correlation of the oligomeric structure of the enzyme with the presence of half of the sites reactivity. Stable dimers from ALDH1A1 were generated by the fusion of GFP in the C-terminus of the protein. The active site of the enzyme seemed to be modified by the mutation, with respect to substrate specificity. Some kinetic properties of the mutant resembled those of ALDH3A1 in that the fusion dimer did not show the *burst phase* and was less sensitive to the action of specific modulators of the activity. Interestingly, this mutant showed better activity with malondialdehyde and acrolein and was resistant to inactivation by these compounds. The kinetic profile of the mutant showed two hyperbolic components when the substrates were varied, revealing two active sites with different affinities. The ALDH1A1-GFP dimeric mutant showed full site reactivity, suggesting that the oligomeric structure is important to determine the half-site reactivity

Contenido.

Esta tesis se encuentra dividida en 12 capítulos. En el capítulo 1 se describen generalidades acerca de la formación de diferentes aldehídos con implicaciones toxicas a nivel celular. Los capítulos 2 al 4 contienen información detallada acerca de la función y estructura de diferentes isoformas de aldehído deshidrogenasas, mecanismo de reacción, parámetros cinéticos reportados y su participación en diferentes padecimientos que involucran la generación de estrés oxidante; mientras que los capítulos 5 a 7 incluyen justificación, hipótesis, objetivos y estrategia experimental. En los capítulos 8 y 9 se muestran los resultados del proyecto central que se refiere a la relación que existe entre la reactividad de la mitad de los sitios en ALDH1A1 con el estado de oligomerización (Yoval-Sánchez, B., 2013); mientras que en el capítulo 10 se expone la relevancia de las diferentes ALDHs en la desintoxicación de aldehídos producto de la lipoperoxidación, así como la descripción de los diferentes residuos que podrían ser clave en la protección de estas enzimas ante estos compuestos altamente tóxicos (Yoval-Sánchez, B., 2012). Finalmente en el capítulo 11 se reporta la participación de estas enzimas en el metabolismo del etanol en el protista *Euglena gracilis*, evidenciando así la importancia de estas enzimas no sólo en el metabolismo de organismos superiores sino también en organismos unicelulares (Yoval-Sánchez, B. 2011). En el capítulo 12 se incluyen las referencias.

Índice **Página**

Abreviaturas

ALDH1A1	Aldehído deshidrogenasa humana clase 1.
ALDH2	Aldehído deshidrogenasa humana clase 2.
ALDH3A1	Aldehído deshidrogenasa humana clase 3.
ALDH1A1-D80G/S82A	mutante de aldehído deshidrogenasa clase 1 con cambios en D80G y S82A.
GFP	proteína verde fluorescente.
ALDH1A1-D80G/S82A-GFP	fusión de la mutante ALDH1A1-D80G/S82A con GFP.
4-HNE	4-hidroxi-2-nonenal.
MDA	Malondialdehído.
MAO	Monoaminooxidasa.
DOPAL	3-4, Dihidroxifenilacetaldehído.
DOPAC	3-4, Dihidroxifenilacético.
AD	Alzheimer disease (Enfermedad de alzheimer).
NASH	Esteatohepatitis no alcohólica.
LPO	Lipoperoxidación
PAHs	Hidrocarburos policíclicos.
XREs	Elementos de respuesta a xenobióticos.

1. Generación de aldehídos tóxicos.

Los aldehídos son especies generadas durante numerosos procesos fisiológicos a partir de una amplia variedad de precursores endógenos y exógenos. Son compuestos orgánicos que contienen grupos carbonilo, lo que los hace ser altamente reactivos y citotóxicos. Se ha estimado que el máximo consumo diario de aldehídos insaturados en humanos es de 5 mg/kg, mientras que el consumo total de aldehídos llega a ser de aproximadamente 7mg/kg [40, 41]. Los aldehídos se pueden dividir en 4 clases generales de carbonilos: 1) alcanales saturados, como formaldehído, acetaldehído y hexanal; 2) alquenales insaturados, como la acroleína, 4-hidroxi-2-nonenal y crotonaldehído. Estos representan un grupo de aldehídos altamente reactivos que contienen dos centros electrofílicos (Fig. 1). Un carbono parcialmente positivo C1 o C3, en el cual las moléculas pueden sufrir un ataque nucleofílico. Se ha sugerido que estos aldehídos reaccionan de manera primaria con el grupo sulfhidrilo de la cisteína, el grupo ε-amino de la lisina y el grupo imidazol de la histidina en las proteínas, a través de una reacción de adición de Michael o de la formación de una base de Schiff [42-45]; 3) aldehídos aromáticos, como benzaldehído, DOPAL y DOPEGAL y 4) dicarbonilos como el glioxal y el malondialdehído.

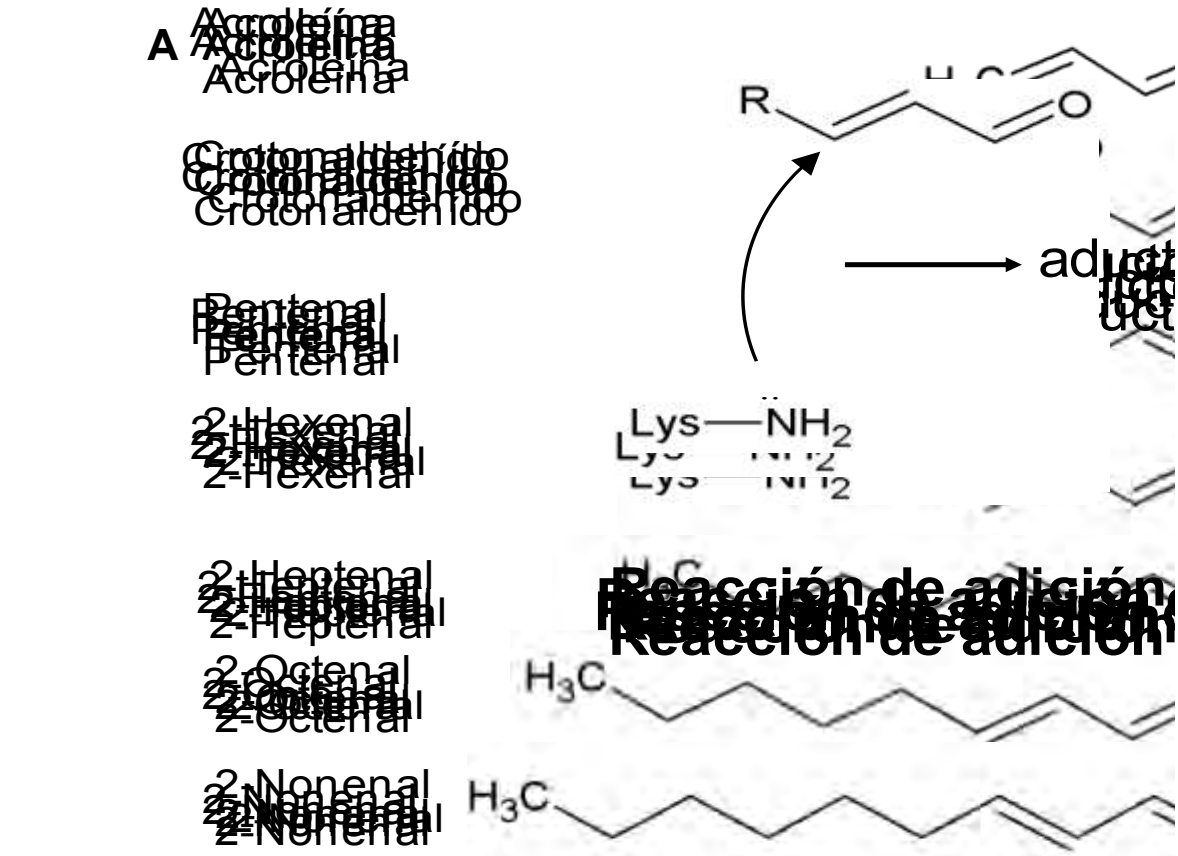

Figura 1. A. Estructura química de los 2-alquenales. B. Reacciones de formación de aductos.

Fig. 4. Estructura química de los 2-alquenales y reacciones de formación de aductos

Estos compuestos se encuentran altamente distribuidos en la naturaleza y de manera ubicua en el ambiente. Varios aldehídos, incluyendo al formaldehido, acetaldehído y acroleína son producidos durante la combustión y están presentes en el smog y el humo del cigarro [42, 47]. Los escapes de los vehículos representan la principal fuente de contaminación del aire por aldehídos, a través de la emisión directa de estos y a través de la emisión de hidrocarburos, los cuales posteriormente derivan en aldehídos. Los aldehídos también se generan en una amplia cantidad de procesos industriales [48]. Una gran cantidad de aldehídos alifáticos y aromáticos, incluyendo el citral, benzaldehído, acetaldehído y formaldehido, existen de manera natural en varios alimentos, particularmente en frutas y vegetales, a los cuales proporcionan olor y sabor [2]. En los animales, los aldehídos incluyendo la acroleína, benzaldehído y hexanal, actúan como moléculas de comunicación y tienen roles en la atracción o defensa [50]. Los aldehídos también son generados como intermediarios fisiológicos durante la biotransformación de muchos compuestos endógenos, incluyendo lípidos, aminoácidos, neurotransmisores y carbohidratos. Por ejemplo, a partir de la peroxidación lipídica se generan más de 200 especies de aldehídos , incluyendo el 4-HNE y MDA [51]. Aunque algunos aldehídos son esenciales para llevar a cabo diversos procesos biológicos normales, muchos son citotóxicos e incluso carcinogénicos [52]. Por ejemplo, a bajas concentraciones la acroleína puede inducir apoptosis por mecanismos que involucran la activación de caspasas y muerte mitocondrial [53-55]. Sin embargo, a concentraciones altas la acroleína genera muerte celular por necrosis. Este fenómeno también se ha observado para el HNE [56, 57]. A diferencia de los radicales libres, los aldehídos tienen una vida

media relativamente larga y debido a ello no sólo reaccionan en el sitio donde se generan, sino que pueden difundir o ser transportados a sitios lejanos de donde se generan [42]. Varias líneas de investigación muestran que la modificación oxidativa de proteínas y la subsecuente acumulación de éstas, se presenta en las células durante el envejecimiento, el estrés oxidante y en diferentes estados patológicos incluyendo enfermedades prematuras como distrofia muscular, artritis reumatoide y aterosclerosis [58-61]. Los compuestos más importantes que dan origen a la modificación de estas proteínas pueden ser representados por aldehídos como cetoaldehídos, 2-alquenales y 4-hidroxi-2-alquenales [42, 45, 61]. Estos aldehídos reactivos son considerados mediadores importantes del daño celular debido a su capacidad de modificar biomoléculas de manera covalente, lo cual puede alterar funciones celulares importantes y pueden causar mutaciones [42].

Capítulo 2. Función y estructura de las aldehído deshidrogenasas.

Entre algunos de los principales mecanismos de desintoxicación de aldehídos con los que cuenta la célula se encuentra la familia de las aldehído deshidrogenasas. Estas enzimas se encuentran ampliamente distribuidas tanto en bacterias como en humanos, son un grupo de enzimas que catalizan la conversión de una amplia variedad de aldehídos endógenamente y exógenamente generados a sus correspondientes ácidos en una reacción dependiente de $NAD(P)^+$ [1]; al mismo tiempo, protegen a la célula de los efectos dañinos que estos compuestos pueden producir [2, 3]. Para nombrar cada gen de estas enzimas, se utiliza el símbolo ALDH, usado como abreviación de aldehído deshidrogenasa; seguido de un número arábigo que representa la familia a la cual pertenece, cuando se requiere se usa una letra indicando la subfamilia y un segundo número arábigo indica el gene individual dentro de la subfamilia [147]. A nivel de secuencia de aminoácidos, la aldehído deshidrogenasa humana clase 1 (ALDH1A1) y aldehído deshidrogenasa humana clase 2 (ALDH2), ambas tetraméricas, comparten cerca del 70% de identidad, mientras que con la aldehído deshidrogenasa humana clase 3, que es un dímero (ALDH3A1), sólo comparten un 30% de identidad. Las primeras dos enzimas presentan una extensión de 56 aminoácidos en el N-terminal (el tamaño del monómero de estas enzimas es de alrededor de 500 aminoácidos con respecto a ALDH3A1. La aldehído deshidrogenasa clase 3 no posee esos 56 aminoácidos en el N-terminal, pero posee una extensión de 17 aminoácidos en el extremo C-terminal (este monómero posee 453 aminoácidos), que interactúa con el otro monómero para formar el dímero. A pesar de estas diferencias en la estructura primaria, los monómeros de todas las isoenzimas

poseen en esencia la misma estructura tridimensional [4-6]. Por otro lado, se ha demostrado que el N-terminal de las ALDHs tetraméricas es importante para la estabilidad [7] y plegamiento [8] de la proteína. En contraste, el C-terminal de la proteína se extiende a través de la interfase dímero-dímero y es capaz de formar un ancla entre miembros de cada par de dímeros [9], por lo que parece ser importante para la oligomerización de la proteína en tetrámeros. Cada una de las isoenzimas posee tres dominios; el dominio catalítico, el dominio de unión de la coenzima y el dominio de oligomerización [6]. El dominio de oligomerización comprende tres hebras β antiparalelas, las cuales están involucradas en la interacción entre subunidades tanto en el dímero como en el tetrámero (Fig. 2) [5, 12].

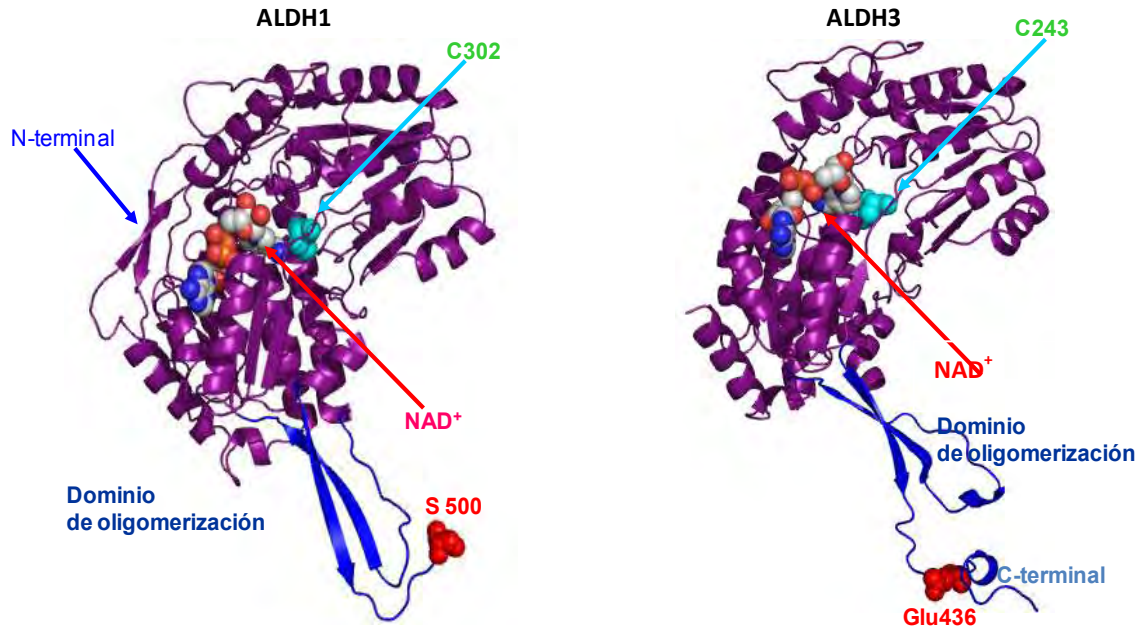

Figura 2. Estructura terciaria de las subunidades de las enzimas ALDH1A1 y ALDH3A1. (Rodríguez-Zavala and Weiner, 2000).

En cuanto a la especificidad por sustrato, ALDH1A1 y ALDH2 prefieren aldehídos alifáticos tales como, el acetaldehído y el propionaldehído, mientras que la ALDH3A1 es preferencialmente más afín por aldehídos aromáticos tal como el benzaldehído. La especificidad por sustrato de cada isoenzima se encuentra determinada por los aminoácidos que forman el túnel del sitio activo [6]. Estos residuos pueden ayudar a discriminar entre aldehídos aromáticos, alifáticos y otros [13].

Es interesante observar que mientras los residuos de Cys se encuentran posicionados de manera similar en ambas enzimas, las moléculas de NAD^+ tienen diferentes orientaciones dentro de cada isozima [13]. Las estructuras del complejo binario entre la enzima y el NAD^+ muestran que el conjunto de aminoácidos que rodea al anillo de nicotinamida favorecen una conformación de la coenzima más expuesta en el caso de ALDH3A1, mientras que el anillo se encuentra más escondido en el caso de ALDH2, pues al parecer, el "*core"* de aminoácidos es más hidrofóbico lo cual puede favorecer o desfavorecer la salida del producto [13].

Capítulo 3. Mecanismo general de reacción de las ALDHs.

La oxidación de aldehídos por estas enzimas es dependiente de $NAD(P)^+$ e involucra una reacción nucleofílica del sustrato con la Cys 302 localizada en el sitio activo, resultando en la formación de un intermediario tiohemiacetal, seguido de la transferencia del hidruro al NAD^+ para formar el NADH, originando un intermediario tioéster, que es hidrolizado a ácido carboxílico, producto de la reacción que involucra la activación de una molécula de H_2O por la base general que es un residuo de glutamato adyacente (E268) (Figura 3) [14].

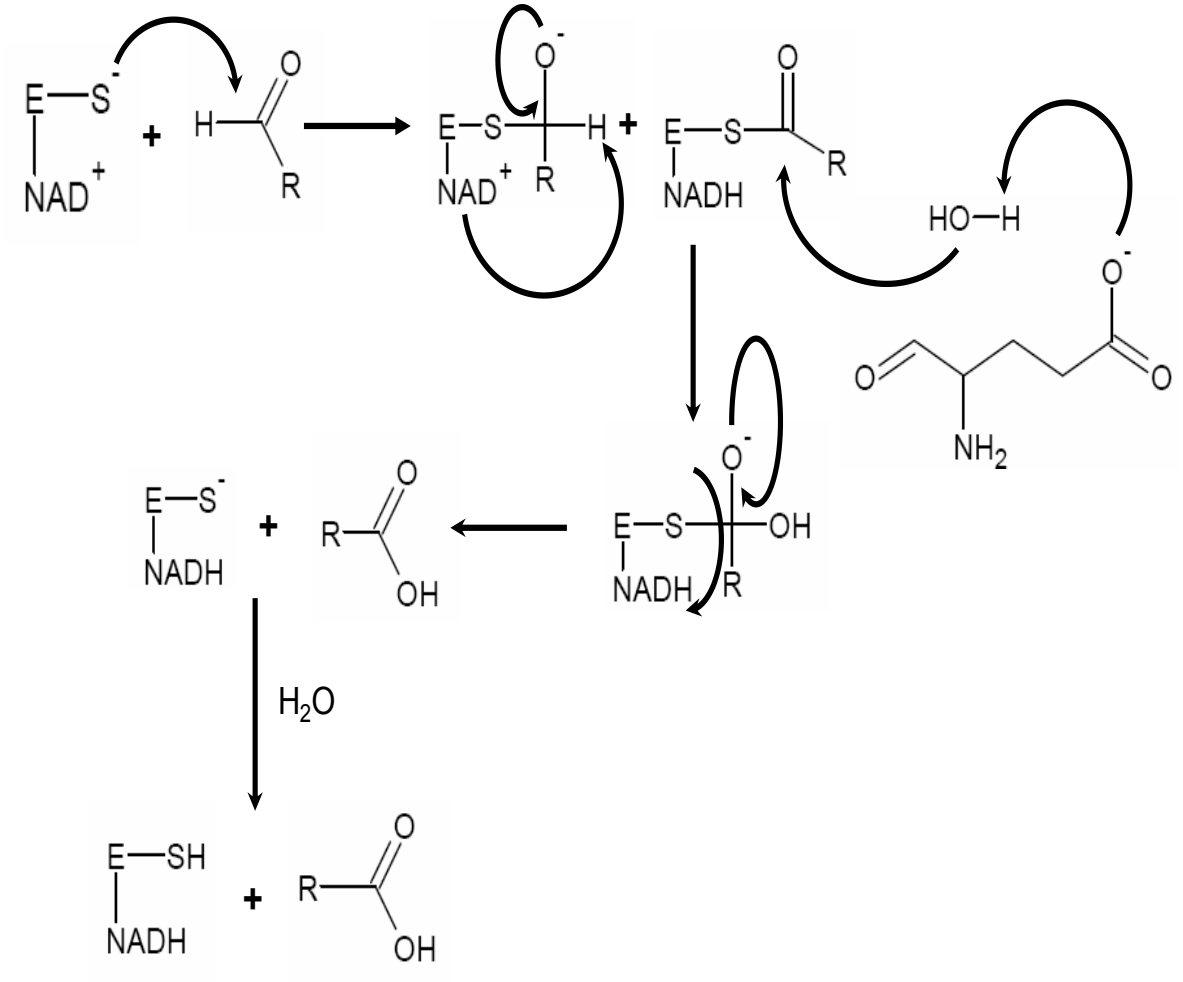

Figura 3. Representación del mecanismo catalítico de las ALDHs.

En general, el mecanismo cinético de reacción de estas enzimas es secuencial ordenado [14,13]. Es decir, primero se une el NAD^+ a la enzima, posteriormente se incorpora el aldehído, ocurre la liberación del ácido y como último paso, la liberación de la coenzima reducida, dejando a la enzima libre para que ocurra un nuevo ciclo catalítico. A pesar de que los diversos miembros de la superfamilia de las aldehído deshidrogenasas (ALDHs) comparten ciertas características específicas a nivel estructural y funcional, el paso limitante para cada una de las enzimas difiere: a) para ALDH1A1 el paso limitante es la liberación del NADH *(k9* en la figura 4*)*, b) desacilación o liberación del ácido para ALDH2 *(k7* en la figura 4*)* y c) la transferencia del hidruro para ALDH3A1 *(k5* en la figura 4*)* [15, 16, 13].

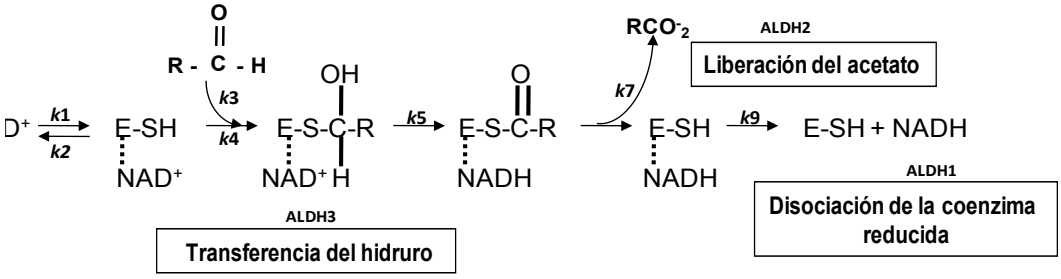

Figura 4. Mecanismo general de reacción de las aldehído deshidrogenasas.

El hecho de que el paso limitante se encuentre después de la formación de la coenzima reducida (NADH), permite que ocurra lo que se conoce como *"burst"* antes del estado estacionario. Esto es, el NADH se forma en los sitios activos en el primer ciclo catalítico sin ser liberado al medio, lo cual se puede determinar mediante la fluorescencia emitida por el NADH generado como producto de la reacción. Del delta de fluorescencia obtenido se puede cuantificar el número de sitios activos funcionales en la enzima y se ha determinado que para las enzimas

tetraméricas, la magnitud del *"burst"* antes del estado estacionario corresponde a 2 nmoles de NADH formado por nanomol de enzima [15, 18, 19]**.** Esto se conoce como reactividad de la mitad de los sitios, característica compartida sólo por algunos miembros de las ALDHs [23-20-22]; ya que, de los cuatro sitios activos que se encuentran en las enzimas tetraméricas sólo 2 son funcionales. Esto último permite diferenciar entre ALDH1A1 (tetramérica) y ALDH3A1 (dimérica), pues en el caso de esta última, al ser el paso limitante la transferencia del hidruro (Figura 4), el estado estacionario se alcanza de manera inmediata; esto impide cuantificar el número de moles de NADH generados en el ***primer*** ciclo catalítico y por ello se desconoce si esta enzima dimérica cuenta con reactividad de la mitad de los sitios o si ambos son funcionales. Es muy interesante observar que la contribución de los diferentes aminoácidos no esenciales en el sitio catalítico puedan afectar de diferente manera los parámetros cinéticos de cada una de las isoenzimas, explicando así la diferencia que existe entre ellas en preferencia y afinidad por los sustratos así como en el paso limitante de la reacción [13].

Con respecto a las ALDHs tetraméricas un punto clave en el mecanismo de la reacción y en la comunicación entre las subunidades que conforman el tetrámero justamente es el fenómeno de la reactividad de la mitad de los sitios y éste hasta la fecha ha permanecido sin explicación alguna. No se ha dilucidado si ésta condición se da previa a la unión de los sustratos o bien la unión del ligando afecta el reconocimiento de la subunidad adyacente por el sustrato. Una apropiada descripción para este fenómeno podría ser la cooperatividad negativa extrema. Esto implica que una vía de comunicación debería existir para transmitir las

consecuencias estructurales de la unión de los ligandos. Se cree que las transiciones orden-desorden en la conformación de la enzima juegan un rol clave en la unión de la coenzima y la catálisis [23].

Estudios previos, realizados en la enzima tetramérica ALDH2; al titular con NADH y monitorear los cambios de fluorescencia en la enzima debidos a la unión de este compuesto, muestran una estequiometria de 2 moléculas de NADH unidas por tetrámero [15]. Sin embargo, todas las estructuras cristalográficas disponibles de las formas tetraméricas de ALDH, muestran claramente 4 moléculas de coenzima unidas por tetrámero [6, 20, 5, 26].

En cuanto al sitio de unión del NAD^+ se ha observado mediante estudios de cristalografía de rayos X que durante el ciclo catalítico, el anillo de nicotinamida del NAD^+ fluctúa entre dos conformaciones: una con el anillo de nicotinamida extendida, que favorece la transferencia del hidruro y la otra con el anillo de nicotinamida contraído, la cual favorece la acción de la base general para que se lleve a cabo la desacilación [6,5, 7, 31].

3.1 Etapas limitantes en el mecanismo de reacción de las ALDHs.

Como se mencionó previamente, las diferentes isoenzimas de ALDH comparten el mismo mecanismo de reacción para la oxidación de los aldehídos (Figuras 3 y 4). A pesar de la similitud en sus reacciones, ALDH1A1 y ALDH2 difieren en el paso limitante de la reacción y pueden ser diferenciadas en función de cómo es afectada su velocidad máxima en presencia de iones Mg^{2+}. En el caso de ALDH1A1, la etapa limitante de la reacción es la disociación de la coenzima reducida [32], mientras que para ALDH2 el paso limitante es la desacilación [33, 34]. Ambas enzimas son afectadas por los iones Mg^{2+}, pues este ion incrementa la velocidad de la desacilación y disminuye la velocidad de disociación de la coenzima reducida; no se ha observado efecto alguno del Mg^{2+} sobre la transferencia del hidruro, paso limitante de la ALDH3A1 [35]. Por lo tanto, cuando se ensaya la actividad de estas enzimas bajo condiciones de *Vmax*, el Mg^{2+} inhibe la actividad de ALDH1A1 y activa a ALDH2, lo cual ayuda a predecir cuál es su respectiva etapa limitante [35]. En el complejo binario enzima-NAD^+, se ha observado que el ión Mg^{2+} interactúa con el grupo pirofosfato del NAD^+ en el caso de ALDH1 y ALDH2; lo cual no se observa para la isozima ALDH3, pues al determinarse la estructura binaria en presencia del ión divalente, no se detecta ningún enlace entre el Mg^{2+} y el NAD^+ o la enzima. Por otro lado, también se han evaluado las constantes de disociación del NAD^+ y NADH (K_{ia} y K_{iq}, respectivamente) las cuales disminuyen en presencia de Mg^{2+} tanto para ALDH1

como para ALDH2, lo cual implica que la presencia de este ión favorece que la coenzima se una más fuertemente a cada isoenzima [6, 5, 7, 4].

Capítulo 4. Contribución de las ALDHs en la respuesta ante el estrés oxidante generado en algunos padecimientos.

Cuando se generan altos niveles de estrés oxidante en la célula, de tal manera que los niveles de ROS superan la capacidad antioxidante, se pueden generar daños irreversibles en la célula, ocasionados por un incremento en la lipoperoxidación y sus productos. Uno de los principales mecanismos de defensa antioxidante en la célula es llevado a cabo a través de la participación de las aldehído deshidrogenasas (Figura 5); estas enzimas se encuentran localizadas en diferentes compartimentos dentro de la célula, como son: citosol, mitocondria, núcleo y retículo endoplásmico. Como se mencionó en capítulos previos, estas enzimas son capaces de convertir una amplia variedad de aldehídos a su correspondiente ácido carboxílico. Esta capacidad les permite prevenir la acumulación de aldehídos derivados de procesos tanto endógenos como exógenos, al mismo tiempo que mantienen la homeostasis de dichos compuestos en la célula impidiendo la generación de daño oxidante a nivel celular y tisular. La familia de las ALDHs, no solo juega un papel importante en la desintoxicación de la célula; también participa de manera importante en la biosíntesis de *novo* de moléculas que son preponderantes a nivel fisiológico, como se describe más adelante y de manera detallada en este capítulo. Debido a que las diferentes isoformas de ALDHs se encuentran ampliamente distribuidas en el organismo, su

actividad es crucial para regular la concentración de aldehídos a diferentes niveles.

Es por ello que en esta sección se resalta la participación de las tres principales isoformas de aldehído deshidrogenasas (ALDH1A1, ALDH2 y ALDH3A1), en diferentes procesos tanto fisiológicos como patológicos que involucran altos niveles de estrés oxidante.

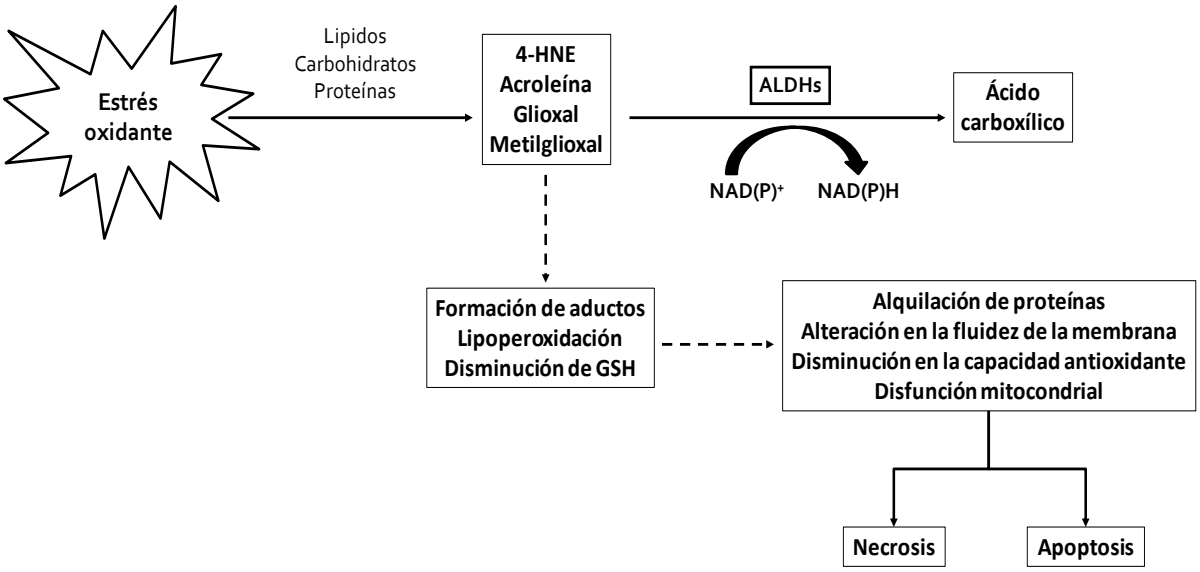

Modificado de Marchitti, et al. 2007

Figura 5. Consecuencias de la toxicidad de los aldehídos y reacción general de desintoxicación catalizada por las ALDHs.

4.1. ALDH1A1

ALDH1A1 es una enzima citosólica ubicuamente distribuida en varios tejidos, incluyendo hígado, riñón, pulmón, cerebro, ojos, testículos y células rojas [61, 62,63, 64, 65, 66]. Tiene un papel importante en la desintoxicación de aldehídos generados de la lipoperoxidación producida por luz UV, protegiendo de esta

manera el cristalino de los ojos [67]. También, se ha observado una alta actividad de esta enzima en la oxidación de aldofosfamida y tiene un rol importante en la desintoxicación de algunos fármacos usados contra el cáncer, como lo son las oxazafosforinas [68, 69]. Se ha observado que algunas células cancerosas adquieren resistencia a estos fármacos, debido a que en ellas existe una sobre-expresión de ALDH1A1, que actualmente se utiliza como biomarcador de células cancerosas [70-72].

En cultivos de hepatocitos, la supresión de ALDH1A1 reduce tanto la oxidación de ω-ácidos grasos y la producción de especies reactivas de oxígeno [73]. En el cerebro humano, ALDH1A1 se expresa de manera importante en las neuronas dopaminérgicas [74]. En estas neuronas, ALDH1A1 se encuentra bajo el control de Pitx3, un factor transcripcional que puede regular la especificidad y mantenimiento de poblaciones distintas de neuronas dopaminérgicas, a través de la regulación de ALDH1A1 [75, 76]. En el sistema nervioso central (CNS), la monoaminooxidasa (MAO) metaboliza la dopamina a su metabolito aldehído 3, 4-dihidroxifenilacetaldehído (DOPAL). La literatura sugiere que el DOPAL puede ser neurotóxico y su acumulación puede llevar a la muerte celular asociada con patologías de tipo neurológico [77]. ALDH1A1 juega un rol crítico en mantener bajos los niveles de DOPAL, por catalizar la conversión del DOPAL a ácido 3,4-dihidroxifenilacético DOPAC contrarrestando así la neurodegeneración [74, 77].

La ALDH1A1 cataliza la oxidación irreversible de retinal a ácido retinoico. Mientras que las propiedades de absorber la luz del aldehído retinal son un elemento necesario para la visión, los isómeros all-trans-ácido retinoico y 9-cis-ácido

retinoico, son ligandos para 2 familias de receptores nucleares de retinoides, el receptor retinoico (RAR) y el receptor retinoide X (RXR) que son mediadores en la expresión de genes durante el crecimiento y desarrollo [78].

Debido a la participación de la ALDH1A1 en los procesos ya mencionados, es importante conocer los valores de afinidad *(Km)* de ésta enzima, en relación a diferentes aldehídos generados a nivel endógeno y exógeno (Tabla A), pues dicho parámetro cinético se encuentra estrechamente relacionado con su capacidad de desintoxicación.

Tabla A. Afinidad de ALDH1A1 por algunos aldehídos de importancia fisiológica.

Aldehído	*Km*	Referencia
all-trans y 9-cis retinal	<0.1	79,80
Acetaldehído	4.5 -180	136, 138, 139
Aldofosfamida	51	81
Acroleína	4-5	82
4-HNE	1-2	82
malondialdehído	4-30	82
propionaldehído	5.8 -12	83, 84, 137, 139

Los valores de afinidad están reportados en unidades de μM

4.2. ALDH2

La ALDH2 es una enzima mitocondrial, la cual tiene una alta afinidad por el acetaldehído y juega un papel muy importante en su desintoxicación. Tanto el etanol como el acetaldehído son neurotóxicos y se ha reportado que el consumo excesivo de etanol puede participar en el avance de la enfermedad de alzheimer (Ohta and Oshawa, 2006). El 50% de la población asiática es sensible a la ingesta alcohólica y diversos reportes indican que esto se debe a la presencia de un polimorfismo en el alelo ALDH2*2, esta variante contiene una lisina en lugar de un glutamato en la posición 487 (E487K) y esta modificación puntual se ha asociado con una deficiencia en la actividad de ALDH2 [5]. En la estructura cristalográfica de ALDH2 se puede observar que el E487 forma puentes de hidrogeno con los residuos R264 y R475, dichas interacciones ayudan a estabilizar la interfase dímero-dímero de esta enzima y mantienen la integridad estructural del sitio de unión del NAD^+; en la variante ALDH2*2 la presencia de una lisina en la posición 487 rompe esas interacciones, con lo cual se altera el arreglo estructural de la enzima y esto ocasiona una reducción de 10 veces en el valor de la constante *kcat* e incrementa 200 veces el valor de *Km* por NAD^+ [148]. Al ser una mutante de tipo dominante, los individuos que la poseen muestran una clara reacción adversa al etanol, lo cual es causado por los altos niveles de acetaldehído generado y acumulado en el organismo [5, 85, 86]. Por otro lado, se ha observado que en células de cordón umbilical (HUVEC) transfectadas con el gen de la ALDH2, disminuyen los niveles de acetaldehído, como reflejo de esto, también disminuye

la generación de ROS, la apoptosis y la activación de moléculas marcadoras de estrés, como ERK1/2 y p38 MAP cinasa, las cuales se inducen por la presencia del acetaldehído. Estos resultados indican el potencial terapéutico de la enzima ALDH2 en la prevención del daño celular inducido por el consumo de etanol [87].

En la enfermedad de Alzheimer (AD), también se ha observado una importante participación de esta enzima. La AD se caracteriza clínicamente por la pérdida progresiva de la memoria, esto se debe particularmente a la pérdida de las conexiones neurofibrilares que genera perdida de la sinapsis [88]. Es un desorden neurodegenerativo generalmente asociado con la edad. En la enfermedad de Alzheimer las células neuronales están sometidas a altos niveles de estrés oxidante [89] y este estrés se manifiesta por la peroxidación lipídica y por la oxidación de proteínas. Existe evidencia que muestra que la peroxidación lipídica es un mecanismo importante de la neurodegeneración en la AD, inducida por el péptido β-amiloide (Aβ), el cual es un péptido de 39-43 aminoácidos que conforma el centro de las placas seniles (SP) [88], se ha reportado que su presencia induce la oxidación de proteínas y la peroxidación lipídica en membranas celulares del cerebro, dichos efectos pueden ser inhibidos por la presencia de agentes anti-oxidantes [90-96]. Dos de los principales productos generados a partir de estos procesos son el HNE y la acroleína [95], los que a su vez actúan alterando la conformación de diferentes proteínas de membrana generando toxicidad para las neuronas [43, 71, 95, 97]. La concentración de HNE se encuentra elevada en múltiples regiones del cerebro y en el fluído cerebro espinal (CSF) en la enfermedad de Alzheimer [98]. Los aductos de proteínas-HNE también se

encuentran elevados [99]. Se ha observado que el HNE es neurotóxico para las neuronas del hipocampo de ratas, posiblemente por que altera la homeostasis del Ca^{2+} y reduce la actividad de la Na^{+}/K^{+}-ATPasa [95] y daña el transporte de glucosa [100]. Es por ello, que resalta la importancia de la participación de las ALDHs en este tipo de padecimientos, pues se han encontrado altos niveles de ALDH2 en la corteza cerebral, hipocampo (glia y placas seniles), ganglios basales, mesencéfalo y cerebelo. La actividad de la ALDH2 se observó significativamente incrementada en la corteza temporal de pacientes con AD, mientras que esto no se observó en los controles. Estos resultados sugieren que el incremento en actividad de ALDH2 es uno de los mecanismos de desintoxicación y protección de la corteza cerebral en la AD [64]. También, se ha identificado a la ALDH2 como una enzima cuya activación correlaciona con la disminución de daño al miocardio en un corazón isquémico. En un modelo de roedores, cuando se administra ALDA-1 (un activador específico de ALDH2) antes de un evento isquémico el tamaño del infarto se reduce un 60% [101]. El 4-HNE es uno de los principales compuestos que se acumulan durante un evento isquémico cardiaco, se ha propuesto que la eliminación de este compuesto por la ALDH2 puede ser uno de los mecanismos por los cuales esta enzima protege al corazón del daño isquémico [101, 102]. La ALDH2 posee un grupo tiol en el sitio activo que es sensible a reacciones de oxido-reducción y que vuelve a esta enzima más propensa a la inactivación [13]. Más específicamente, se ha observado que tratamientos largos con nitroglicerina pueden llegar a inactivar a la ALDH2, debido a la sobreproducción de especies reactivas de oxígeno generadas en la mitocondria [103, 104]. También, se ha observado que el estrés oxidativo generado por una hiperglicemia crónica puede

afectar la actividad de la ALDH2 y que la inhibición de esta enzima puede estar involucrada en la disfunción ventricular izquierda en corazones diabéticos. Otros estudios muestran que una dieta rica en fructosa o sus metabolitos como gliceraldehído y glicolaldehído pueden inducir esteatohepatitis no-alcohólica (NASH) en ratas y este padecimiento se ha asociado con un incremento en los marcadores de estrés oxidante [105], pues estos compuestos pueden ser oxidados por las ERO para formar productos altamente tóxicos o genotóxicos, tal como el glioxal. En hepatocitos, gliceraldehído, glicolaldehído y glioxal son eliminados a través de la ALDH2, ya que se observó que cuando se usan inhibidores de esta enzima la citotoxicidad de estos aldehídos se incrementa, así como también, la proporción de proteínas carboniladas, revelando de esta manera la importancia de esta enzima en diversos padecimientos como la esteatohepatitis no alcohólica (NASH) [140].

En la tabla que se presenta a continuación (Tabla B), se muestran las afinidades de la enzima ALDH2 por algunos aldehídos

Tabla B. Afinidad de ALDH2 por algunos aldehídos de importancia fisiológica.

Aldehído	***Km***	**Referencia**
Acetaldehído	<3.5	106, 107, 139
Acroleína	1	82
4-HNE	0.9	82
Malondialdehído	26	82
Propionaldehído	0.2 - 1.2	15, 83, 84, 108, 138, 139

Los valores de afinidad están reportados en unidades de μM

4.3. ALDH3A1

La familia de ALDH3 está constituida por enzimas que tienen un rol específico en el metabolismo de la peroxidación de lípidos. Se ha encontrado una alta actividad de ALDH3 en cornea, estomago, hígado, retículo endoplásmico, tracto urinario y en algunos tipos de cáncer [66, 109, 141, 142, 143, 144].

ALDH3A1 puede también regular la proliferación y el ciclo celular. Líneas celulares que expresan altos niveles de ALDH3A1 son más resistentes a los efectos antiproliferativos de los aldehídos derivados de la LPO [110] y la inhibición o deficiencia de ALDH3A1 reduce la velocidad de crecimiento celular, esto debido probablemente a la acumulación de los aldehídos generados [111]. En adición a su localización citosólica, se ha determinado que ALDH3A1 también se encuentra presente en el núcleo, dónde parece participar en la regulación del ciclo celular mediante mecanismos aun no bien determinados. Se ha observado que, durante la sobre-expresión de la ALDH3A1, hay una regulación a la baja de las ciclinas A, B y E, el factor de transcripción E2F1 y p21, proteínas reguladoras del ciclo celular [112]. En experimentos *in vitro*, se ha observado que ALDH3A1 puede reducir el daño al DNA y la apoptosis generada a partir de varios compuestos tóxicos incluyendo peróxido de hidrogeno, mitomicina C y etopósido, a través de modular el ciclo celular, generando un cierto retraso en éste para facilitar su reparación [113].

Aunque los mecanismos a través de los cuales la ALDH3A1 puede influenciar la proliferación celular no se han esclarecido completamente, es probable que se

incluyan la modulación de genes involucrados en la regulación transcripcional, crecimiento celular, diferenciación, apoptosis y/o los efectos de los productos de la peroxidación lipídica, la cual también tiene la capacidad de modular la expresión de genes a través de algunos de sus productos. Por ejemplo, ALDH3A1 se encuentra altamente expresada en muestras de pacientes con cáncer de pulmón (NSCLC) [114]; en este tipo de células, el crecimiento y la proliferación celular se afectan significativamente cuando la actividad de ALDH3A1 es reducida por siRNA u otros inhibidores, esto se debe probablemente a la capacidad que tiene esta enzima de afectar un amplio espectro de genes que tienen diversos roles en las células. Estos genes incluyen CCL20, GPR37, DDX3Y, ID4, GPC6, RPS4Y1, EIF1AY y HMGA2 y están involucrados en la regulación transcripcional, el crecimiento celular, la diferenciación y la apoptosis [115-117]. La ALDH3A1 también tiene un rol importante en el metabolismo de los aldehídos derivados de la peroxidación lipídica, tal como alcanales y alquenales de cadena mediana y 4-hidroxialquenales. Existen diversos factores capaces de inducir estrés oxidante, incluyendo el metabolismo de xenobióticos, la exposición a la radiación UV o la exposición a agentes pro-oxidantes [118, 119]. El 4-HNE es el pro-oxidante más reactivo y citotóxico de los aldehídos producto de la peroxidación lipídica [120]. Este aldehído causa una variedad de efectos en los sistemas biológicos, por ejemplo, induce la disminución del glutatión [121], inhibe la síntesis de DNA y RNA [122] inhibe la respiración mitocondrial [123] e induce ciertos cambios morfológicos [124]. Los efectos del 4-HNE, como los de otros aldehídos, se correlacionan no sólo con el grado de peroxidación lipídica, sino también con la actividad de las enzimas capaces de metabolizar estos aldehídos. Entre estas enzimas se

encuentra la ALDH3A1, de modo que un incremento en la expresión de esta enzima hace que tanto las células normales como las células tumorales sean más resistentes al efecto de los productos de la peroxidación lipídica [125]. Las células tumorales de pulmón A549, expresan altos niveles de la enzima ALDH3A1, esta línea celular es menos susceptible a los efectos antiproliferativos del 4-HNE, comparada con células de hepatoma humano HepG2 o SK-HEP-1, las cuales presentan una menor expresión de ALDH3A1 [126].

Una de las funciones propuestas para ALDH3A1 es la desintoxicación de aldehídos formados durante la peroxidación lipídica inducida por UV como ocurre en la cornea humana en la cual esta enzima constituye de 20-40% de las proteínas totales solubles en agua [114, 127]. Experimentos de inmunohistoquímica han revelado la expresión de ésta enzima en células epiteliales y queratinocitos del estroma corneal [128]. Este efecto protector de la ALDH3A1 ante la presencia de HNE fue demostrado en células transfectadas de la cornea que carecían de la enzima de manera endógena. Las células transfectadas fueron más resistentes a la apoptosis inducida por HNE que las que no fueron transfectadas con el gen de ALDH3A1. La expresión de ALDH3A1 también previene la formación de aductos con proteínas en la cornea [129]. ALDH3A1 es inducida en otros tejidos neoplásicos y líneas celulares [130] y su expresión es afectada diferencialmente por hormonas como progesterona y cortisona, sugiriendo un rol potencial dependiente de hormonas en algunos tumores [131]. La expresión de ALDH3A1 también, es inducida por varios xenobióticos, incluyendo hidrocarburos policiclicos (PAHs) y 3-metilcolantreno, a

través de múltiples elementos de respuesta a xenobióticos (XREs) [132, 133]. Todos estos datos sugieren que la ALDH3A1 es un elemento regulatotrio del sistema de defensa celular. En la tabla que se muestra a continuación (Tabla C) se reportan las afinidades de la enzima ALDH3 por algunos aldehídos.

Tabla C. Afinidad de ALDH3 por algunos aldehídos de importancia fisiológica.

Aldehído	*Km*	Referencia
acroleína	921	82
4-HNE	46	82
malondialdehído	3500	82
benzaldehído	215	134

Los valores de afinidad están reportados en unidades de μM

Como se pudo apreciar en este capítulo, es relevante conocer la importancia fisiológica de esta familia de enzimas, pues a través de modular su actividad se pueden generar diversas aplicaciones tanto biomédicas como a nivel industrial. Es por ello que conocer a detalle su mecanismo cinético es crucial para poder diseñar estrategias que nos permitan manipular su actividad y eficiencia.

Capítulo 5. Justificación.

En un trabajo previo reportado por Rodríguez-Zavala *et al* 2002, se evidenció la importancia que podrían tener los enlaces iónicos en la región de la interfase dímero-dímero en el mantenimiento de la estructura tetramérica de la enzima ALDH1A1, por lo cual, se generó una doble mutante de ésta, modificando dos residuos por subunidad, D80G y S82A, los cuales forman enlaces iónicos con residuos de la interfase dímero/dímero de la enzima silvestre [9] (Figura 6). Esto se hizo con el objetivo de romper esas interacciones y dilucidar las bases estructurales que definen a las ALDH como dímeros o tetrámeros.

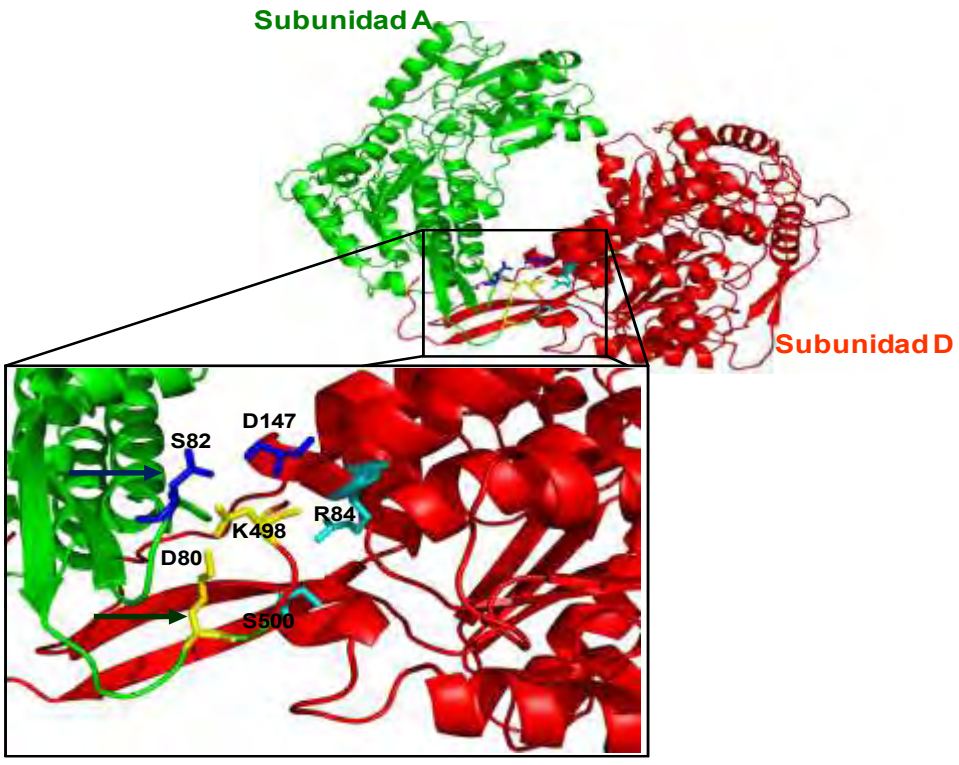

Figura 6. Residuos modificados involucrados en la interfase dímero-dímero de ALDH1A1.

Las mutaciones realizadas en la región de la interfase dímero-dímero no favorecieron la disociación completa de dímeros a partir del tetrámero de ALDH1; sin embargo, en el perfil de exclusión molecular se observó una mezcla de dímeros y tetrámeros, donde la prevalencia de una u otra especie fue dependiente de la concentración de proteína. Por otro lado, se observó que esta mutante sólo cuenta con el 10% de actividad específica comparada con la enzima silvestre [9]. Con estos datos se demuestra que a pesar de que se rompieron interacciones en la región de la interfase dímero-dímero, esto no fue suficiente para disociar el tetrámero; sin embargo, estos residuos son sumamente importantes en esa región pues lograron desestabilizarlo, lo cual se reflejó en la disminución de la actividad específica.

Una explicación de por qué se disminuyó la actividad de esta doble mutante, es que al desestabilizar el tetrámero en la región de la interfase dímero-dímero, se expone al solvente una región altamente hidrofóbica, cuyos residuos por efecto hidrofóbico tienden a esconderse del solvente (Figura 7), ocasionando un cambio conformacional del sitio activo de la enzima a larga distancia, y como consecuencia disminuyendo drásticamente la actividad.

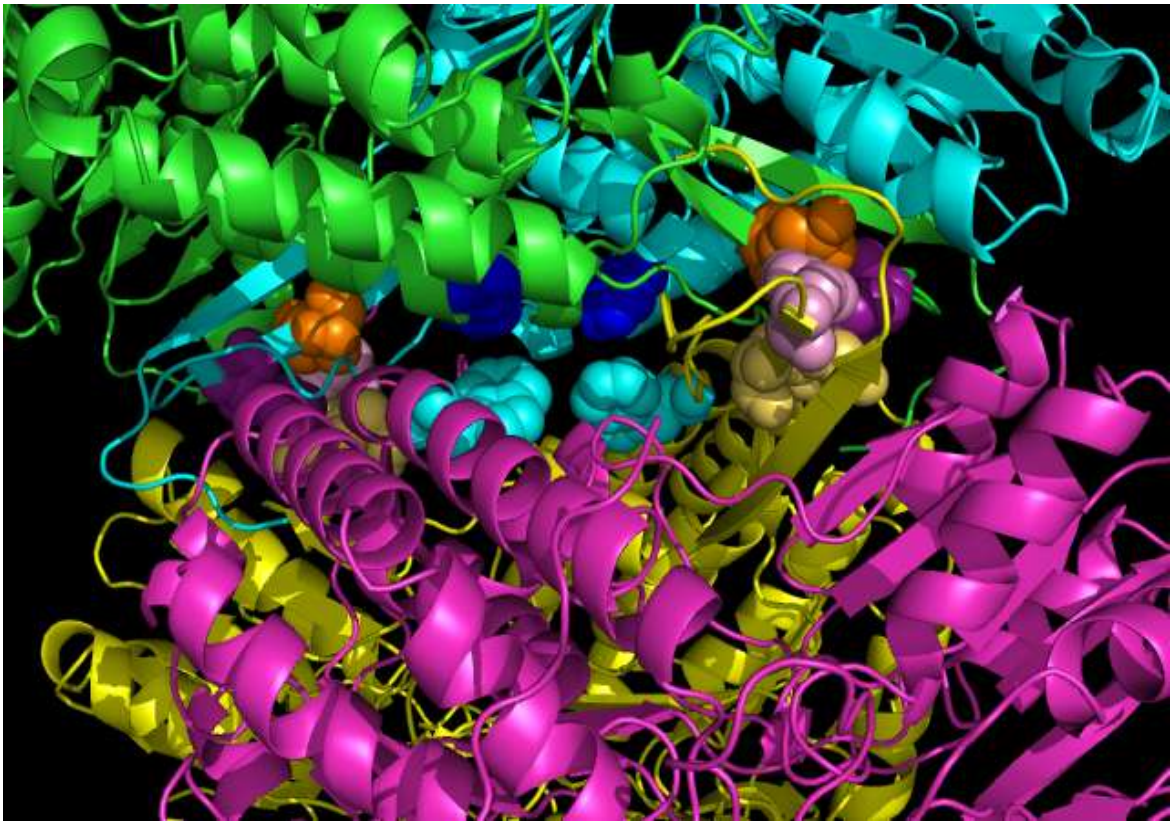

Figura 7. Región hidrofóbica de la interfase dímero-dímero en la ALDH1A1. Los residuos que se muestran en la figura son F151, W135, Y153, correspondientes a cada subunidad que conforma el tetrámero.

Como se mencionó previamente el fenómeno de la reactividad de la mitad de los sitios que ocurre en las aldehído deshidrogenasas tetraméricas no ha sido bien dilucidado. Por lo tanto, si se estabiliza la región hidrofóbica de la interfase dímero-dímero de la mutante ALDH1A1-D80G/S82A, estaremos contribuyendo a la desestabilización del tetrámero y a la separación de los dímeros; con lo cual podremos determinar si la reactividad de medio sitio depende de la formación del tetrámero.

6.1 Hipótesis

La reactividad de la mitad de los sitios en ALDH1A1 depende de la formación del tetrámero

6.2 Objetivo general

Generar dímeros estables de ALDH1A1 y determinar si la reactividad de la mitad de los sitios de ALDH1A1 humana depende de su estado de oligomerización.

6.3 Objetivos particulares

1. Determinar los parámetros cinéticos de la mutante ALDH1A1- D80G/S82A.
2. Establecer condiciones de estabilización mediante métodos físico-químicos para ALDH1A1-D80G/S82A que desplacen el equilibrio dímero-tetrámero hacia la formación de dímeros.
3. Estabilizar los dímeros generados de la doble mutante, mediante mutagénesis sitio dirigida al fusionar la proteína GFP en el C-terminal de ALDH1A1- D80G/S82A.
4. Sobre-expresar y purificar a la mutante obtenida.
5. Determinar el estado de oligomerización de ALDH1A1-D80G/S82A-GFP
6. Caracterizar cinéticamente a los dímeros ALDH1-D80G/S82A-GFP obtenidos.
7. Determinar la estabilidad estructural y del sitio activo de la mutante obtenida.
8. Dilucidar el paso limitante de la reacción.
9. Determinar la presencia de *"burst"* antes del estado estacionario y con ello, el número de sitios activos funcionales en los dímeros generados.

7. Estrategia experimental.

A continuación se muestra de manera resumida la metodología empleada en la realización de este proyecto, los detalles se describen el el artículo publicado y denominado: *"New Insights into the Half-of-the-Sites Reactivity of Human Aldehyde Dehydrogenase 1A1".* Proteins: structure function and bioinformatics. 81:8, 1285-1490.

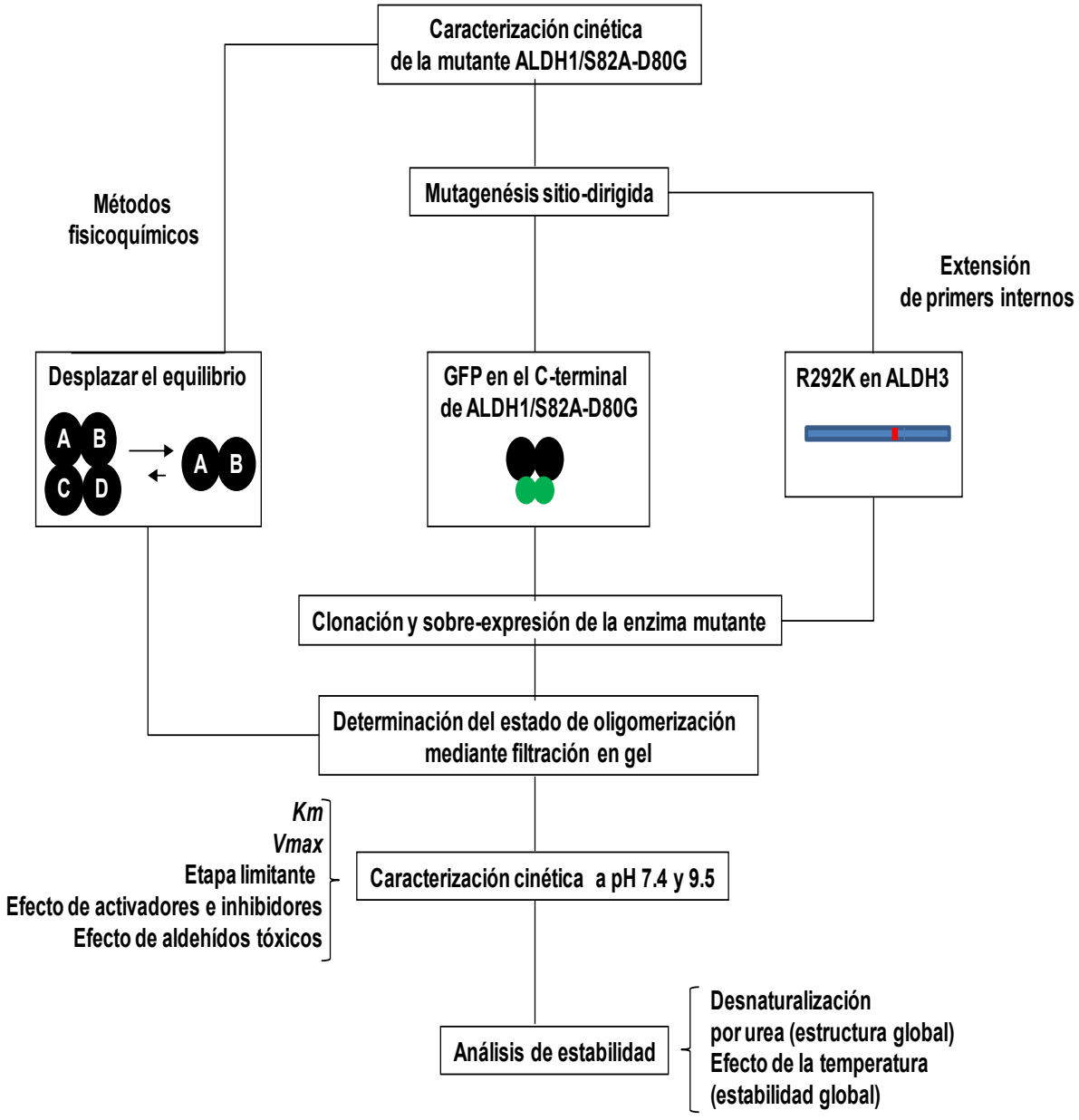

Capítulo 8. Resultados

La finalidad de este proyecto fue dilucidar si existía una dependencia de la reactividad de la mitad de los sitios con el estado de oligomerización en las ALDHs tetraméricas; pues esto nos permitiría comprender mejor el mecanismo de reacción de estas enzimas y usar esta información como una herramienta para posteriormente mejorar su eficiencia catalítica, pues se ha propuesto que la modulación de la actividad de estas enzimas se podría utilizar en el tratamiento de enfermedades que involucren incrementos en el estrés oxidante.

A continuación se describe un resumen de los resultados obtenidos.

8.1 Datos no publicados sección A.

En un inicio se determinaron los parámetros cinéticos de la enzima mutante ALDH1A1-D80G/S82A, pues como se menciona en los antecedentes, en un trabajo previo [9], se determinó que esta mutante se encuentra como una mezcla de dímeros y tetrámeros de manera dependiente de la concentración de proteína y la actividad observada en la mezcla parece indicar que el dímero generado posee muy baja actividad o es inactivo. Es por ello, que esta mutante se utilizó para intentar formar dímeros estables y activos de la enzima tetramérica ALDH1A1. Se encontró que esta enzima mutante tiene una *Km* de 136$\pm$70 μM por NAD^+, esto es 12 veces mayor que la enzima nativa (11 μM). Lo mismo ocurrió con la *Km* por el propionaldehído (189$\pm$86 μM) al compararse con la enzima nativa (12μM), en la que se observa un incremento de 16 veces. En cuanto a la *Vmax*, se observó una disminución de 11 veces con respecto a la enzima nativa (Tabla 1). Lo anterior, indica que las mutaciones de los residuos D80G y S82A en

ALDH1A1 generan una enzima poco estable y que el sitio activo de la enzima se está deformando de manera indirecta por un efecto de comunicación a distancia, pues las mutaciones realizadas se encuentran lejos del sitio activo.

Tabla 1. Comparación de los parámetros cinéticos de ALDH1A1 y ALDH1A1-D8OG/S82A.

	ALDH1A1	ALDH1A1-D80G/S82A
Km_{NAD+}	11	136 ± 70
$Km_{Propionaldehído}$	12	189 ± 86
Vmax	200	17.54

**Km en μM y Vmax en nmol $min^{-1}mg^{-1}$*

Como primera aproximación, se intentó dimerizar y estabilizar a ALDH1A1-D80G/S82A mediante métodos físico-químicos; la primera estrategia fue variar la fuerza iónica en el buffer de reacción, con el fin de promover la disociación del tetraméro en la mutante y evaluar los parámetros cinéticos así como el estado de oligomerización en las diferentes condiciones. Al evaluar la actividad de la enzima mutante variando las condiciones de fuerza iónica se observó un incremento de 3 veces en la actividad cuando I=1 con respecto a I= 0.025 (Figura 8A). Lo anterior, podría sugerir que el estado dimérico de la mutante se favorece a baja fuerza iónica y el rearreglo del estado tetramérico se favorece en condiciones de alta fuerza iónica. Lo contrario ocurre para la enzima nativa, pues al incrementar la fuerza iónica del medio ésta va perdiendo actividad indicando una posible aglomeración de subunidades de ALDH1A1 que podrían estar impidiendo la adecuada entrada de los sustratos (Figura 8B). Debido a estos resultados se

decidió realizar el análisis cinético en condiciones de baja (I=0.025) y alta (I=0.662) fuerza iónica. Se observó que a baja fuerza iónica la *Km* de la enzima mutante por el propionaldehído aumenta 44 veces, indicando una drástica disminución en la afinidad, al comparase con la enzima ensayada en condiciones de alta fuerza iónica (I= 0.662) (Tabla 2, pág. 42). Se utilizó como control de estos experimentos la ALDH1A1 nativa y en ésta no se observó el efecto encontrado para la mutante, pues los parámetros cinéticos no se modificaron. A este respecto, se corrió una cromatografía de exclusión molecular en condiciones de baja fuerza iónica y en el cromatograma se observó un pico asimétrico, con un ligero desplazamiento hacia la región donde debe eluir el dímero; sin embargo, la mayor proporción de la enzima eluyó en la región correspondiente a un tetrámero (Figura 8C), estos datos se muestran más claramente al procesar los datos del cromatograma obtenido como se muestra en la figura 8D. Como control de este análisis se usó a la enzima tetramérica fenilacetaldehído deshidrogenasa (PAD) y se observó que en ésta la disminución de la fuerza iónica no influyó en su estado de oligomerización.

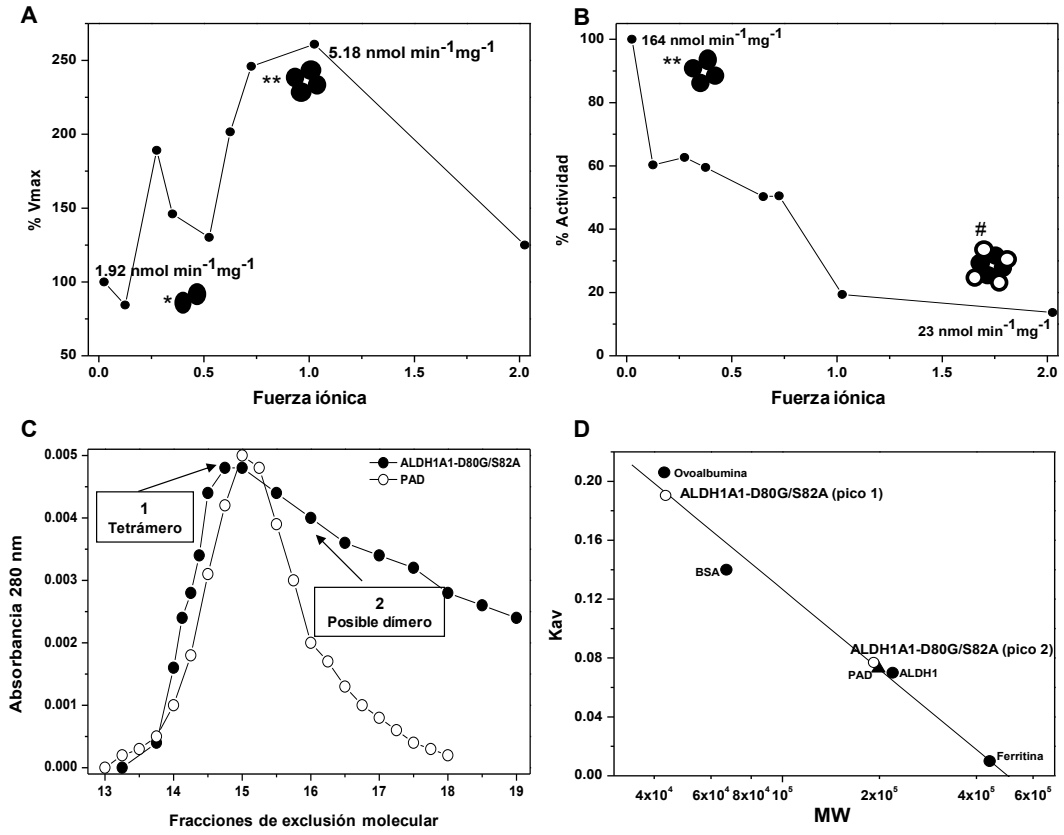

Figura 8. A) y B) Efecto de la fuerza iónica sobre la actividad de ALDH1A1-D80G/S82A y ALDH1A1 respectivamente. C) Perfil de elución de las enzimas de la cromatografía de exclusión molecular en condiciones de baja fuerza iónica. ● ALDH1-D80G/S82A, ○ PAD. D) Curva de calibración de las fracciones obtenidas en la exclusión molecular. *Dímero, **Tetrámero, # Agregado de alto peso molecular.

Por otro lado, se exploró el efecto de algunos solventes orgánicos y detergentes sobre la actividad y estado de oligomerización de ALDH1A1-D80G/S82A, incrementando la hidrofobicidad del medio, con ello, disminuyendo el efecto hidrofóbico sobre las regiones no polares expuestas de la proteína por las mutaciones. Estos compuestos fueron: tritón X-100, tween 20, polioxietilen-10-trideciléter ($iC_{13}E_{10}$), PEG-8000, DMSO, N-N,DMF, Acetonitrilo e Isopropanol. A continuación, se describen los resultados obtenidos para cada compuesto.

Tritón y DMSO.

En el caso del detergente tritón X-100, se observó un efecto de activación de al menos tres veces (de 2.5 a 7.95 nmol*min^{-1} mg^{-1}) para ALDH1A1-D80G/S82A a concentraciones crecientes de este compuesto, observándose el mayor efecto con 0.6% de tritón. A su vez, la enzima mostró una *Km* por NAD^{+} de 130 μM y un desplazamiento del equilibrio de tetrámero a dímero en la cromatografía de exclusión molecular, esta vez observándose dos picos en el perfil de elución (Figura 9).

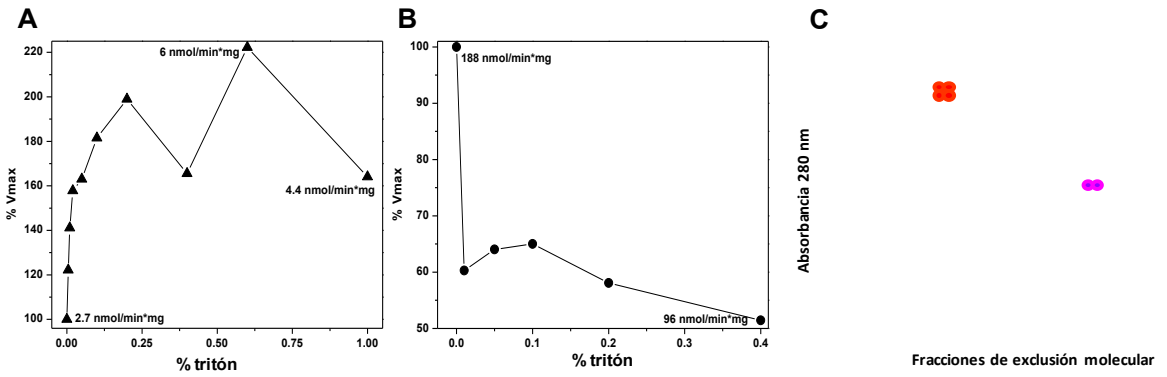

Figura 9. A) y B) Efecto del tritón sobre la actividad de ALDH1A1-D80G/S82A y ALDH1A1, respectivamente. C) Perfil de elución de la cromatografía de exclusión molecular en presencia de tritón 0.1%.

Posteriormente, se probó el efecto del solvente orgánico DMSO sobre la actividad de ALDH1A1-D80G/S82A. La actividad se incrementó al menos 16 veces (de 4 a 70 nmol*min^{-1}mg^{-1} con 30-35% de DMSO), lo cual es un reflejo de la disminución del efecto hidrofóbico (Fig. 10); en presencia de DMSO al 30% ALDH1A1-D80G/S82A mostró una *Km*=333±140 μM por NAD^{+}, mientras que para el propionaldehído la *Km* fue de 68μM, lo cual podría indicar que el DMSO logra

estabilizar las regiones hidrofóbicas de la enzima expuestas al separar los dímeros. Al analizar el efecto de otros compuestos de carácter hidrofóbico sobre la actividad de ALDH1A1-D80G/S82A, no se observó el efecto de estabilización y activación alcanzado con el DMSO, en ninguno de los compuestos evaluados. (Figura 11).

Tabla 2. Efecto de la fuerza iónica y cambio de hidrofobicidad en el medio sobre la afinidad de ALDH1A1-D80G/S82A por los substratos y el estado de oligomerización.

	ALDH1-D80G/S82A			
	Km **NAD^+** ***(μM)***	***Km*** **Propionaldehído** ***(μM)***	**Burst**	**Estado de oligomerización**
PPi 100mM pH 9.5 I=0.662	133±70 (3)	189±86 (3)	N.D.	Tetrámero
Tris 50mM pH 8 I=0.025	502 (2)	8400 (1)	No	Tetrámero-Dímero
Tritón 0.6%	206±88 (3)	96 (2)	No	Tetrámero-Dímero
DMSO 30%	**330±140 (3)**	**41±26 (4)**	**Si 2nmolNADH/ nmol enzima**	**?**

N.D. no detectado

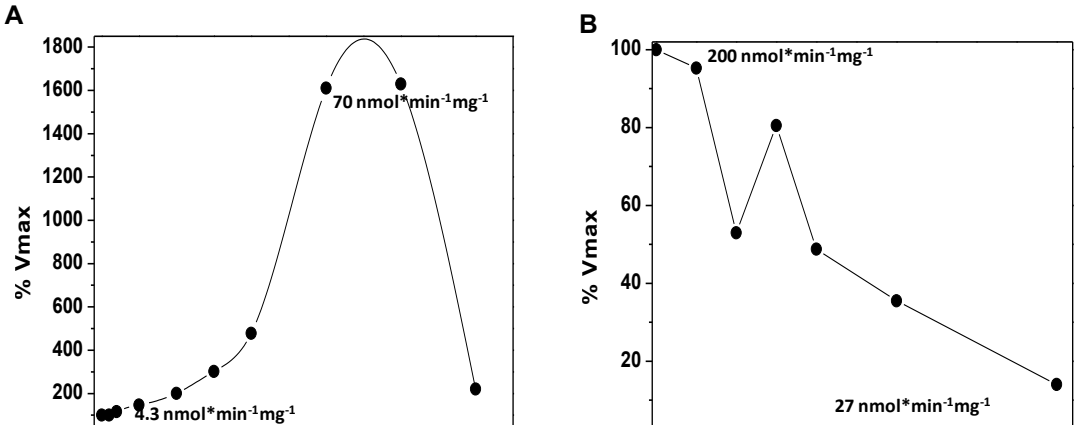

Figura 10. A) y B) Efecto del DMSO sobre la actividad de ALDH1A1-D80G/S82A y ALDH1A1, respectivamente.

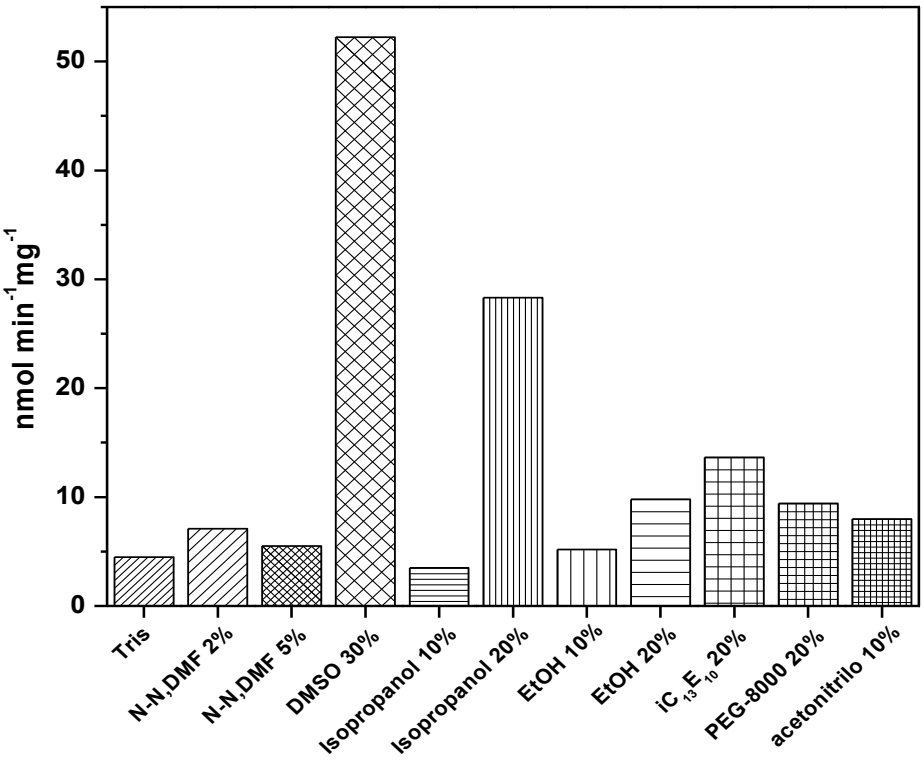

Figura 11. Actividad de ALDH1A1-D80G/S82A en presencia de diferentes compuestos de carácter hidrofóbico.

Reactividad de la mitad de los sitios.

Para determinar si la enzima mutante (ALDH1A1-D80G/S82A) en las diferentes condiciones de ensayo, cuenta o no con reactividad de la mitad de los sitios, fue necesario determinar el *"burs*t" antes del estado estacionario (Fig.12). Este ensayo se realizó en tres diferentes condiciones: 1). Tris 50 mM pH 8, 2) Tritón 0.6% y 3) DMSO 30%, siendo ésta última la única condición en la que se observó la presencia de *"burst",* el cual tuvo una magnitud de 2.053 nmol NADH/nmol enzima, tal como está reportado para la enzima silvestre. Entonces, si ALDH1A1-D80G/S82A fuera dimérica en presencia de DMSO y con un *"burst"* de 2 nmol NADH/nmol enzima, esto indicaría que las dos subunidades existentes cuentan con un sitio activo funcional, por lo tanto, la enzima tendría reactividad de sitio completo. Para corroborar esto, más adelante se muestra en análisis del estado de oligomerización de esta mutante en presencia de DMSO 30%. En caso de no existir la presencia de *"burst",* esto indicaría que el paso limitante se encuentra previo a la generación de NADH.

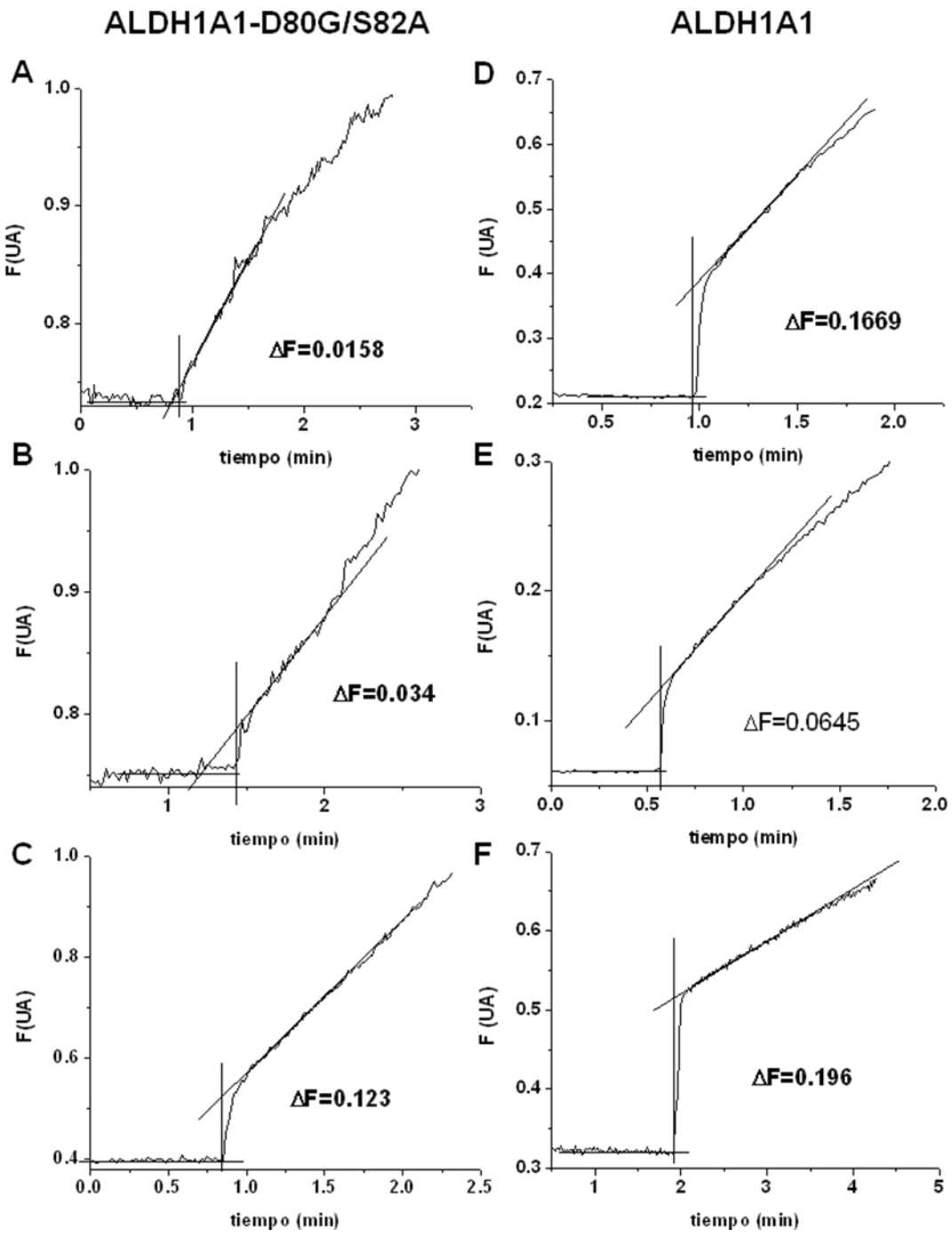

Figura 12. Determinacion del *"burst"* antes del estado estacionario de la reacción. A, B y C, ALDH1A1-D80G/S82A; D, E y F, control ALDH1A1, en presencia de tris 50 mM pH 8, tritón 0.6%, DMSO 30%, respectivamente.

Análisis del estado de oligomerización.

Al realizar el análisis de exclusión molecular de ALDH1A1-D80G/S82A en presencia de DMSO, los resultados no fueron claros, ya que la enzima eluyó de la columna en fracciones intermedias entre el dímero y el tetrámero, mientras que el control ALDH1A1 en las mismas condiciones eluyó como tetrámero (Figura 13).

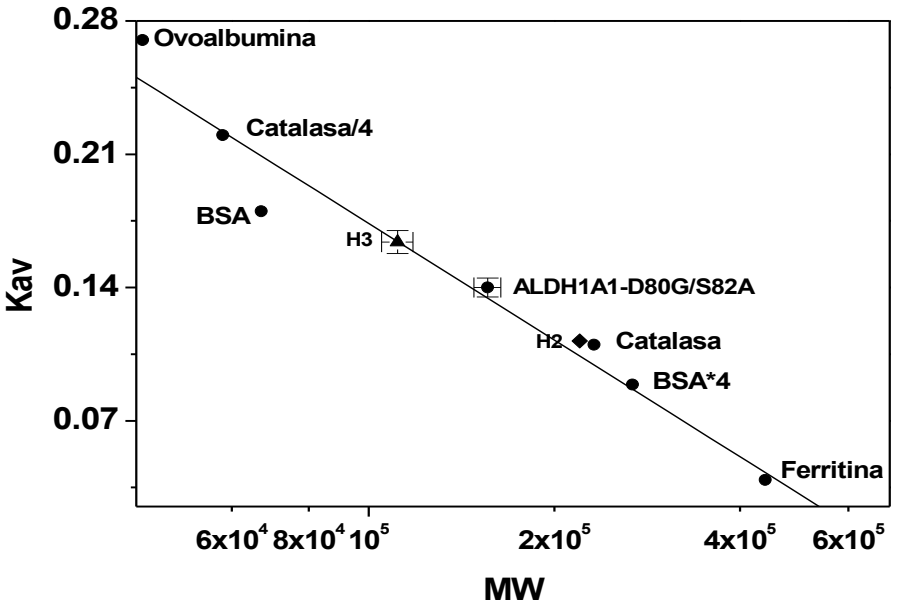

Figura 13. Curva de calibración de la columna de exclusión molecular en presencia de DMSO.

Debido a que los resultados obtenidos hasta este punto no fueron concluyentes, se optó por realizar mutagénesis sitio dirigida en la región del C-terminal, tal como se describe a continuación y más detalladamente en el artículo publicado.

8.2 Datos publicados.

El fenómeno de la reactividad de la mitad de los sitios en las aldehído deshidrogenasas es un evento poco estudiado y de gran relevancia, pues la dilucidación acerca de éste, nos puede llevar a conocer de manera más profunda el mecanismo de regulación estructural de esta enzimas y con ello proponer nuevas estrategias de modulación sobre su actividad en diferentes procesos no sólo a nivel fisiológico, sino también con fines biotecnológicos.

Weiner et al. (1976) demostró que las ALDHs poseen reactividad de la mitad de los sitios, esto es, que de las subunidades que conforman un homotetrámero, solo funcionan dos. Se sabe que estas enzimas se encuentran arregladas como un par de dímeros, pero no se ha dilucidado si uno de los dímeros es activo y el otro inactivo, o bien, si una subunidad de cada par de dímeros es la que cumple con la función catalítica. Este hecho es el que nos llevó a proponer la dependencia del estado de oligomerización en este fenómeno; pues existe la posibilidad de que al estructurarse el par de dímeros en forma tetramérica, sea cuando una de las subunidades de cada dímero pierda su capacidad catalítica.

Parte de los resultados obtenidos a este respecto se publicaron en el siguiente artículo:

Yoval-Sánchez, Belem[1]; Pardo, Juan Pablo[2]; Rodríguez-Zavala, Jose[1*] (2013). *"New Insights into the Half-of-the-Sites Reactivity of Human Aldehyde Dehydrogenase 1A1".* Proteins: structure function and bioinformatics. DOI: 10.1002/prot.24274.

PROTEINS

New insights into the half-of-the-sites reactivity of human aldehyde dehydrogenase 1A1

Belem Yoval-Sánchez,[1] Juan Pablo Pardo,[2] and Jose S. Rodriguez-Zavala[1]*

[1] Departamento de Bioquímica, Instituto Nacional de Cardiología, Mexico D.F., Mexico

[2] Departamento de Bioquímica, Facultad de Medicina, Universidad Nacional Autónoma de México, México D.F., Mexico

ABSTRACT

Aldehyde dehydrogenases (ALDHs) couple the oxidation of aldehydes to the reduction of $NAD(P)^+$. These enzymes have gained importance as they have been related to the detoxification of aldehydes generated in several diseases involving oxidative stress. It has been determined that tetrameric ALDHs work only with two of their four active sites (half-of-the-sites reactivity), but the mechanistic reason for this feature remains unknown. In this study, tetrameric human aldehyde dehydrogenase class 1A1 (ALDH1A1) was dimerized to study the correlation of the oligomeric structure with the presence of half-of-the-sites reactivity. Stable dimers from ALDH1A1 were generated by combining the mutation of two residues of the dimer–dimer interface in the tetramer (previously shown to render a low-active and unstable enzyme) and the fusion of green fluorescent protein (GFP) in the C-terminus of the mutant. Some kinetic properties of the GFP-fusion mutant resembled those of human aldehyde dehydrogenase class 3A1, a native dimer, in that the fusion dimer did not show *burst* in the generation of nicotinamide adenine dinucleotide (NADH) and was less sensitive to the action of specific modulators. The presence of primary isotope effect indicated that the rate-limiting step changed from NADH release to hydride transfer. The mutant showed higher activity with malondialdehyde and acrolein and was more resistant to inactivation by acrolein compared with the wild type. The mutant kinetic profile showed two hyperbolic components when the substrates were varied, suggesting the presence of two active sites with different affinities and catalytic capacities. In conclusion, the ALDH1A1–GFP dimeric mutant exhibits full site reactivity, suggesting that only the tetrameric structure induces the half-of-the-sites reactivity.

Proteins 2013; 00:000–000.

Key words: half-of-the-sites reactivity; ALDH1A1; GFP-fusion; acrolein; rate-limiting step; presteady state burst.

INTRODUCTION

Aldehyde dehydrogenases (ALDHs) catalyze the oxidation of a wide variety of aldehydes to their corresponding less reactive acids, aiding the cell to detoxify these compounds.[1,2] The oxidation of aldehydes by these enzymes is $NAD(P)^+$ dependent and their expression is tissue specific. Human aldehyde dehydrogenase class 1A1 (ALDH1A1) is a cytosolic enzyme ubiquitously distributed in tissues including liver, kidney, lung, brain, eye, lens, testis, and red cells.[3–7] This enzyme is a homotetramer composed of subunits with a molecular mass of 55 kDa. The subunits are arranged in the tetramer such that the protein is a dimer of dimers.[8] ALDH2 is a mitochondrial enzyme, also arranged as a tetramer that is mainly expressed in liver, heart, and brain,[5,9,10] whereas human aldehyde dehydrogenase class 3A1 (ALDH3A1) is dimeric, located in the cytosol and strongly expressed in stomach, liver, lung, and the eye.[3,11,12] ALDH2 and ALDH3A1 share 70 and 30% of identity, respectively, with ALDH1A1,[1,2] but their tertiary structures overlap perfectly.[8,10,13] In spite of the similarity at the structural level, they have very distinct substrate specificity, besides their oligomeric state (dimer vs. tetramer). Although the residues responsible for the activity are conserved among the three enzymes, the substrate specificity of the

Abbreviations: ALDHs, aldehyde dehydrogenases; ALDH1A1, human aldehyde dehydrogenase class 1A1; ALDH2, human aldehyde dehydrogenase class 2; ALDH3A1, human aldehyde dehydrogenase class 3A1; ALDH1A1-D80G/S82A, mutant of human aldehyde dehydrogenase with changes D80G and S82A; ALDH1A1-GFP, fusion of mutant ALDH1A1-D80G/S82A with GFP; GFP, green fluorescent protein.

Grant sponsor: CONACyT México; Grant number: 166463; Fellowship number: 220714

*Correspondence to: Jose S. Rodriguez-Zavala, Departamento de Bioquímica, Instituto Nacional de Cardiología, Juan Badiano No. 1, Seccion XVI, Tlalpan, México D.F. 14080, México. E-mail: rodjos@cardiologia.org.mx, rzjs@yahoo.com.

Received 19 November 2012; Revised 2 February 2013; Accepted 12 February 2013
Published online 27 February 2013 in Wiley Online Library (wileyonlinelibrary.com) DOI: 10.1002/prot.24274

isozymes appears to be determined by the differences in the rest of the amino acids comprising the active site.[8,10,13]

Aldehyde dehydrogenases share the same sequential ordered kinetic mechanism for aldehyde oxidation, with $NAD(P)^+$ binding first.[14–16] ALDH1A1, ALDH2, and ALDH3A1 can be distinguished from each other by the rate-limiting step of the reaction. For ALDH1A1 the rate-limiting step is coenzyme dissociation[16] and this step is affected by Mg^{2+} ions inhibiting the activity.[17] For ALDH2, the rate-limiting step is deacylation[18,19] and this step is enhanced in the presence of Mg^{2+}.[17] The rate-limiting step for the human class 3A1 isozyme is hydride transfer[20] and Mg^{2+} has no effect on the activity.[17] As a consequence of the different rate-limiting steps, ALDH1A1 and ALDH2 exhibit half-of-the-sites reactivity which is revealed by a presteady state burst of a magnitude of 2 nmol nicotinamide adenine dinucleotide (NADH) per nanomole of enzyme,[19,21] whereas the burst is not observed in ALDH3A1.

It has been determined that ALDHs participate in the detoxification of lipid aldehydes generated in several diseases involving oxidative stress[9,22–28] and their activities have been related with the resistance of cancer cells to chemical or radiation treatments.[29–31] It has also been shown that the activation of ALDH2 protects the heart against the damage induced by ischemia/reperfusion episodes.[9,32] A preponderant role of ALDH1A1 and ALDH3A1 has been established in protecting the eye structures against the damage caused by the light-induced increase in lipid peroxidation products, preventing the formation of cataracts.[6,14,33] Furthermore, it has been proposed that the activation of ALDH1A1 would be an alternative therapeutic/preventive approach against cataractogenesis.[33]

An important role of ALDH2 in the bioactivation of organic nitrate vasodilators has been elucidated[34–38] and has been shown that the inactivation of this enzyme is in part responsible for nitroglycerin tolerance in patients after continuous treatment.[37,39–41] Recent data suggest that ALDH1A1 may also be involved in organic nitrate vasodilators metabolism.[36,42] In this regard, a differential selectivity for these substrates by ALDH2 and ALDH1A1 was also observed, showing that both enzymes liberate nitric oxide from nitroglycerin, isosorbide dinitrate, and nicrorandil, but only ALDH1A1 metabolized isosorbide-2-mononitrate and isosorbide-5-mononitrate.[42] Thus, the understanding of the mechanisms that regulate the activity of these ALDHs may eventually have biomedical implications.

In a previous study, a mutant of ALDH1A1 (ALDH1A1-D80G/S82A) was generated, in which the dimer–dimer interface of the tetramer was destabilized, to analyze the nature of the interactions that maintain bound the subunits that comprise the tetramer.[43] The changes in the interface residues disrupted a salt bridge and prevented the formation of a hydrogen bond. The resulting mutant was a mixture of dimers and tetramers, where the predominant oligomeric species depended on the protein concentration. The dimer could not be separated from the mixture and seemed to be inactive, which made difficult its kinetic characterization. The maximal activity obtained for the dimer/tetramer mixture was only 10% compared with the wild type (WT).[43] Additionally, this mutant showed a dramatic diminution in stability as assayed by urea denaturation.[43]

In this study, the GFP protein was fused to the C-terminus of the mutant ALDH1A1-D80G/S82A, to impose a steric impediment to the formation of the tetramer, as a strategy to stabilize the mutant as a dimer, and thus be able to analyze the kinetic properties and the correlation of the half-of-the-sites reactivity with the oligomeric structure of the enzyme.

MATERIALS AND METHODS

Chemicals

Acetaldehyde, acrolein, bicinchoninic acid protein assay kit, chloroacetaldehyde, glyceraldehyde, isopropyl β-D-1-thiogalactopyranoside (IPTG), magnesium chloride, NAD^+, and NADH were from Sigma-Aldrich (St. Louis, MO); plasmid purification and DNA gel extraction kits were from Qiagen (Valencia, CA); glycerol was from J. T. Baker (Phillipsburg, NJ); restriction enzymes, Vent polymerase, and DNA T4 ligase were from New England Biolabs (Ipswich, MA); Molecular weight calibration kits and sephacryl S300 were from GE Healthcare (Piscataway, NJ).

Site-directed mutagenesis

The nucleotide sequence encoding the GFP protein was amplified by polymerase chain reaction, inserting EcoR1 and Hind III restriction site sequences flanking the N- and C-terminus, respectively, for a further subcloning step. Then, the GFP sequence was inserted at the C-terminus of a previously generated mutant ALDH1A1-D80G/S82A,[43] contained in the pT7-7 expression vector.

Overexpression and purification of the recombinant enzyme

The vectors containing the DNA-encoding ALDH1A1, ALDH1A1-D80G/S82A, and ALDH1A1–GFP were transformed in *Escherichia coli* BL21(DE3) pLysS strain. For protein expression, 1 L of 2XYT growth medium was inoculated with 20 mL of an overnight culture of the transformed cells and incubated in the presence of 100 μg/mL ampicillin and 25 μg/mL chloramphenicol, at 37°C until reaching an optical density of 0.5 at 600 nm. Protein expression was induced by addition of 0.4 m*M* IPTG and the incubation was continued for 12 h.

Cells were harvested by centrifuging at 5000 rpm and washed twice with 100 mL saline solution. Then, the cells were resuspended in a buffer composed of 50 m*M* sodium phosphate (pH 7.5), 500 m*M* NaCl, and 20 m*M* 2-mercaptoethanol (buffer A) at 4 C. Cells were disrupted by 15 cycles of 15 s sonication/1 min rest on ice. The extract was centrifuged at 45,000 rpm for 30 min. Clarified cell lysate containing the recombinant enzymes was applied into a Nickel Chelating Sepharose column previously equilibrated with buffer A. Then, the column was washed with 50 mL of 20 m*M* imidazole in buffer A and the recombinant protein was eluted from the column using a 100 mL linear gradient of imidazole (0–500 m*M*).

The pure enzyme was concentrated by using Amicon filters of molecular mass cutoff limit of 50,000 kDa (Millipore, Billerica, MA) and stored at −20 C with 50% of glycerol until use. For the experiments, the enzyme was washed with assay buffer and concentrated using an Amicon filter before use. The protein concentration was determined with the bicinchoninic acid assay kit, using bovine serum albumin as standard.

Molecular weight analysis

Size exclusion analysis was performed using a 1.5 × 85 cm sephacryl S-300 gel filtration column. The protein (200–500 µg) was injected into the column and eluted with buffer containing 100 m*M* sodium phosphate, 100 m*M* NaCl, and 0.025% mercaptoethanol. The protein was detected recording the absorbance at 280 nm.

Enzyme kinetics

ALDH activity was assayed in a buffer containing 100 m*M* sodium pyrophosphate (pH 9.5) or in buffer composed of 100 m*M* sodium phosphate, 100 m*M* NaCl, and 0.025% mercaptoethanol (pH 7.4) at 25 C in the presence of 4 m*M* NAD^+. The reaction was started with the addition of different aldehydes. Activity measurements were carried out using a Shimadzu UV-1800 spectrophotometer, following the increase in absorbance at 340 nm owing to the formation of NADH.

The dissociation constant for NAD^+ (K_d) was determined using an Aminco-Bowman Series 2 spectrofluorometer. Spectra of pure enzyme (64 µg) were obtained in the presence of increasing concentrations of NAD^+ using an excitation wavelength of 298 nm and collecting the emission at 338 nm. The inner filter effect of NAD^+ was corrected using the equation described by Lakowicz[44]:

$$F_c = F_{obs} \times 10^{(A_{ex} + A_{em})/2}$$

where F_c is the corrected fluorescence, F_{obs} is the observed fluorescence, A_{ex} is the absorbance of the solution at a given excitation wavelength, and A_{em} is the absorbance of the solution at the emission wavelength.

Determination of the rate-limiting step of the reaction

Several protocols were used as reported previously[21,43,45]: (i) The presteady state burst magnitude of NADH formation was determined with an Aminco-Bowman Series 2 fluorometer. Enzyme (50, 100, and 200 µg) and NAD^+ was incubated in 100 m*M* sodium pyrophosphate (pH 9.5), and NAD^+ to establish a baseline. NAD^+ concentration was 10 times the value of the K_m. The reaction was initiated with the addition of a saturating concentration of aldehyde. (ii) The activity of the purified enzyme was assayed in the presence of several aldehydes containing electron-withdrawing or electron-donating substituent groups under V_{max} conditions, to look for a differential effect of the substituents on the enzyme activity. (iii) The activity of the enzymes was determined in the presence or the absence of Mg^{2+}. (iv) The primary isotope effect on the aldehyde oxidation was determined using [^{2}H]-acetaldehyde and compared with the activity of the enzyme with acetaldehyde.

Stability assays

Urea denaturation was determined by incubating the enzyme (40 µg) for 2 h at the desired urea concentration in assay buffer at 25 C. The change in intrinsic fluorescence was measured using an Aminco Bowman Series 2 spectrofluorometer equipped with stirrer and temperature controller. The excitation wavelength used was 290 nm, and the emission spectra were acquired from 300 to 400 nm.

For thermostability assays, protein (20 µg) was incubated at the indicated temperature. Then, at the indicated times, an aliquot of the sample was poured into a cuvette containing the assay buffer and the substrates at 25 C, for activity measurement as indicated above.

Enzyme inactivation by acrolein or arsenite

Protein (20 µg) was incubated in the absence or in the presence of 200 µ*M* acrolein. At the indicated times, an aliquot was retrieved and supplemented with 4 m*M* NAD^+ to start the reaction and determine the remaining activity. For the arsenite assay, the enzyme was incubated in the presence of 2 m*M* NAD^+, and 1 or 2 m*M* sodium arsenite. Then, the reaction was started by the addition of aldehyde, and activity was compared with the control without arsenite.

Structural Modeling of ALDH1A1-GFP

Model of dimeric ALDH1A1-D80G/S82A mutant was obtained using the SWISS-MODEL software (available at http://swissmodel.expasy.org/).[46–48] Then, the monomers of GFP were docked to the dimer of ALDH1A1-D80G/S82A using the program ClusPro 2.0[49,50] to

generate the model of ALDH1A1–GFP. The best docking orientation was selected, considering that the GFP protein was bound to the C-terminus of the ALDH1A1-D80G/S82A mutant, restricting its movement to what would be the dimer–dimer interface of ALDH1A1. Analysis of the structure and generation of the figures was performed with PyMOL (http://pymol.sourceforge.net/).

RESULTS AND DISCUSSION

Stabilization of the mutant ALDH1A1-S82A/D80G by the fusion of the green fluorescent protein

The ALDH1A1-S82A/D80G mutant was subjected to different conditions of ionic strength, pH, and medium polarity (hydrophobicity) in an attempt to stabilize the protein as a dimer; however, none of these conditions was successful (data not shown). Further, as another strategy to stabilize the enzyme as a dimer, the green fluorescent protein (GFP) was fused to the C-terminus of the mutant, with the objective to impose a steric effect in the dimer–dimer interface and block the formation of the tetramer. In this regard, it was previously observed that the fusion of peptides of different size, or the GFP, to the C-terminus of WT ALDH1A1 was unable to disrupt the tetrameric structure,[43,51] indicating that the interactions that maintain the oligomeric structure are very strong.

The purified fusion protein ALDH1A1–GFP showed a band with the molecular mass expected for the subunit around 85 kDa after sodium dodecyl sulfate polyacrylamide gel electrophoresis (SDS-PAGE), corresponding to the sum of the masses of GFP and ALDH1A1-S82A/D80G [Fig. 1(a)]. The enzyme preparations used in this study showed purity exceeding 95% (data not shown).

The purified mutant enzyme was analyzed by gel filtration to determine its oligomerization state. ALDH1A1–GFP eluted from the column as a symmetric peak corresponding to a mass of 170 ± 15 kDa [Fig. 1(b)], indicating that the fusion of the mutant of ALDH1A1 with GFP was successful in stabilizing the enzyme as dimers. As controls, the enzymes ALDH1A1 and ALDH3A1 eluted at fractions corresponding to the masses of the tetramer and dimer, respectively [Fig. 1(b)].

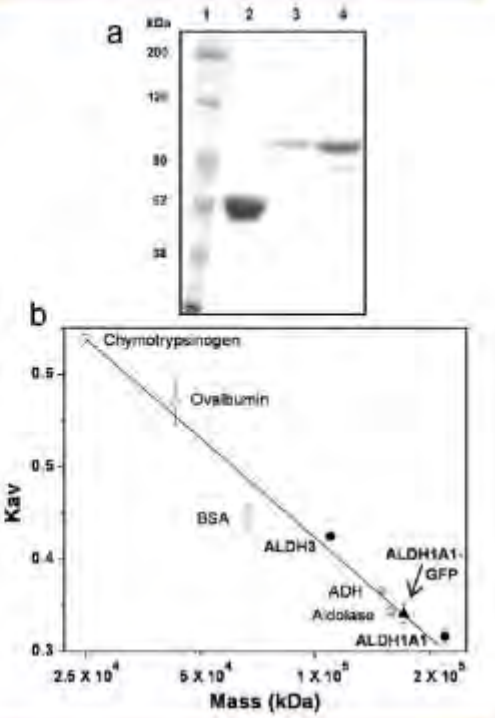

Figure 1

a. Coomassie-stained SDS-PAGE of purified ALDH1A1–GFP mutant. Line 1, molecular weight marker; line 2, ALDH1A1; lines 3 and 4, ALDH1A1–GFP. This figure is representative of runs with at least three independent protein preparations. b. Determination of the oligomerization state of the mutant ALDH1A1–GFP by gel filtration. ▲, ALDH1A1–GFP. Column calibration was accomplished using the following proteins: chymotrypsinogen, 25 kDa; ovalbumin, 43 kDa; bovine serum albumin, 67 kDa; ALDH3A1, 110 kDa; alcohol dehydrogenase, 150 kDa; aldolase, 158 kDa; ALDH1A1, 220 kDa. Data are mean ± SE of results with three independent protein preparations.

Kinetic analyses of ALDH1A1-GFP

The stabilized dimer of ALDH1A1–GFP showed two kinetic components, suggesting the presence of two binding sites with different affinities and catalytic abilities (Table I). The *Km1* for NAD^+ was fourfold higher than the WT and threefold lower than the mutant without the GFP fusion (Table I), whereas the value of *Km2* was 14-fold higher than the WT and similar to the mutant ALDH1A1-S82A/D80G. The Kd1 for this coenzyme was about three to four times higher than that in the WT and ALDH1A1-S82A/D80G, whereas the Kd2 was sixfold and 1.7-fold higher than that of the WT and ALDH1A1-S82A/D80G, respectively.

It is also worth noting that although the determination of Kd of ALDH1A1 and NAD^+ also showed two components (Table I), as reported previously,[52] the presence of two distinct types of sites is not reflected in the kinetic behavior of the WT enzyme, because half of the sites is inactive. The decrease in the affinity for NAD^+ in the mutant enzyme was probably owing to the conformational changes induced by a long distance effect upon the GFP binding to the dimer–dimer interface region.

On the other hand, the ALDH1A1–GFP mutant was more catalytically able than ALDH1A1-S82A/D80G with

Table I
Kinetic Parameters of the Mutants of ALDH1A1

	ALDH1A1		ALDH1A1-S82A/C86G		ALDH1A1-GFP		
K_{m1} (μM)[a]	11[a]		136 ± 0.07 (*n* = 3)		42 ± 16 (*n* = 3)		
K_{m2} (μM)[a]			8 ± 2 (*n* = 3)		157 ± 38 (*n* = 3)		
K_{m1} (μM)[a]	7.6 ± 1.7[b]		245 ± 50 (*n* = 3)		24 ± 2 (*n* = 3)		
K_{m2} (μM)[a]	67 ± 5[b]				412 ± 147 (*n* = 3)		
	K_m	V_m	K_m	V_m	K_{m1}	V_{m1}	V_{m2}
Propanal	12[a]	200[a]	189 ± 86 (*n* = 3)	13 ± 4 (*n* = 3)	124 × 10^3 (*n* = 2)	247 (*n* = 2)	
Glyceraldehyde	595 (*n* = 2)	414 (*n* = 2)	n.d.	n.d.	542 ± 36 (*n* = 3)	17 × 10^3 ± 3 × 10^3 (*n* = 3)	129 ± 29 (*n* = 3)	1348 ± 378 (*n* = 3)
Acrolein	9 ± 1.7[b] (*n* = 3)	868 ± 112[b] (*n* = 3)	n.d.	n.d.	5 ± 1.8 (*n* = 3)	92 ± 32 (*n* = 3)	887 ± 213 (*n* = 3)	3398 ± 168 (*n* = 3)
Malondialdehyde	4.3 ± 0.8[b] (*n* = 3)	230 ± 18[b] (*n* = 3)	n.d.	n.d.	41 ± 17 (*n* = 3)	128 ± 24 (*n* = 3)	2960 ± 587 (*n* = 3)	6889 ± 330 (*n* = 3)

[a] and [b] Values from Rodriguez-Zavala and Weiner 2002[13] and Royal-Sánchez and Rodríguez-Zavala,[52] respectively. n.d., activity below 2 mmol/min/mg. K_m and K_{m1} values in μM; V_m values in mmol/min/mg.

a V_{max} value 20-fold higher, and slightly more active than ALDH1A1 WT, when propanal was the substrate (Table I), suggesting that the GFP-fusion effectively stabilized the hydrophobic region of the dimer–dimer interface and indirectly restructured the active site favoring the catalysis. Nevertheless, the affinity of the GFP-fusion mutant for this aldehyde decreased several times as compared with the WT enzyme, indicating that the optimal conformation of the active site was not completely restored.

Activity of ALDH1A1–GFP was assayed with different aldehydes to evaluate substrate specificity (Table I). In contrast to the WT enzyme, the mutant showed very low activity with aliphatic aldehydes such as acetaldehyde and propanal and had no activity with aromatic aldehydes such as benzaldehyde, nitrobenzaldehyde, methoxybenzaldehyde, or phenylacetaldehyde (data not shown). Nevertheless, ALDH1A1–GFP showed very high activity with glyceraldehyde, acrolein, and malondialdehyde (Table I). The activity with these last aldehydes was 5-, 14-, and 30-fold higher, respectively, than that observed with propionaldehyde. The increase in the catalytic ability of the mutant enzyme suggests that the release of NADH (which is rate-limiting step for ALDH1A1 WT) is no longer the rate-limiting step of the reaction for the GFP-fusion mutant. This was further investigated by different methods and is described and discussed in the next section.

In addition, kinetics of the mutant enzyme with glyceraldehyde, acrolein, and malondialdehyde as substrates also showed two components, suggesting the presence of two binding sites with different affinities (Fig. 2(a,b)). The second kinetic component with propanal was absent because of the high substrate concentrations required for the assay as the mutant showed a very low affinity for this substrate (Table I). These results indicated that both active sites in the dimeric mutant participated in the activity and thus this mutant presented full-site reactivity.

It has been proposed that the half-of-the-sites reactivity of ALDHs may be the result of extreme negative cooperativity among the subunits in the tetramer.[53,54] Our data showed that the disruption of the communication between subunits in the mutant ALDH1A1–GFP unleashed the activity of the subunits otherwise silenced upon the binding of the substrates in the WT enzyme. Thus, the results of Table I and Figure 2 suggest that the half-of-the-sites reactivity of tetrameric ALDHs emerges from the crosscommunication between dimer–dimer subunits. These results also showed that ALDH1A1–GFP preferred aldehydes with a more hydrophilic chain such as glyceraldehyde, acrolein, and malondialdehyde, instead of acetaldehyde and propanal, suggesting a rearrangement of the amino acids that interact with the aldehyde. In turn, the lack of ALDH1A1–GFP activity with aromatic aldehydes and 4-HNE (a lipid aldehyde with a long side chain) suggests that the volume of the aldehyde-binding site and/or access to it has been restricted.

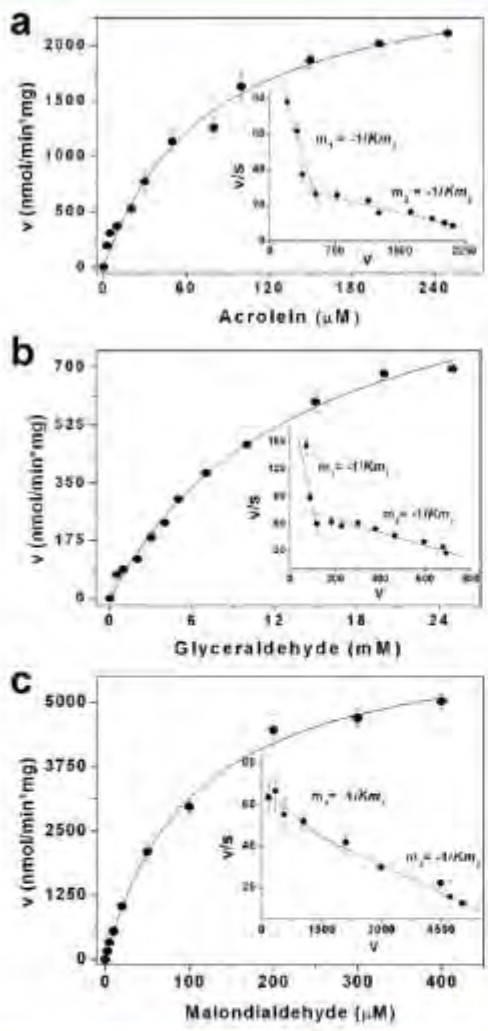

Figure 2

Kinetics of ALDH1A1–GFP with different substrates. a: acrolein; b: glyceraldehyde, and c: malondialdehyde. Line represents the fitting of the data to the Michaelis–Menten equation. Insets, Scatchard plots of the data, showing the presence of two components, corresponding to two sites with different affinities for the substrates. Plots are mean ± SE of results with three independent protein preparations and kinetic constants determined are listed in Table I.

Rate-limiting step

As indicated above, the activity of the GFP-fusion mutant increased several-fold as compared with the WT (Table I), but this was observed only with some substrates. The increased catalytic ability of the mutant may be related to a change in the rate-determining step of the reaction. For ALDH1A1, the rate-limiting step is the release of the reduced coenzyme,[16] the last step in the catalytic cycle. Therefore, different strategies were assayed to determine the rate-limiting step of the mutant. First, it was determined that the presteady state NADH burst, a well-documented feature of the WT enzyme [Fig. 3(a)], was absent in the mutant [Fig. 3(b)]. Second, it was observed that the WT enzyme activity was inhibited (64%) by Mg^{2+} at pH 7.4, in agreement with the previous reports,[17,21] whereas the ALDH1A1–GFP activity was not affected by Mg^{2+} (Table II). The absence of the presteady state burst and Mg^{2+} effect indicated that the rate-limiting step in the mutant enzyme was now located before the release of products.

To further assess the change in the rate-limiting step of the mutant enzyme, its activity was determined using chloracetaldehyde as substrate. The rationale of this experiment is that the electron-withdrawing effect of the chlorine atom would make it harder to remove the hydride, slowing down the aldehyde oxidation which would be potentiated in enzymes where the rate-determining step of the reaction is certainly the hydride transfer.[21,25] Indeed, a decrease of 40% in the activity of

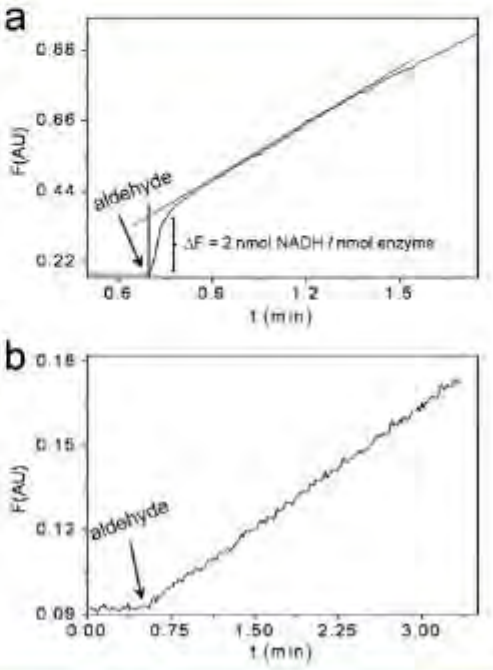

Figure 3

Assay for the presence of burst. Representative analysis of the presteady state reaction, showing the burst of WT ALDH1A1 (a) and the absence of burst in the case of ALDH1A1–GFP (b). The plots are representative of results with at least three independent protein preparations.

Table II
Effect of Different Modulator of the Activity of ALDH3 on ALDH1A1 and ALDH1A1-GFP

	ALDH1A1		ALDH1A1-GFP	
	pH 9.5	pH 7.4	pH 9.5	pH 7.4
Control	100	100	100	100
Mg^{2+} (1 mM)	86 ± 2	36 ± 2	107 ± 7	92 ± 11
Acetaldehyde	100	100	100	n.d.
Chloroacetaldehyde	87 ± 3	100 ± 7	65 ± 4	n.d.
[^{2}H]-acetaldehyde	96 ± 12	96 ± 4	18 ± 2	n.d.
Arsenite experiments				
Control	100	100	100	100
1 mM	47 ± 5	48 ± 8	98 ± 12	103 ± 8
2 mM	31 ± 4	28 ± 3	101 ± 8	104 ± 6

n.d., activity below 2 nmol/min × mg. Activity is expressed as mean ± SD of % V_{max} ($n = 3$).

ALDH1A1-GFP was attained with chloracetaldehyde, compared with the activity with acetaldehyde, whereas essentially the same activity was found for ALDH1A1 with either substrate (Table II).

Primary isotope effect was also evaluated. The rationale of this experiment is that the presence of deuterium in the aldehyde functional group, instead of hydrogen, makes the bond more stable, increasing the activation energy required to disrupt it. As a consequence, the hydride transfer would be more difficult and slower with a deuterated aldehyde, and if this is the rate limiting then the overall reaction would be lower. Again, the mutant enzyme activity with [^{2}H]-acetaldehyde was 80% lower than that attained with acetaldehyde, whereas no difference was observed with either substrate for the WT

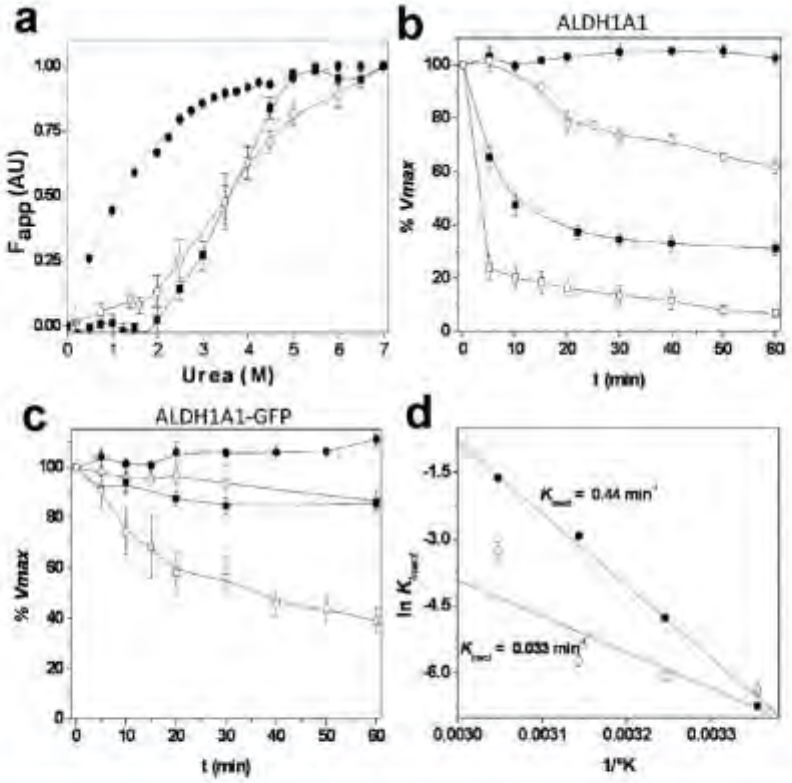

Figure 4
Assessment of the stability of the mutant enzyme (a) urea denaturation profiles of ALDH1A1 (■), ALDH1A1-GFP (○), and ALDH1A1-S82A/D80G (●). Data of ALDH1A1-S82A/D80G were adapted with permission from Ref. 43. Copyright 2002 American Chemical Society. b and c: Temperature inactivation profiles of ALDH1A1 and ALDH1A1-GFP, respectively at, ●, 25°C; □, 35°C; ■, 45°C; and □, 55°C. d: Determination of the thermal inactivation constants of ALDH1A1 (●) and ALDH1A1-GFP (○). Results are mean ± SE of experiments with three independent protein preparations.

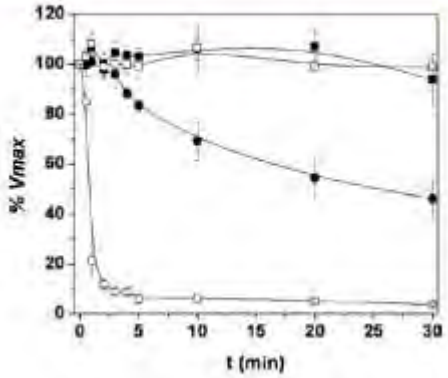

Figure 5

Effect of acrolein on the activity of ALDH1A1 and ALDH1A1–GFP. Remaining activity of ALDH1A1 and ALDH1A1–GFP, respectively, in the absence (●, ■) or the presence (○, □) of 200 μ*M* acrolein through time. Results are mean ± SE of experiments with three independent protein preparations.

enzyme (Table II). Together, these results indicated that the disruption of the oligomeric structure induced a change in the rate-limiting step of the reaction from coenzyme dissociation to hydride transfer, which is the rate-determining step reported for ALDH3A1.[20]

Stability analyses

As the ALDH1A1-S82A/D80G double mutant was previously found to be extremely unstable,[43] urea denaturation assays were conducted to assess whether the stability of the GFP-fusion mutant enzyme was preserved or improved. Denaturation of ALDH1A1 and ALDH1A1–GFP was apparent at urea concentrations higher than 2*M*, reaching half of the denaturation at 3.5 and 3.4*M* urea, respectively (Fig. 4(a)), whereas ALDH1A1-S82A/D80G started to denature at urea concentrations below 0.5*M*, reaching half of the denaturation at 1.2*M* urea. Interestingly, the denaturation pattern of ALDH1A1–GFP showed a component that resisted urea concentrations higher than 4.5*M*, concentration at which WT ALDH1A1 was almost completely denatured. The molecular component conferring higher stability may very likely be linked to the GFP portion of the protein as it has been reported that GFP possess high resistance to temperature and urea denaturation.[56]

Thermostability analysis was conducted as another approach to determine whether there was a restoration of the active site stability in the mutant ALDH1A1-S82A/D80G by the fusion of GFP. ALDH1A1–GFP was indeed more thermostable than ALDH1A1, particularly in the range of 45–55°C (Fig. 4(b,c)), with a thermal denaturation constant value more than 10 times lower than that of the WT enzyme (Fig. 4(d)). As it has been shown that GFP has high thermostability,[56] the coupling of this protein to the dimer–dimer interacting surface may protect sensitive residues of this region against temperature denaturation, indirectly stabilizing and protecting the whole structure of the enzyme.

Similarly, when the mutant enzyme was assayed for its sensitivity to acrolein, it showed a higher resistance against this compound compared to ALDH1A1 (Fig. 5). ALDH1A1 lost the activity within few seconds of the acrolein addition, whereas ALDH1A1–GFP remained active after 20–30 min of incubation (Fig. 5). The conformational change induced by the fusion of GFP may rearrange the active site, promoting the hiding of sensitive residues that may react with acrolein. In this regard, it has been proposed that Cys301 in the aldehyde-binding site and Lys352 in the NAD^+-binding site may be the targets for enzyme inactivation in ALDH1A1.[52]

Arsenite has been used as a diagnostic reagent for dithiols as it exhibits a very high affinity for vicinal thi-

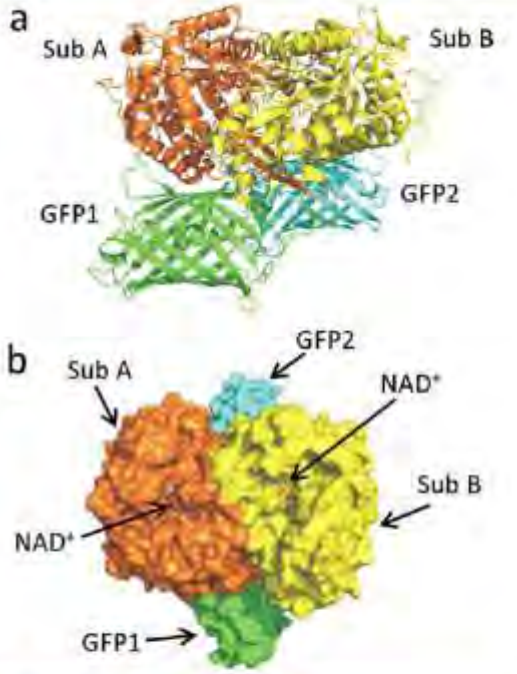

Figure 6

Model of the three-dimensional structure of the mutant ALDH1A1–GFP. The model was generated as described under the Materials and Methods section. a: Cartoon representation of the dimer of ALDH1A1–GFP; the subunits A (orange) and B (yellow) of ALDH1A1 S82A/D80G are shown coupled with two monomers of GFP (green and cyan). b: Top view of the surface representation of the structure of the mutant ALDH1A1–GFP. The position of subunits A and B, monomers of GFP and NAD^+ in the coenzyme-binding site is shown.

ols.[57,58] Thus, to evaluate the accessibility of the active site thiol groups, the mutant and WT enzymes were incubated with arsenite. ALDH1A1–GFP was insensitive to arsenite inhibition, whereas the WT enzyme was strongly inhibited by this anion (Table II). These results further support the proposal that the target cysteine for inactivation (Cys301) may not longer be accessible in the active site of ALDH1A1–GFP.

Tridimensional structural model of the mutant dimeric enzyme

A model of the possible coupling of the GFP to the dimer of ALDH1A1–GFP was generated by docking the monomers of GFP, to a model of the dimer of ALDH1A1-S82A/D80G (Fig. 6). In the model, the subunits of GFP are located in the dimer of ALDH1A1-S82A/D80G, covering part of the exposed surface for contact with the opposite dimer in the tetrameric structure. The model does not certainly explain the differences in K_m and V_m values of the active sites in the dimeric mutant, which may be related to an asymmetrical accommodation of the GFP monomers in the interface, exerting a higher stabilization to one subunit than the other. However, the model helps to visualize the possible coupling of the GFP monomers in the exposed interface of the tetramer. The crystal structure of the mutant would be required to elucidate all these proposals.

CONCLUSIONS

The fusion of GFP to the C-terminus of mutant ALDH1A1-S82A/D80G successfully stabilized the protein into dimers of ALDH1A1. It is shown that the half-of-the-sites reactivity of tetrameric enzymes is linked to the generation of dimers as the generation of single dimers of ALDH1A1 revealed activity of both sites. This last finding suggests that in ALDH3A1, which is a dimer, full site reactivity is also occurring, and as both sites possess the same affinity for the substrates, only one hyperbolic kinetic component is observed. The fusion of ALDH1A1-S82A/D80G with GFP also conferred increased stability to thermal denaturation, and resistance against acrolein inactivation, one of the most toxic aldehydes by-products of lipid peroxidation.

ACKNOWLEDGMENTS

The authors thank the program of Doctorado en Ciencias Biomédicas. Facultad de Medicina UNAM.

REFERENCES

1. Lindahl R. Aldehyde dehydrogenases and their role in carcinogenesis. Crit Rev Biochem Mol Biol 1992;27:283–335.
2. Vasiliou V, Pappa A, Petersen DR. Role of aldehyde dehydrogenases in endogenous and xenobiotic metabolism. Chem Biol Interact 2000;129:1–19.
3. Hempel J, Bahr-Lindstrom H, Jornvall H. Aldehyde dehydrogenase from human liver. Primary structure of the cytoplasmic isoenzyme. Eur J Biochem 1984;141:21–35.
4. Yoshida A, Hsu LC, Dave V. Retinal oxidation activity and biological role of human cytosolic aldehyde dehydrogenase. Enzyme 1992;46:239–244.
5. Pickle MI, Olson SI, Markesbery WR, Montine TJ. Expression and activities of aldo-keto oxidoreductases in Alzheimer disease. J Neuropathol Exp Neurol 2001;60:686–695.
6. Lassen N, Bateman BB, Estey T, Kuszak JR, Nees DW, Piatigorsky J, Duester G, Day BJ, Huang J, Hines LM, Vasiliou V. Multiple and additive functions of ALDH3A1 and ALDH1A1. Cataract phenotype and ocular oxidative damage in Aldh3a1 (-/-)/ Aldh1a1 (-/-) knock-out mice. J Biol Chem 2007;282:25668–25676.
7. Patel M, Lu L, Zander DS, Sreerama L, Coco D, Moreb JS. ALDH1A1 and ALDH3A1 expression in lung cancers: Correlation with histologic type and potential precursors. Lung Cancer 2008; 59:340–349.
8. Moore SA, Baker HM, Blythe TJ, Kitson KE, Kitson TM, Baker EN. Sheep liver cytosolic aldehyde dehydrogenase: the structure reveals the basis for the retinal specificity of class 1 aldehyde dehydrogenases. Structure 1998;6:1541–1551.
9. Chen CH, Budas GR, Churchill EN, Disatnik MH, Hurley TD, Mochly-Rosen D. Activation of aldehyde dehydrogenase-2 reduces ischemic damage to the heart. Science 2008;321:1493–1495.
10. Steinmetz C, Xie P, Weiner H, Hurley TD. Structure of mitochondrial aldehyde dehydrogenase: the genetic component of ethanol aversion. Structure 1997;5:701–711.
11. Yoshida A, Rzhetsky A, Hsu LC, Chang C. Human aldehyde dehydrogenase gene family. Eur J Biochem 1998;251:549–557.
12. Perozich J, Nicholas H, Lindahl R, Hempel J. The big book of aldehyde dehydrogenase sequences: an overview of the extended family. Adv Exp Med Biol 1999;463:45–52.
13. Liu ZJ, Sun YJ, Rose J, Chung YJ, Hsiao CD, Chang WR, Kuo I, Perozich J, Lindahl R, Hempel J, Wang BC. The first structure of an aldehyde dehydrogenase reveals novel interactions between NAD and the Rossmann fold. Nat Struct Biol 1997;4:317–326.
14. Bradbury SL, Jakoby WB. Ordered binding of substrates to yeast aldehyde dehydrogenase. J Biol Chem 1971;246:1834–1840.
15. Bradbury SL, Jakoby WB. Ligand interactions with yeast aldehyde dehydrogenase. J Biol Chem 1971;246:6929–6932.
16. Blackwell LJ, Mutton RL, MacGibbon AKH, Hardman, MJ, Buckley PD. Evidence that the slow conformation change controlling NADH release from the enzyme is rate-limiting during the oxidation of propionaldehyde by aldehyde dehydrogenase. Biochem J 1987;242: 803–808.
17. Ho KK, Allali-Hassani A, Hurley TD, Weiner H. Differential effects of Mg^{2+} ions on the individual kinetic steps of human cytosolic and mitochondrial aldehyde dehydrogenases. Biochemistry 2005;44: 8022–8029.
18. Feldman R, Weiner H. Horse liver aldehyde dehydrogenase. II. Kinetics and mechanistic implications of the dehydrogenase and esterase activity. J Biol Chem 1972;247:267–272.
19. Weiner H, Ho JH, Sanny CG. Rate-limiting steps for the esterase and dehydrogenase reaction catalyzed by horse liver aldehyde dehydrogenase. J Biol Chem 1976;251:3853–3855.
20. Mann CJ, Weiner H. Differences in the roles of conserved glutamic acid residues in the active site of human class 3 and class 2 aldehyde dehydrogenases. Protein Sci 1999;8:1922–1929.
21. Rodríguez-Zavala JS, Allali-Hassani A, Weiner H. Characterization of *E. coli* tetrameric aldehyde dehydrogenases with atypical properties compared to other aldehyde dehydrogenases. Protein Sci 2006;15:1387–1396.
22. Yokoyama A, Muramatsu T, Ohmori T, Makimoto H, Higuchi S, Matsushita S, Yoshino K, Maruyama K, Nakano M, Ishii H. Multiple primary esophageal and concurrent upper aerodigestive tract cancer and the aldehyde dehydrogenase-2 genotype of Japanese alcoholics. Cancer 1996;77:1986–1198.

23. Sreerama L, Sladek NE. Class 1 and class 3 aldehyde dehydrogenase levels in the human tumor cell lines currently used by the National Cancer Institute to screen for potentially useful antitumor agents. Adv Exp Med Biol 1997;414:81–94.
24. Zhai Y, Sperkova Z, Napoli JL. Cellular expression of retinaldehyde dehydrogenase types 1 and 2: effects of vitamin A status on testis mRNA. J Cell Physiol 2001;186:220–232.
25. Tanel A, Averill-Bates DA. Inhibition of acrolein-induced apoptosis by the antioxidant N-acetylcysteine. J Pharmacol Exp Ther 2007; 321:73–83.
26. Wenzl MV, Beretta M, Gorren A, Zeller A, Bürul PK, Gruber K, Russwurm M, Koesling D, Schmidt K, Mayer B. Role of the general base Glu-268 in nitroglycerin bioactivation and superoxide formation by aldehyde dehydrogenase 2. J Biol Chem 2009;284:19878–19886.
27. Marcato P, Dean CA, Giacomantonio CA, Lee P. Aldehyde dehydrogenase activity of breast cancer stem cells is primarily due to isoform ALDH1A3 and its expression is predictive of metastasis. Stem Cells 2011;29:32–45.
28. Yang K, Feng C, Lin H, Bruce WR, O'brien PJ. Cytotoxic molecular mechanism and cytoprotection by enzymic metabolism for glyceraldehyde, hydroxypyruvate and glycolaldehyde. Chem Biol Interact 2011;191:315–321.
29. Muzio G, Canuto RA, Trombetta A, Maggiora M. Inhibition of cytosolic class 3 aldehyde dehydrogenase by antisense oligonucleotides in rat hepatoma cells. Chem Biol Interact 2001;130–132:219–225.
30. Marchitti SA, Brocker C, Stagos D, Vasiliou V. Non-P450 aldehyde oxidizing enzymes: the aldehyde dehydrogenase superfamily. Expert Opin Drug Metab Toxicol 2008;4:697–720.
31. Muzio G, Maggiora M, Paiuzzi E, Oraldi M, Canuto RA. Aldehyde dehydrogenases and cell proliferation. Free Radic Biol Med 2012; 52:735–746.
32. Gong D, Zhang Y, Zhang H, Gu H, Jiang Q, Hu S. Aldehyde dehydrogenase-2 activation during cardioplegic arrest enhances the cardioprotection against myocardial ischemia-reperfusion injury. Cardiovasc Toxicol 2012;12:350–358.
33. Chowdhury S, Xiao T, Vergara LA, Srivastava S, Nees D, Piatigorsky J, Ansari NH. Invest Ophthalmol Vis Sci 2005;46:259–267.
34. Chen Z, Zhang J, Stamler JS. Identification of the enzymatic mechanism of nitroglycerin bioactivation. Proc Natl Acad Sci USA 2002; 99:8306–8311.
35. Chen Z, Foster MW, Zhang J, Mao L, Rockman HA, Kawamoto K, Kitagawa K, Nakayama KI, Hess DT, Stamler JS. An essential role for mitochondrial aldehyde dehydrogenase in nitroglycerin bioactivation. Proc Natl Acad Sci USA 2005;102:12159–12164.
36. Beretta M, Gruber K, Kollau A, Russwurm M, Koesling D, Goessler W, Keung WM, Schmidt K, Mayer B. Bioactivation of nitroglycerin by purified mitochondrial and cytosolic aldehyde dehydrogenases. J Biol Chem 2008;283:17873–17880.
37. Griesberger M, Kollau A, Wölkart G, Wenzl MV, Beretta M, Russwurm M, Koesling D, Schmidt K, Gorren AC, Mayer B. Bioactivation of pentaerythrityl tetranitrate by mitochondrial aldehyde dehydrogenase. Mol Pharmacol 2011;79:541–548.
38. Beretta M, Wölkart G, Scherrenbauer M, Griesberger M, Neubauer B, Schmidt K, Sacherer M, Heinzel FR, Kohlwein SD, Mayer B. Vascular bioactivation of nitroglycerin is catalyzed by cytosolic aldehyde dehydrogenase-2. Circ Res 2012;110:385–393.
39. Wenzl MV, Beretta M, Griesberger M, Russwurm M, Koesling D, Schmidt K, Mayer B, Gorren AC. Site-directed mutagenesis of aldehyde dehydrogenase-2 suggests three distinct pathways of nitroglycerin biotransformation. Mol Pharmacol 2011;80:258–266.
40. Sun L, Ferreira JC, Mochly-Rosen D. ALDH2 activator inhibits increased myocardial infarction injury by nitroglycerin tolerance. Sci Transl Med 2011;3:107–111.
41. Lang BS, Gorren AC, Oberdorfer G, Wenzl MV, Furdui CM, Poole LB, Mayer B, Gruber K. Vascular bioactivation of nitroglycerin by aldehyde dehydrogenase-2: reaction intermediates revealed by crystallography and mass spectrometry. J Biol Chem 2012;287:38124–38134.
42. Tsou PS, Page NA, Lee SG, Fung SM, Keung WM, Fung HL. Differential metabolism of organic nitrates by aldehyde dehydrogenase 1a1 and 2: substrate selectivity, enzyme inactivation, and active cysteine sites. AAPS J 2012;15:548–555.
43. Rodriguez-Zavala JS, Weiner H. Structural aspects of aldehyde dehydrogenase that influence dimer-tetramer formation. Biochemistry 2002;41:8229–8237.
44. Lakowicz JR. Principles of fluorescence spectroscopy. New York: Plenum Press; 1983. p 44.
45. Rodriguez-Zavala JS. Enhancement of coenzyme binding by a single point mutation at the coenzyme binding domain of *E. coli* lactaldehyde dehydrogenase. Protein Sci 2008;17:563–570.
46. Peitsch MC. Protein modeling by E-mail. Biotechnology 1995;13: 658–660.
47. Guex N, Peitsch MC. SWISS-MODEL and the Swiss-PdbViewer: an environment for comparative protein modeling. Electrophoresis 1997;18:2714–2723.
48. Schwede T, Kopp J, Guex N, Peitsch MC. SWISS-MODEL: automated protein homology-modeling server. Nucleic Acids Res 2003;31:3381–3385.
49. Kozakov D, Hall DR, Beglov D, Brenke R, Comeau SR, Shen Y, Li K, Zheng J, Vakili P, Paschalidis IC, Vajda S. Achieving reliability and high accuracy in automated protein docking: Cluspro, PIPER, SDU, and stability analysis in CAPRI rounds 13–19. Proteins 2010; 78:3124–3130.
50. Kozakov D, Brenke R, Comeau SR, Vajda S. PIPER: an FFT-based protein docking program with pairwise potentials. Proteins 2006;65: 392–406.
51. Rodriguez-Zavala JS, Weiner H. Role of the C-terminal tail on the quaternary structure of aldehyde dehydrogenases. Chem Biol Interact 2001;130–132:151–160.
52. Yoval-Sánchez B, Rodriguez-Zavala JS. Differences in susceptibility to inactivation of human aldehyde dehydrogenases by lipid peroxidation byproducts. Chem Res Toxicol 2012;25:722–729.
53. Ambroziak W, Kosley LL, Pietruszko R. Human aldehyde dehydrogenase: coenzyme binding studies. Biochemistry 1989;28:5367–5373.
54. Larson HN, Weiner H, Hurley TD. Disruption of the coenzyme binding site and dimer interface revealed in the crystal structure of mitochondrial aldehyde dehydrogenase "Asian" variant. J Biol Chem 2005;280:30550–30556.
55. Farres J, Wang X, Takahashi K, Cunningham SJ, Wang TT, Weiner H. Effects of changing glutamate 487 to lysine in rat and human liver mitochondrial aldehyde dehydrogenase. J Biol Chem 1994;269: 13854–13860.
56. Chalfie M, Kain SR.Green fluorescent protein: properties, applications and protocols (Methods of Biochemical Analysis, Vol.47). New York: John Wiley & Sons; 2005. pp 48–50.
57. Zahler WL, Cleland WW. A specific and sensitive assay for disulfides. J Biol Chem 1968;243:716–719.
58. Snow ET. Metal carcinogenesis: mechanistic implications. Pharmacol Ther 1992;53:31–65.

8.3 Datos no publicados sección B.

En el presente estudio se mostró la obtención de una aldehído deshidrogenasa dimérica y estable mediante la fusión de la proteína verde fluorescente (GFP) en el C-terminal de la secuencia de ALDH1A1 y con ello se demuestra la relevancia de la estructura oligomérica con respecto a la reactividad de la mitad de los sitios, ya que en la mutante dimérica se revelan dos sitios activos y estos son funcionales. Sin embargo, el sitio activo de esta mutante se modificó y con ello la especificidad por sus sustratos. Se evidenció la modificación del sitio activo en la mutante ALDH1A1-GFP al analizar el efecto de diferentes inhibidores reportados para ALDHs y ADH donde los valores de *Ki* obtenidos se encuentran en el rango de 0.02 – 1.5 μM [145]. Los datos obtenidos se muestran en la siguiente tabla:

Tabla 3. Efecto de inhibidores de ALDHs y ADH sobre la actividad de ALDH1A1-GFP.

Cumarina (μM)	**% *Vmax***	**Daidzina (μM)**	**% *Vmax***	**Disulfiram (μM)**	**% *Vmax***	**Pirazol (μM)**	**% *Vmax***
0	100	0	100	0	100	0	100
15	115	1	101	1	119	20	87
30	95	15	138	10	138	100	88
45	100			20	124		

**Experimentos realizados a pH 7.4*

Como se puede observar estos compuestos no ejercieron su efecto de inhibición en la mutante ALDH1A1-GFP, indicando un cambio en el arreglo tridimensional de la estructura del sitio activo; por lo cual se decidió explorar cambios a nivel estructural en esta enzima mutante. Para ello se determinó la accesibilidad de los triptófanos al solvente en ALDH1A1 y en ALDH1A1-GFP, al determinar las

constantes de Stern-Volmer *(Ksv)* titulando con acrilamida que es un *"quencher"* neutro de la fluorescencia [146], con el fin de determinar si el sitio activo se había reducido y por esta razón se modificaron los parámetros cinéticos de la enzima mutante. El análisis se realizó en presencia y ausencia de los sustratos. Se encontró que la accesibilidad de los triptófanos al solvente de la enzima mutante disminuye un 28% en presencia de NAD^+ mientras que el área de ALDH1A1 disminuye un 33% de área expuesta; lo cual sugiere que el volumen del sitio activo en la mutante ALDH1A1-GFP efectivamente se encuentra reducido (Figura 12).

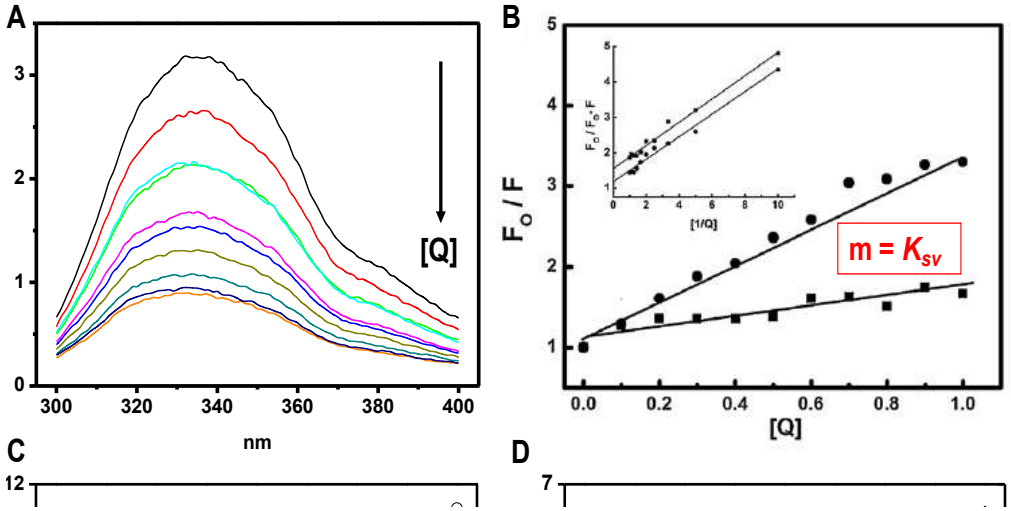

Figura 12. Determinación del área expuesta al solvente. A. Espectros de emisión de fluorescencia al adicionar concentraciones crecientes de acrilamida a la proteína. B. Cálculo del área expuesta al solvente. C y D. Determinación del área expuesta al solvente para ALDH1A1 y ALDH1A1-GFP, respectivamente. ○, en ausencia de sustratos; ●, en presencia de NAD^+; ◇, en presencia de propionaldehído.

En cuanto al arreglo tridimensional de la GFP en la mutante generada, esta se puede arreglar como monómero o como dímero. Para explorar estas posibilidades, se realizó una curva de desnaturalización por urea y se observó que a una concentración de 2 M, ambas proteínas (ALDH1A1 y ALDH1A1-GFP) aún conservan su estructura cuaternaria (Figura 13A y 13B). Con esta información se determinó la relación entre los picos máximos de excitación ($\mathbf{R_{395/475}}$), ya que se ha reportado que, cuando la GFP se encuentra en forma de monómero la $\mathbf{R_{395/475}}$ es menor que cuando se encuentra en forma dimérica. Al realizar el experimento sin urea la $\mathbf{R_{395/475}}$ encontrada fue de 2.75, mientras que a 2 M de urea la $\mathbf{R_{395/475}}$ fue de 2.4 (Figura 13C y 13D), indicando con ello que antes de la exposición a la urea, la GFP en la enzima mutante se encuentra en forma dimérica. Esto último explicaría el incremento en los valores de los parámetros cinéticos obtenidos para la mutante generada y el hecho de que no se haya observado efecto de los inhibidores sobre la actividad enzimática; pues al estar los monómeros de GFP acoplados en forma dimérica en la interfase de los dímeros de ALDH1A1, este arreglo, probablemente reduce la accesibilidad de los diferentes sustratos al sitio activo y por ende se modifique la afinidad y velocidad máxima de la mutante.

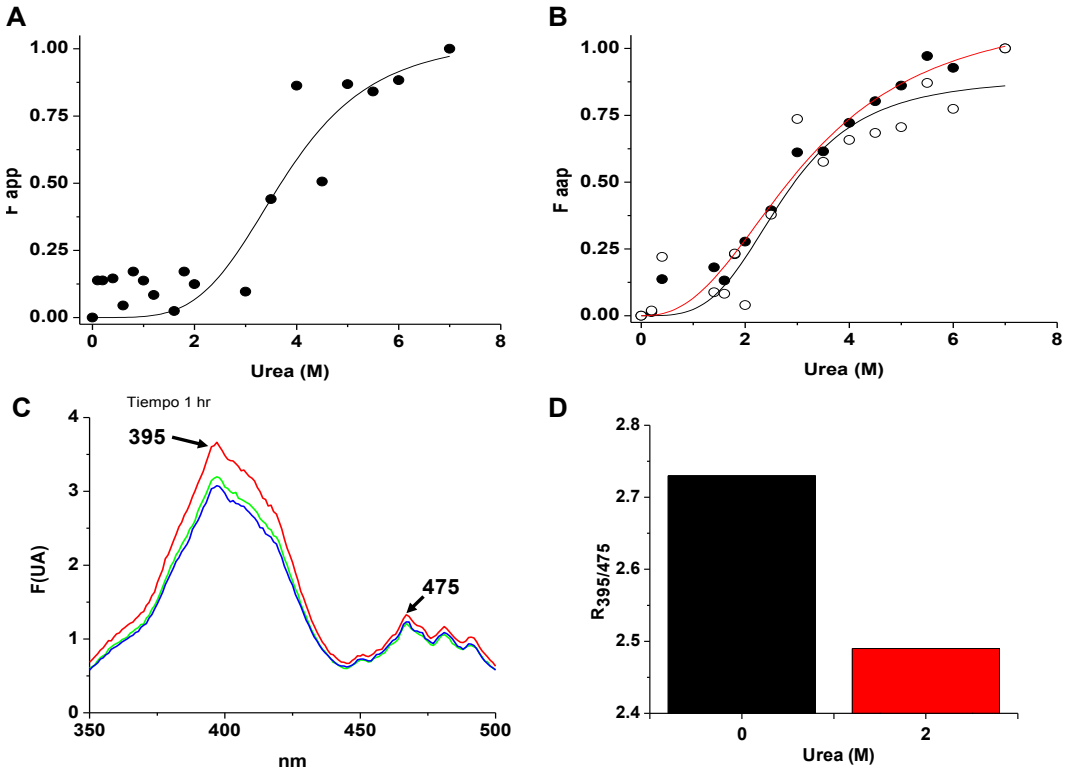

Figura 13. Determinación del arreglo oligomérico de la GFP en la mutante. Desnaturalización por urea, A y B. ALDH1A1 y ALDH1A1-GFP, respectivamente. C. Espectros de emisión de la GFP en la mutante ALDH1A1-GFP. D. Relación entre los máximos de emisión a 0 y 2M de urea para ALDH1A1-GFP, indicando la asociación de la proteína en forma de monómero o dímero.

Capítulo 9. Discusión general

El trabajo realizado en esta tesis demuestra que la fusión de la proteína verde fluorescente (GFP) en el C-terminal de la mutante ALDH1A1-S82A/D80G, fue exitosa para estabilizar a la enzima ALDH1A1 en dímeros; además de que se pone en evidencia la dependencia existente de la reactividad de la mitad de los sitios en las enzimas tetraméricas, con el estado de oligomerización. Esto nos lleva a sugerir que la ALDH3A1, que presenta una conformación dimérica posee reactividad de sitio completo; puesto que, una vez que los dímeros de ALDH1A1 fueron generados, se observó que cada subunidad en el dímero es funcional y activa. La fusión de ALDH1A1-D8OG/S82A con GFP no solo ayudó a explicar el fenómeno de la reactividad de la mitad de los sitios, sino que también le confirió a la enzima mayor estabilidad térmica y resistencia a la inactivación por acción de la acroleína, uno de los principales productos de la peroxidación lipídica. Todo lo anterior contribuye al mejor entendimiento del mecanismo cinético de las ALDHs y ofrece un panorama de cómo poder regular su actividad en los diferentes padecimientos en los que se encuentran relacionadas, ya sea mediante terapia génica o bien en el área de diseño de fármacos moduladores de su actividad; incluso en el área biotecnológica, produciendo a través de ellas algún aldehído de importancia industrial.

9.1. Conclusiones generales.

Las bases estructurales de la reactividad de la mitad de los sitios en las ALDHs tetraméricas no han sido completamente explicadas hasta el momento; Steinmetz, C. et al. (1997) y Ni, L. (1999), relacionaron la reactividad de la mitad de los sitios con las dos diferentes conformaciones que puede tomar el anillo de nicotinamida del NAD^+ en el sitio activo, mientras que Zhou and Weiner (2000), muestran que el efecto de una subunidad en las propiedades de otra ocurre entre las subunidades que pertenecen al mismo dímero y no entre el par de dímeros. Esto último refuerza nuestros datos, al demostrar que una enzima tetramérica con la mitad de sus sitios activos, al ser estabilizada en dímeros, despierta la capacidad catalítica en cada una de las subunidades que lo conforman y aun cuando cada subunidad muestra una afinidad diferente por sus sustratos; este hallazgo se puede interpretar como reactividad de sitio completo; con lo cual el objetivo de este trabajo queda cubierto.

Capítulo 10. Susceptibilidad de las aldehído deshidrogensas humanas a productos de la peroxidación lípidica.

Las aldehído deshidrogenasas participan de manera importante en la desintoxicación de compuestos generados a partir de la LPO, por lo que su contribución en la desintoxicación de estos compuestos en padecimientos que involucran altos niveles de estrés oxidante, las convierte en enzimas esenciales en el organismo. Por otro lado, a través de su modulación se pueden regular diversos procesos del crecimiento y desarrollo celular. Además, mediante el conocimiento de su secuencia, estructura y propiedades cinéticas se pueden diseñar estrategias que puedan contribuir a eliminar los carbonilos causales de diferentes patologías.

En el trabajo que se muestra a continuación se evaluó el efecto de diferentes aldehídos lipídicos sobre la actividad de las tres principales isoformas de aldehído deshidrogenasas (ALDH1A1, ALDH2 y ALDH3A1), encontrando que la ALDH3A1 es la isoforma más resistente al efecto de la acroleína, 4-HNE y malondialdehído, esto al compararse con las isoformas ALDH1A1 y ALDH2. Dicho hallazgo nos llevó a analizar la secuencia de aminoácidos involucrados en el reconocimiento del NAD^+ y del aldehído en el sitio activo de las diferentes isoformas, con el fin de determinar los residuos responsables de la protección o inactivación en las ALDHs frente a diferentes aldehídos producto de la lipoperoxidación. Los datos se muestran y discuten de manera detallada en el siguiente artículo.

10.1. Artículo publicado.

Chemical Research in Toxicology

Article

pubs.acs.org/crt

Differences in Susceptibility to Inactivation of Human Aldehyde Dehydrogenases by Lipid Peroxidation Byproducts

Belem Yoval-Sánchez[†] and José S. Rodriguez-Zavala*[,†]

[†]Departamento de Bioquímica, Instituto Nacional de Cardiología, México D.F., Mexico

ABSTRACT: Aldehyde dehydrogenases (ALDHs) are involved in the detoxification of aldehydes generated as byproducts of lipid peroxidation. In this work, it was determined that, among the three most studied human ALDH isoforms, ALDH2 showed the highest catalytic efficiency for oxidation of acrolein, 4-hydroxy-2-nonenal (4-HNE), and malondialdehyde. ALDH1A1 also exhibited significant activity with these substrates, whereas ALDH3A1 only showed activity with 4-HNE. ALDH2 was also the most sensitive isoform to irreversible inactivation by these compounds. Remarkably, ALDH3A1 was insensitive to these aldehydes even at concentrations as high as 20 mM. Formation of adducts of ALDH1A1 and ALDH2 with acrolein increased their K_d values for NAD^+ by 2- and 3-fold, respectively. NADH exerted a higher protection than propionaldehyde to the inactivation by acrolein, and this protection was additive. These results suggested that both binding sites, those for aldehyde and NAD^+ in ALDH2, are targets for the inactivation by lipid peroxidation products. Thus, with the advantage of being relatively inactivation-insensitive, ALDH1A1 and ALDH3A1 may be actively participating in the detoxification of these aldehydes in the cells.

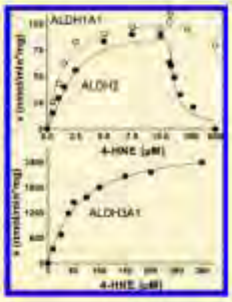

INTRODUCTION

The lipid peroxidation products malondialdehyde, acrolein, and 4-hydroxy-2-nonenal (4-HNE) have been implicated in the etiology and pathogenesis of many diseases that involve an increase in oxidative stress such as atherosclerosis,[1−3] diabetes,[4] alcoholic liver disease,[5] and other diseases related to obesity and metabolic syndrome,[6,7] as well as neurodegenerative diseases such as Alzheimer's, Parkinson's,[8−13] and multiple sclerosis.[14] Toxicity of these compounds is related to the formation of adducts with proteins[15,16] and DNA,[17−19] causing enzyme inactivation and DNA damage that may promote mutagenesis.[18−21]

Aldehyde dehydrogenases (ALDHs) are involved in the oxidation of these aldehydes into their corresponding acids, which are less toxic and easier to eliminate. Expression of ALDHs is tissue specific. For instance, ALDH1A1 in the cytosol and ALDH2 in the mitochondrial matrix are ubiquitously distributed in the mammalian organism including the liver, brain, heart, and gastrointestinal tract.[22−26] ALDH3A1 is expressed mainly in the gastrointestinal tract and at a low level in the liver.[24] In addition, both ALDH1A1 and ALDH3A1 are expressed at a very high level in the cornea, while ALDH1A1 is also highly expressed in the lens.[24,27]

It has been proposed that ALDH2 has an important role in the elimination of lipid peroxidation byproducts in neurodegenerative diseases, as increased contents of this enzyme have been detected in the brain of Alzheimer patients.[28] In addition, a protective role of ALDH2 in incidents of ischemia-reperfusion of the heart has been proposed.[29,30] Diminution of the cardiac infarct size has been observed after the activation of ALDH2 by ALDA-1 in a rat model[29,31,32] or after the overexpression of the enzyme in a mouse model.[33]

In the eye, the generation of oxidative stress induced by light promotes the production of toxic aldehydes, and a role for ALDH1A1 and ALDH3A1 in the detoxification of these aldehydes has also been proposed.[34,35] Indeed, ALDH3A1 has been involved in multiple antioxidant tasks such as the metabolism of endogenous and exogenous aldehydes, UV-light absorption, production of NADPH, as a ROS scavenger, and structural or chaperone-like activity.[34,36−38]

Most studies on the role of ALDHs in the detoxification of lipid peroxidation products have focused on ALDH2[31] and ALDH5A1,[39] the mitochondrial enzymes, as this organelle is the main source of reactive oxygen species in the cell. Superoxide ions are generated in the mitochondrial matrix mainly at sites I and III of the respiratory chain;[40] site III also releases superoxide to the cytosolic side of the mitochondrial inner membrane.[41−43] Thus, cytosolic ALDHs (ALDH1A1 and ALDH3A1) may also be relevant in detoxifying lipid peroxidation products. In the present work, the kinetics of human ALDH1A1, ALDH2, and ALDH3A1 with lipid peroxidation byproduct were evaluated along with their susceptibility to inactivation by these toxic compounds.

MATERIALS AND METHODS

Caution: *Acrolein is extremely hazardous and should be handled carefully avoiding skin contact and inhalation.*

Chemicals. Acrolein, glycerol, 4-HNE, imidazole, IPTG (Isopropyl β-D-1-thiogalactopyranoside), malondialdehyde, 2-mercaptoethanol, NAD^+, NADH, nickel chloride, propionaldehyde, sodium chloride, sodium pyrophosphate, and trehalose where from Sigma-Aldrich (St. Louis, MO, USA). Enzymes Nde I, Hind III, T4-ligase, and Vent DNA polymerase were form New England Biolabs (Ipswich, MA, USA). Chelating Sepharose fast flow was from GE Healthcare (Piscataway, NJ, USA).

Received: November 30, 2011
Published: February 16, 2012

dx.doi.org/10.1021/tx200518d | Chem. Res. Toxicol. 2012, 25, 722−729

Table 1. Kinetic Parameters of Human ALDHs with Acrolein, 4-HNE, and Malondialdehyde at pH 7.4[a]

	ALDH1A1			ALDH2			ALDH3A1		
	acrolein	HNE	malon	acrolein	HNE	malon	acrolein	HNE	malon
K_m (μM)	5.4 ± 1.0	17 ± 0.9	30 ± 11	1.1 ± 0.3	0.9 ± 0.4	26 ± 4	921 ± 614	46 ± 19	1500 ± 1500
V_{max} (nmol/min*mg)	530 ± 32	120 ± 13	142 ± 30	250 ± 17	99 ± 10	110 ± 28	1205 ± 91	2347 ± 93	264 ± 33
V_{max}/K_m	150 ± 44	68 ± 10	5.4 ± 2.7	243 ± 74	126 ± 40	21 ± 3	1.6 ± 0.7	64 ± 18	0.09 ± 0.09
$K_{i\,sub}$ (μM)	>2 mM			22 ± 4*	55 ± 5**				

[a]Results are the mean ± SD of experiments with three independent enzyme purifications. * and **, $p < 0.01$ compared with Table 2.

Expression and Purification of the Recombinant Enzymes. The plasmids containing the DNA sequences encoding the ALDH1A1 and ALDH3A1 proteins were kindly provided by Dr. Henry Weiner from the Department of Biochemistry, Purdue University. Full-length human ALDH2 cDNA was purchased from ATCC (Manassas, VA, USA) (Cat. No. MGC-1806, GenBank ID: BC002967). The ALDH2 encoding sequence was amplified by PCR, removing the mitochondrial import signal sequence (18 amino acids) and the resulting fragment cloned into the NdeI/HindIII sites of vector pT7−7 (containing an N-terminus His-Tag), using the following primer set: GGGAATTCCATATGTCAGCCGCCGCCACC and GATCCCAAGCTTGGGTTATGAGTTCTTCTGAGG. *E. coli* BL21 (DE3)pLysS strain was transformed with the vectors containing the His-Tag constructs. The proteins were overexpressed as reported previously.[41,42] The cells were harvested by centrifugation at 3000*g* and washed twice with 100 mL of saline solution. Then, cells were resuspended in a buffer containing 50 mM sodium phosphate (pH 7.5), 500 mM sodium chloride, and 20 mM 2-mercaptoethanol and disrupted by sonication at 4 °C; the sonicated cell suspension was centrifuged at 100,000*g* for 30 min. The supernatant containing the recombinant protein was applied to a 20-mL Chelating-Sepharose column packed with nickel and equilibrated with the buffer described above at 4 °C. The column was washed with 50 mM imidazole in the same buffer, and the protein was eluted applying a 100-mL total volume of a 50−500 mM linear imidazole gradient. Fractions with activity were pooled, and ALDH1A1 and ALDH2 were concentrated using Amicon filters of 50,000 kDa molecular weight cutoff, while ALDH3A1 was concentrated using Amicon filters of 30,000 kDa molecular weight cutoff. Then, the enzymes were washed with a buffer containing 100 mM sodium phosphate (pH 7.5), 100 mM sodium chloride, and 0.025% 2-mercaptoethanol to eliminate imidazole. Pure enzymes were concentrated and stored at 4 °C in the presence of 1 M trehalose for short time storage or in the presence of 50% glycerol at −20 °C for longtime storage. Proteins were stable for more than 1 month in trehalose or more than 6 months in the presence of glycerol. The protein concentration was determined with the bicinchoninic acid protein assay kit (Sigma-Aldrich), using bovine serum albumin as standard. The enzyme purities were higher than 95% as judged by SDS−PAGE and densitometry.[40]

Activity Assay. Protein (15−30 μg) were added to a buffer containing 100 mM sodium phosphate (pH 7.4), 100 mM sodium chloride, 20 mM 2-mercaptoethanol, and 1−2 mM NAD^+; activity was also assayed in a buffer containing 100 mM tetrasodium pyrophosphate/HCl pH 9.5 and 20 mM 2-mercaptoethanol. The reaction was initiated by the addition of aldehyde. The ALDH activity was measured in a Shimadzu UV-1800 spectrophotometer, following the increase in absorbance at 340 nm due to the formation of NADH. Stock solutions of aldehydes were routinely calibrated by an enzymatic assay. Data were fitted to the Michaelis−Menten equation or to the Michaelis−Menten equation plus substrate inhibition where required, using the Microcal Origin v. 5.0 software.

Determination of the K_d for NAD^+. ALDH1A1 and ALDH2 (75−150 μg) were incubated in 0.5 mL of assay buffer at pH 7.4 without 2-mercaptoethanol or substrates, in the presence of 3 mM acrolein for 10 min. Then, the protein was diluted/concentrated several times in the same buffer to eliminate the unreacted aldehyde. No remaining activity was found after this treatment. To determine the dissociation constants of the native and aldehyde-treated enzymes for NAD^+, the proteins were titrated with the coenzyme, and the changes in intrinsic fluorescence of the enzymes were followed using an excitation of 287 nm and recording the emission spectrum in a range from 300 to 400 nm with the use of an Aminco-Bowman Series 2 spectrofluorometer. The inner filter effect of NAD^+ was corrected using the following equation:[47,48]

$$F_{corr} = F_{obs} \times \text{antilog}[(OD_{ex} + OD_{em})/2]$$

where F_{corr} is the corrected fluorescence, F_{obs} is the observed fluorescence, OD_{ex} is the absorbance of the solution at a given excitation wavelength, and OD_{em} is the absorbance of the solution at the emission wavelength. Data were fitted to the Michaelis−Menten equation.

Enzyme Inactivation Assays. Protein (15−30 μg) was incubated in 100 μL of activity assay buffer without 2-mercaptoethanol or substrates and in the presence of different concentrations of acrolein for 5 min. Then, the enzyme was diluted 20-fold with buffer, and the remaining activity was evaluated as described above, by adding 1 mM NAD^+ and 1 mM propionaldehyde.

Assay of Enzyme Protection by Substrate. ALDH enzyme 1A1 (150−300 μg) was incubated in 1 mL of 100 mM tetrasodium pyrophosphate/HCl buffer at pH 9.5 without 2-mercaptoethanol, with 30 μM acrolein, in the absence or in the presence of either 1 mM propionaldehyde or 0.2 mM NADH, or both, for the indicated times. Then, a 100 μL aliquot was withdrawn and diluted 20-fold with PPi buffer and the remaining activity measured as indicated above.

Statistical Analysis. The software GraphPad Prism, version 5.01, was used for Student's *t* test analysis of the data as indicated in the legends to figures.

RESULTS AND DISCUSSION

The assessment of the human ALDH1A1, ALDH2, and ALDH3A1 activities with the lipid peroxidation byproducts acrolein, 4-HNE, and malondialdehyde revealed the following catalytic efficiency sequence with acrolein: ALDH2 > ALDH1A1 ≫ ALDH3A1 (Table 1). Interestingly, the V_{max} of ALDH3A1 with acrolein was about 5-fold higher than that of ALDH2, but the K_m of ALDH3A1 for acrolein was about 800-fold higher, and hence, the catalytic efficiency of ALDH3A1 with acrolein was very low. The catalytic efficiency sequence with 4-HNE was ALDH2 > ALDH1A1 = ALDH3A1 (Table 1). Then, it seems possible that ALDH1A1 and ALDH3A1 may actively participate in the detoxification of 4-HNE in the cytosol of the cells, under physiological conditions. In fact, it has been shown in a mouse knockout model of these enzymes that their absence promotes the generation of opacity and cataracts in the eye.[34,35] The catalytic efficiency sequence with malondialdehyde was ALDH2 > ALDH1A1 ≫ ALDH3A1 (Table 1). The lower affinity of ALDH3A1 for aliphatic aldehydes was expected as this enzyme prefers aromatic aldehydes as substrate.[40] Nevertheless, the K_m of ALDH3A1 for 4-HNE was in the micromolar range, suggesting that the long hydrophobic chain of this aldehyde can be more efficiently stabilized in the active site pocket than the short chain of acrolein or malondialdehyde.

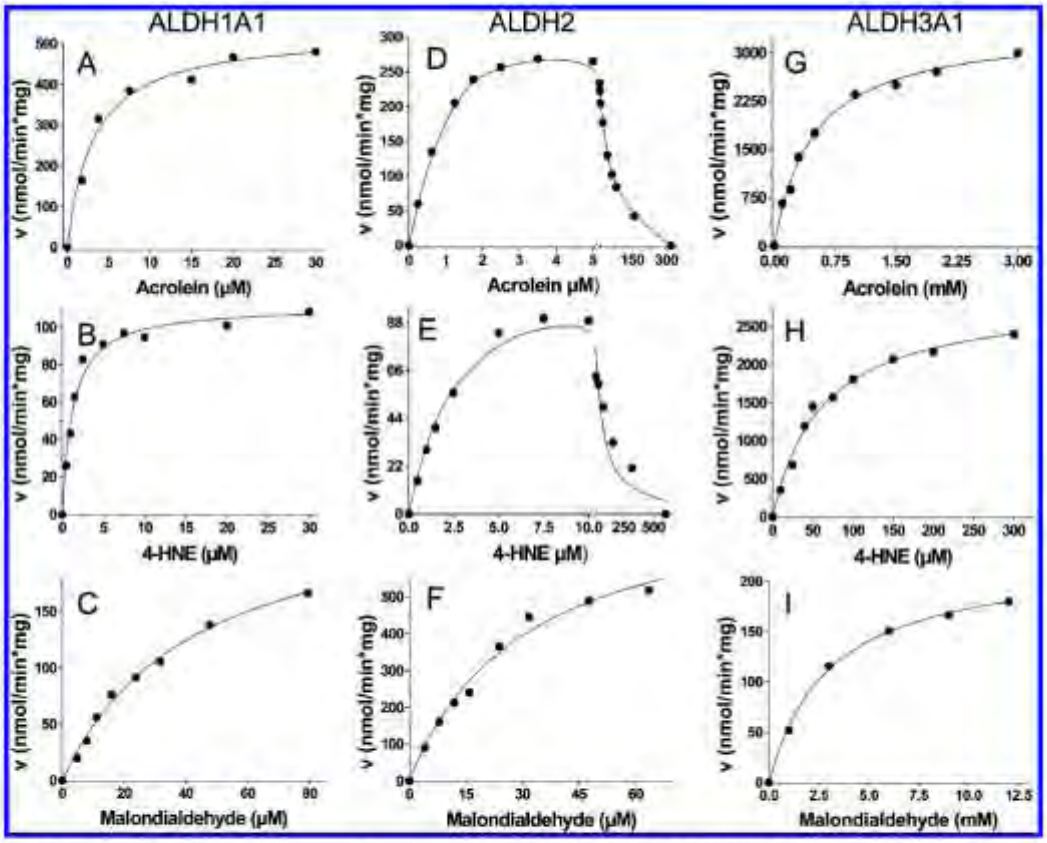

Figure 1. Kinetic profiles of human ALDHs with the lipid peroxidation byproducts at pH 7.4. ALDH1A1, ALDH2, and ALDH3A1 kinetics with acrolein (A, D, and G, respectively), 4-HNE (B, E, and H, respectively), and malondialdehyde (C, F, and I, respectively). Data were fitted to the Michaelis–Menten equation except for panels D and E, which were fitted to the Michaelis–Menten + substrate inhibition equation. Results are representative of experiments with at least 3 independent enzyme purifications.

However, it was observed that ALDH2 was inactivated by both acrolein and 4-HNE; enzyme inactivation occurred at aldehyde concentrations above 10 μM (Figure 1D and E). The irreversible nature of the enzyme inhibition by 4-HNE was further supported by dilution/concentration of the enzyme with fresh buffer and further activity measurement with propionaldehyde and NAD^+. ALDH1A1 was inactivated by acrolein at concentrations above 1 mM (data not shown), while inactivation by 4-HNE was not observed (Figure 1B). Interestingly, ALDH3A1 was not inactivated by any of the aldehydes (Figure 1G–I), even at concentrations as high as 20 mM.

The inactivation of ALDH2 by 4-HNE and of ALDH5A1 by 4-HNE and other lipid peroxidation byproducts has already been documented,[50,51] and it has been proposed that the target of the ALDH2 inactivation is Cys 302. As part of the canonical chemical reaction mechanism, this ALDH-reactive Cys forms an adduct with the aldehyde, which is later released; therefore, this Cys seems unlikely to be the target of HNE inactivation, as the enzyme was able to catalyze the chemical transformation of the aldehyde. Furthermore, ALDH1A1 and ALDH3A1 also possess a reactive cysteine (Cys302 in ALDH1A1 and Cys243 in the equivalent position in ALDH3A1), but these enzymes were insensitive to inactivation by 4-HNE and other aldehydes (Figure 1). Thus, other residues within ALDH2 are most likely targets of the inactivation by these aldehydes.

It has been shown that 4-HNE reacts with nucleophilic amino acids with the following order of preference: Cys > His > Lys, but it does not react with Arg.[52] Therefore, the active site of the three human ALDHs was analyzed for the presence of Cys, His, or Lys residues in an effort to document an explanation of the differences in sensitivity to inactivation by the lipid peroxidation byproducts. To this end, the amino acid sequences of the binding sites for NAD^+ and aldehyde of the three human ALDHs were compared. Analysis of the aldehyde binding site revealed that ALDH2 contains two Cys residues flanking the reactive Cys302 (Figure 2A), which could react with the toxic aldehydes. ALDH1A1 also has a Cys near Cys302, while in the active site of ALDH3A1, only the reactive Cys is present (Figure 2A).

However, it was observed that in the NAD^+ binding site, ALDH2 and ALDH1A1 have a Lys residue, susceptible to be targeted by toxic aldehydes (Figure 2B). In contrast, ALDH3A1 has an Arg residue at the equivalent position (Figure 2B). Considering that the pK_a of Cys and Lys residues is high (pK_a values of 8.18 and 10.53 for the free amino acids, respectively),

dx.doi.org/10.1021/tx2005381 | Chem. Res. Toxicol. 2012, 25, 722–729

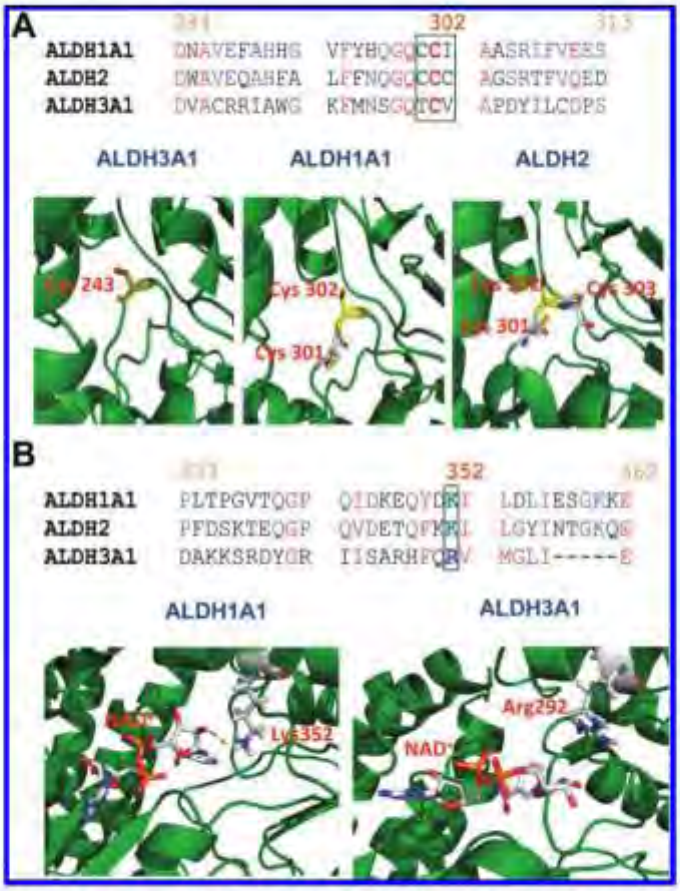

Figure 2. Alignment of the amino acid sequence of the active site of human ALDHs. (A) Sequence of the binding site of aldehyde. Cys302 and adjacent residues are shown in a rectangle in the sequence. A close-up of the binding site of the aldehyde in the structure of the three ALDHs is shown as a cartoon, indicating the Cys residues as sticks, and the reactive Cys (243 in ALDH3A1 and 302 in ALDH1A1 and ALDH2) is indicated at the center. (B) Sequence of the binding site of NAD^+. Residue 352 in the sequence is indicated with a rectangle. A close-up of the binding site of NAD^+ in the structure of ALDH1A1 and ALDH3A1 is shown as a cartoon, and NAD^+ and residue K352 in ALDH1A1 and R292 in ALDH3A1 are shown as sticks.

the effect of the aldehydes on the enzymes was evaluated at pH 9.5 (the optimum for these enzymes) favoring deprotonation, to evaluate whether the enzymes would turn more sensitive to the toxic aldehydes. ALDH2 activity sharply diminished at acrolein concentrations higher than 1 μM (Figure 3D) with a $K_{i\ app}$ value 13 times lower ($p < 0.01$) (Table 2) than that determined at pH 7.4 (Table 1). 4-HNE also inactivated ALDH2 with a higher potency, with the K_i being 3 times lower than that at pH 7.4 ($p < 0.01$) (Figure 3E and Table 2). Under these conditions, ALDH2 was inactivated by malondialdehyde at concentrations above 60 μM (Figure 3F). In turn, the ALDH1A1 activity also became more sensitive to acrolein, starting to inactivate at 60 μM (Figure 3A), while at pH 7.4, this isoform was inactivated by acrolein concentrations higher than 1 mM (Figures 3A and 1A). ALDH1A1 was not inactivated by 4-HNE at either pH (Figure 3B). ALDH3A1 was also insensitive to the toxic aldehydes under alkaline conditions (Figure 3G–I).

ALDH1A1 and ALDH2 sensitivities to acrolein increased with pH (Figure 4). At pH 7.4, ALDH1A1 required more than 300 μM acrolein to reach 50% inactivation, but at pH 9.5, half of the activity was achieved at 70 μM acrolein (Figure 4A). For ALDH2, the effect was more pronounced, as this isoform activity decreased by half with 25 μM acrolein at pH 7.4, whereas only 0.3 μM acrolein was required at pH 9.5 (Figure 4B). The K_m values for the aldehydes did not significantly change for ALDH2 and ALDH1A1 at pH 9.5 versus pH 7.4, but the V_{max} values were higher (Table 2) as this is the pH optimum for these ALDHs. However, ALDH3A1 showed lower V_{max} for the three aldehydes at pH 9.5 (Table 2).

To get further insight on the target for the inactivation by acrolein, experiments of protection by substrate were carried out with ALDH1A1 at pH 9.5. Propionaldehyde partially protected ALDH1A1 from inactivation by acrolein (Figure 4C). To assay the protection of the NAD^+ binding site, NADH was used because in the presence of NAD^+, the enzyme transforms the aldehyde, and it would be difficult to determine if the

dx.doi.org/10.1021/tx2005184 | Chem. Res. Toxicol. 2012, 25, 722–729

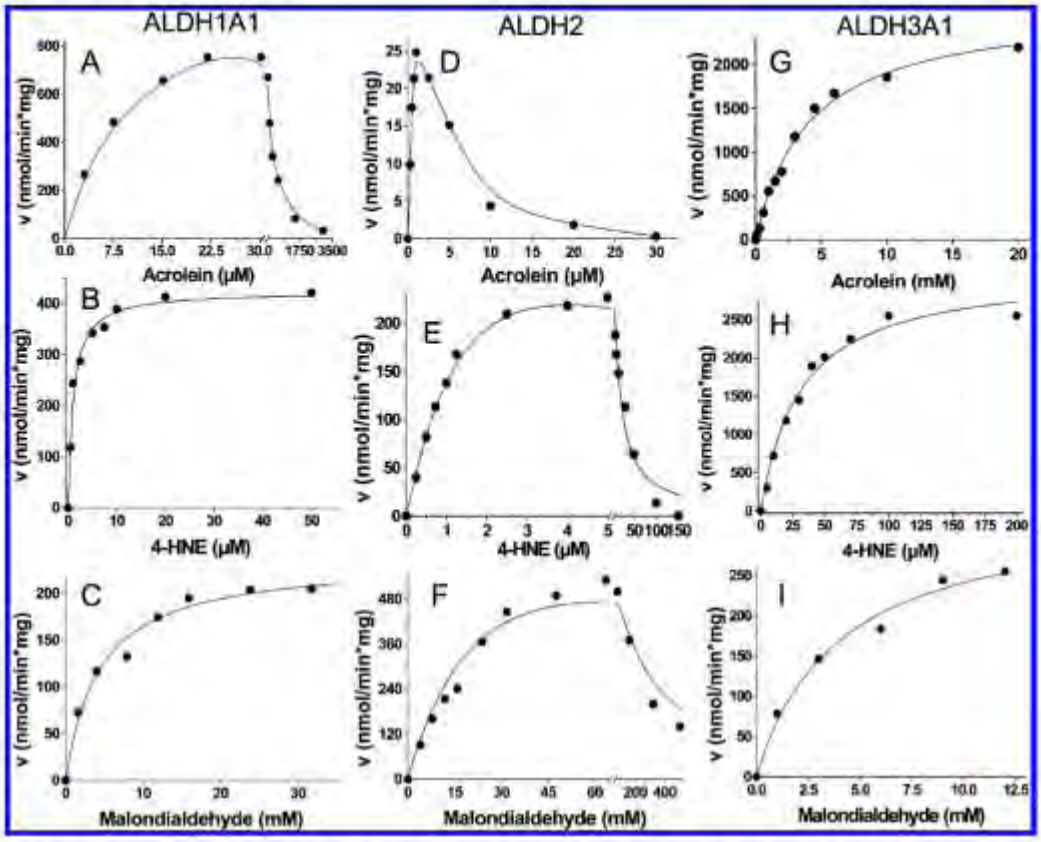

Figure 3. Kinetic profiles of human ALDHs with the lipid peroxidation products at pH 9.5. Kinetics of ALDH1A1, ALDH2, and ALDH3A1 with acrolein, A, D, and G; 4-HNE, B, E, and H, and malonedialdehyde, C, F, and I. Data were fitted to the Michaelis–Menten equation except for panels A, D, E, and F, which were fitted to the Michaelis–Menten + substrate inhibition equation. Results are representative of experiments with at least 3 independent enzyme purifications.

Table 2. Kinetic Parameters of Human ALDHs with Acrolein, 4-HNE, and Malondialdehyde at pH 9.5[a]

	ALDH1A1			ALDH2			ALDH3A1		
	acrolein	HNE	malon	acrolein	HNE	malon	acrolein	HNE	malon
K_m (μM)	8 ± 1.7	1.1 ± 0.3	4.3 ± 0.8	1.2 ± 0.4	4.4 ± 1.4	19 ± 4	2423 ± 738	53 ± 15	2980 ± 370
V_{max} (nmol/min·mg)	866 ± 112	441 ± 51	230 ± 18	89 ± 11	229 ± 34	581 ± 16	1892 ± 289	1457 ± 156	147 ± 42
V_{max}/K_m	100 ± 32	438 ± 133	54 ± 10	72 ± 14	59 ± 13	32 ± 7	0.81 ± 0.16	46 ± 17	0.048 ± 0.006
$K_{i\,app}$ (μM)	122 ± 11			1.6 ± 0.5*	11 ± 2**	198 ± 12			

[a]Results are the mean ± SD of experiments with three independent enzyme purifications. * and **, $p < 0.01$ compared with Table 1.

protection was given by NAD^+, the aldehyde, or the products. It was observed that NADH also protected against inactivation by acrolein and that the protection was higher than that attained with propionaldehyde (Figure 4C). Furthermore, the protection by propionaldehyde and NADH was additive (Figure 4C). These results indicated that the NAD^+ binding site might also be a target for the inactivation of ALDH1A1 and ALDH2 by lipid peroxidation byproducts.

If acrolein reacts with Lys352 in the active sites of ALDH1A1 and ALDH2, the adduct formation would affect the binding of NAD^+. To assay this hypothesis, ALDH1A1 and ALDH2 were exposed to 3 mM acrolein at pH 7.4 for 10 min, and then the K_d of the enzymes for NAD^+ was determined. The titration curves of the tetrameric ALDHs with NAD^+ showed two well-defined components, indicating the presence of two sites with different affinity for NAD^+ (Figure 5A and Table 3). For the enzyme exposed to acrolein, the K_d values increased by about 2-fold ($p < 0.01$) for both NAD^+ sites (Table 3).

Similarly, the ALDH2 K_d values for NAD^+ increased by about two-3-fold ($p < 0.01$) after the formation of the adduct with acrolein (Figure 5B and Table 3). These results supported the proposal that the lipid peroxidation byproducts also react with the NAD^+ binding site in ALDH1A1 and ALDH2. The presence of two sites of high and low affinities for NAD^+ in the tetrameric enzymes may be related to the half site reactivity reported for these enzymes.[53,54] It is worth emphasizing that

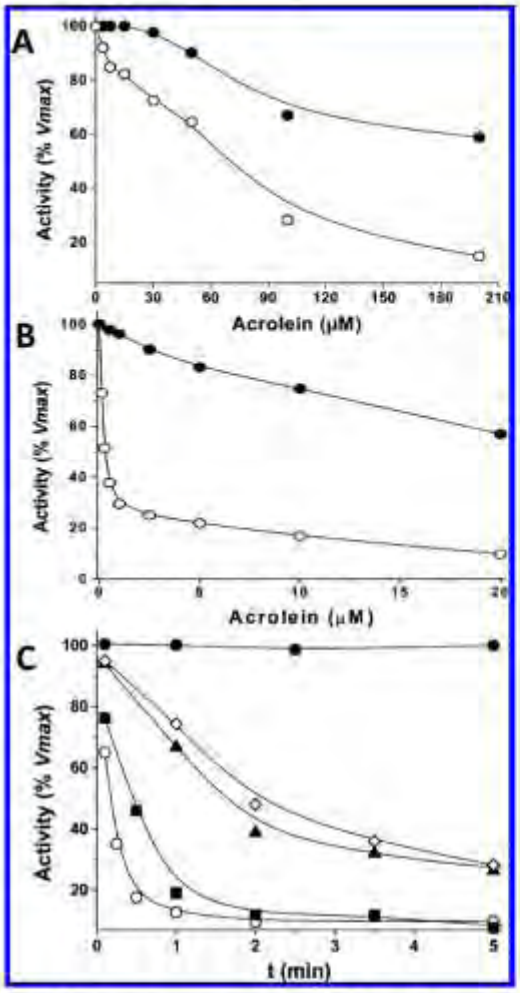

Figure 4. Inactivation of human ALDH1A1 and ALDH2 by acrolein at different pH and protection of the inactivation by substrates. (A) Profile of the inactivation of ALDH1A1 at pH 7.4 (●) and pH 9.5 (○). (B) Profile of the inactivation of ALDH2 at pH 7.4 (●) and pH 9.5 (○). Experiments were conducted as indicated in the Materials and Methods section. (C) Protection by substrates against the inactivation of ALDH1A1 by acrolein. Experiments were conducted as indicated in the Materials and Methods section. ●, control of the incubation of ALDH1A1 in PPi buffer pH 9.5; ○, ALDH1A1 + 30 μM acrolein; ■, ALDH1A1 + 30 μM acrolein + 1 mM propionaldehyde; ▲, ALDH1A1 + 30 μM acrolein + 200 μM NADH; ◇, ALDH1A1 + 30 μM acrolein + 200 μM NADH + 1 mM propionaldehyde. Figures are representative of at least three experiments with different enzyme preparations.

only slight differences in the conformation of the NAD^+ binding site have been observed among the four active sites in the tetramer crystal structure.[55] This article shows the first kinetic data supporting the proposal of two families of active sites in ALDHs with different affinity for NAD^+.

The adduction of the toxic aldehydes with residues Cys301 and Cys303 in ALDH2, Cys301 in ALDH1A1, and Lys352 in both enzymes may inactivate the enzyme by inducing a steric

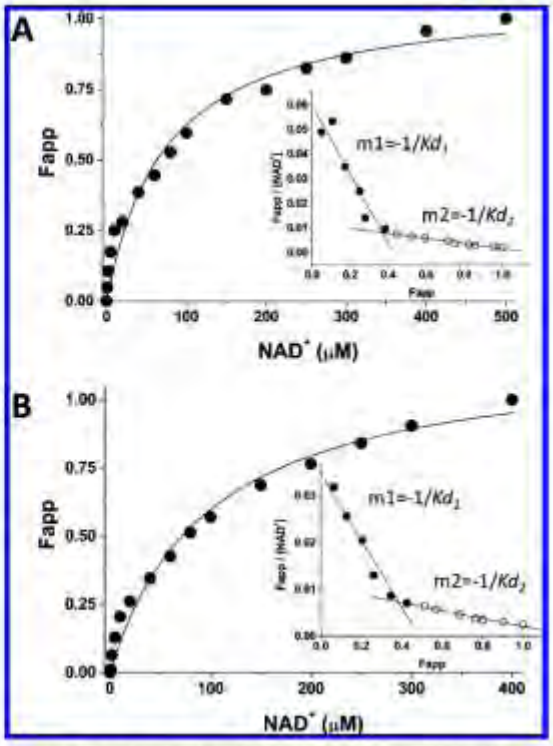

Figure 5. Binding studies of NAD^+ with native ALDH1A1 and acrolein adduct of ALDH1A1. The same experiments were also carried out with ALDH2. Kinetics of binding of native ALDH1A1 (A) and ALDH1A1-acrolein adduct (B) with NAD^+. Solid lines indicate the fitting of the data to the Michaelis–Menten equation to highlight the presence of two components. Insets show the Scatchard plots of the data of A and B, respectively, indicating two well-defined components. Results are representative of at least three experiments with independent enzyme purifications. K_d values determined from the Scatchard analyses of these experiments are shown in Table 3.

Table 3. K_d Values of the ALDHs for NAD^{+a}

	ALDH1A1	ALDH1A1-acrolein	ALDH2	ALDH2-acrolein
K_{d1}	7.0 ± 1.7[b]	19 ± 1[b]	12 ± 5[b]	34 ± 7[b]
K_{d2}	67 ± 5[b,c]	320 ± 16[b,c]	97 ± 14[b]	173 ± 81[b]

[a]Data were obtained from the analysis of the Scatchard plots of the type of experiments shown in Figure 5. Results are the mean ± SD of experiments with four different enzyme purifications. [b], [c], [f], and [h], $p < 0.01$

effect and thus interfering with the correct binding of the substrates to the active site or disrupting protein–substrate interactions. To definitively establish a role for these amino acids as targets of the inactivation of the tetrameric ALDHs by toxic aldehydes, site directed mutagenesis of these residues would be helpful, and is currently in progress in our laboratory.

CONCLUSIONS

Although ALDH2 showed the highest catalytic efficiency toward the toxic aldehydes assayed, this enzyme also was the most sensitive to inactivation by these toxics. Thus, ALDH1A1 and ALDH3A1, with lower activity but with the advantage of

dx.doi.org/10.1021/tx8001941 | Chem. Res. Toxicol. 2008, 21, 722–729

being insensitive to inactivation by interaction with these compounds, may actively participate in the detoxification of these toxic aldehydes in the cell under physiological conditions.

AUTHOR INFORMATION

Corresponding Author

*Departamento de Bioquímica, Instituto Nacional de Cardiología, Juan Badiano No. 1, Seccion XVI, Tlalpan, México D.F. 14080, México. E-mails: rodjos@cardiologia.org.mx; rzjs@yahoo.com.

Funding

This work was supported in part by CONACyT-México grants No. 78775 and 102926.

Notes

The authors declare no competing financial interest.

ABBREVIATIONS

ALDHs, aldehyde dehydrogenases; ALDH1A1, human aldehyde dehydrogenase 1A1; ALDH2, human aldehyde dehydrogenase 2; ALDH3A1, human aldehyde dehydrogenase 3A1; ALDH5A1, succinate-semialdehyde dehydrogenase; 4-HNE, 4-hydroxy-2-nonenal; ALDA-1, ALDH2 activator *N*-(1,3-benzodioxol-5-ylmethyl)-2,6-dichlorobenzamide; F_{obs}, observed fluorescence; F_{corr}, corrected fluorescence; OD_{em}, absorbance of the solution at emission wavelength; OD_{ex}, absorbance of the solution at excitation wavelength; IPTG, (isopropyl β-D-1-thiogalactopyranoside); PCR, polymerase chain reaction.

REFERENCES

(1) Leonarduzzi, G., Chiarpotto, E., Biasi, F., and Poli, G. (2005) 4-Hydroxynonenal and cholesterol oxidation products in atherosclerosis. *Mol. Nutr. Food Res. 49*, 1044–1049.

(2) Poli, G., Sottero, B., Gargiulo, S., and Leonarduzzi, G. (2009) Cholesterol oxidation products in the vascular remodeling due to atherosclerosis. *Mol. Asp. Med. 30*, 180–189.

(3) Srivastava, S., Sithu, S. D., Vladykovskaya, E., Haberzettl, P., Hoetker, D. J., Siddiqui, M. A., Conklin, D. J., D'Souza, S. E., and Bhatnagar, A. (2011) Oral exposure to acrolein exacerbates atherosclerosis in apoE null mice. *Atherosclerosis 215*, 301–308.

(4) Cantero, A. V., Portero-Otin, M., Ayala, V., Auge, N., Sanson, M., Elbaz, M., Thiers, J. C., Pamplona, R., Salvayre, R., and Negre-Salvayre, A. (2007) Methylglyoxal induces advanced glycation end product (AGEs) formation and dysfunction of PDGF receptor-beta: implications for diabetic atherosclerosis. *FASEB J. 21*, 3096–3106.

(5) Yokoyama, A., and Omori, T. (2003) Genetic polymorphisms of alcohol and aldehyde dehydrogenases and risk for esophageal and head and neck cancers. *Jpn. J. Clin. Oncol. 33*, 111–121.

(6) Tinahones, F. J., Murri-Pierri, M., Garrido-Sanchez, L., Garcia-Almeida, J. M., Garcia-Serrano, S., Garcia-Arnes, J., and Garcia-Fuentes, E. (2008) Oxidative stress in severely obese persons is greater in those with insulin resistance. *Obesity 17*, 240–246.

(7) Papazafiropoulou, A., Sklirosb, E., Ioannidisa, A., Apostolou, O., Stamatakis, P., and Sotiropoulos, A. (2011) Serum c, zinc and selenium levels in subjects with and without metabolic syndrome. *J. Endocrinol. Metab. 1*, 92–93.

(8) Sultana, R., and Butterfield, D. A. (2009) Proteomics identification of carbonylated and HNE-bound brain proteins in Alzheimer's disease. *Methods Mol. Biol. 566*, 123–35.

(9) Reed, T. T., Pierce, W. M., Markesbery, W. R., and Butterfield, D. A. (2009) Proteomic identification of HNE-bound proteins in early Alzheimer disease: Insights into the role of lipid peroxidation in the progression of AD. *Brain Res. 1274*, 66–76.

(10) Singh, M., Nam, D. T., Arseneault, M., and Ramassamy, C. (2010) Role of by-products of lipid oxidation in Alzheimer's disease brain: a focus on acrolein. *J. Alzheimers Dis. 21*, 741–56.

(11) Nam, D. T., Arseneault, M., Murthy, V., and Ramassamy, C. (2010) Potential role of acrolein in neurodegeneration and in Alzheimer's disease. *Curr. Mol. Pharmacol. 3*, 66–78.

(12) Burke, W. J. (2003) 3,4-Dihydroxyphenylacetaldehyde: a potential target for neuroprotective therapy in Parkinson's disease. *Curr. Drug. Targets CNS Neurol. Disord. 2*, 143–148.

(13) Burke, W. J., Li, S. W., Williams, E. A., Nonneman, R., and Zahm, D. S. (2003) 3,4-Dihydroxyphenylacetaldehyde is the toxic dopamine metabolite in vivo: implications for Parkinson's disease pathogenesis. *Brain Res. 989*, 205–213.

(14) Koch, M., Mostert, J., Arutjunyan, A. V., Stepanov, M., Teelken, A., Heersema, D., and De Keyser, J. (2007) Plasma lipid peroxidation and progression of disability in multiple sclerosis. *Eur. J. Neurol. 14*, 529–33.

(15) Marquez-Quiñones, A., Cipak, A., Zarkovic, K., Fattel-Fazenda, S., Villa-Treviño, S., Waeg, G., Zarkovic, N., and Guéraud, F. (2010) HNE-protein adducts formation in different pre-carcinogenic stages of hepatitis in LEC rats. *Free Radical Res. 44*, 119–27.

(16) Cai, J., Bhatnagar, A., and Pierce, M. P., Jr (2009) Protein modification by acrolein: formation and stability of cysteine adducts. *Chem. Res. Toxicol. 22*, 708–716.

(17) Falletti, O., and Douki, T. (2008) Low glutathione level favors formation of DNA adducts to 4-hydroxy-2(E)-nonenal, a major lipid peroxidation product. *Chem. Res. Toxicol. 21*, 2097–2105.

(18) Wang, H.-T., Zhang, S., Hu, Y., and Tang, M.-S. (2009) Mutagenicity and sequence specificity of acrolein-DNA adducts. *Chem. Res. Toxicol. 22*, 511–517.

(19) Liu, X. Y., Zhu, M. X., and Xie, J. P. (2010) Mutagenicity of acrolein and acrolein-induced DNA adducts. *Toxicol. Mech. Methods 20*, 36–44.

(20) Feng, Z., Hu, W., Hu, Y., and Tang, M. S. (2006) Acrolein is a major cigarette-related lung cancer agent: Preferential binding at p53 mutational hotspots and inhibition of DNA repair. *Proc. Natl. Acad. Sci. U.S.A. 103*, 15404–15409.

(21) Chung, F. L., Pan, J., Choudhary, S., Roy, R., Hu, W., and Tang, M. S. (2003) Formation of trans-4-hydroxy-2-nonenal- and other enal-derived cyclic DNA adducts from omega-3 and omega-6 polyunsaturated fatty acids and their roles in DNA repair and human p53 gene mutation. *Mutat. Res. 531*, 25–36.

(22) Yoshida, A., Rzhetsky, A., Hsu, L. C., and Chang, C. (1998) Human aldehyde dehydrogenase gene family. *Eur. J. Biochem. 251*, 5492557.

(23) Niederreither, K., Fraulob, V., Garnier, J.-M., Chambon, P., and Dollé, P. (2002) Differential expression of retinoic acid-synthesizing (RALDH) enzymes during fetal development and organ differentiation in the mouse. *Mech. Dev. 110*, 165–171.

(24) King, G., and Holmes, R. (1998) Human ocular aldehyde dehydrogenase isozymes: distribution and properties as major soluble proteins in cornea and lens. *J. Exp. Zool. 282*, 12–17.

(25) Harada S., Agarwal, D. P., H. W. Goedde: Isozyme variations in acetaldehyde dehydrogenase (e.c.1.2.1.3) in human tissues. *Hum. Genet. 44*, 181-185.

(26) Stewart, M. J., Malek, K., and Crabb, D. W. (1996) Distribution of messenger RNAs for aldehyde dehydrogenase 1, aldehyde dehydrogenase 2, and aldehyde dehydrogenase 5 in human tissues. *J. Invest. Med. 44*, 42–46.

(27) Boesch, J. S., Lee, C., and Lindahl, R. G. (1996) Constitutive expression of class 3 aldehyde dehydrogenase in cultured rat corneal epithelium. *J. Biol. Chem. 271*, 5150–5157.

(28) Pickle, M. J., Olson, S. J., Markesbery, W. R., and Montine, T. J. (2001) Expression and activities of aldo-Keto oxidoreductases in Alzheimer disease. *J. Neuropathol. Exp. Neurol. 60*, 686–695.

(29) Chen, C. H., Budas, G. R., Churchill, E. N., Disatnik, M. H., Hurley, T. D., and Mochly-Rosen, D. (2008) Activation of aldehyde dehydrogenase-2 reduces ischemic damage to the heart. *Science 321*, 1493–5.

(30) Wang, J., Wang, H., Hao, P., Xue, L., Wei, S., Zhang, Y., and Chen, Y. (2011) Inhibition of aldehyde dehydrogenase 2 by oxidative

stress is associated with cardiac dysfunction in diabetic rats. *Mol. Med. 17*, 172–9.
(31) Chen, H. H., Sun, L., and Mochly-Rosen, D. (2010) Mitochondrial aldehyde dehydrogenase and cardiac diseases. *Cardiovasc. Res. 88*, 51–57.
(32) Grant, R., Badas, G. R., Disatnik, M. H., Chen, C. H., and Mochly-Rosen, D. (2010) Activation of aldehyde dehydrogenase 2 (ALDH2) confers cardioprotection in protein kinase C epsilon (PKCvarepsilon) knockout mice. *J. Mol. Cell. Cardiol. 48*, 757–764.
(33) Ma, H., Guo, R., Yu, L., Zhang, Y., and Ren, J. (2011) Aldehyde dehydrogenase 2 (ALDH2) rescues myocardial ischaemia/reperfusion injury: role of autophagy paradox and toxic aldehyde. *Eur. Heart J. 32*, 1025–1038.
(34) Choudhary, S., Xiao, T., Vergara, L. A., Srivastava, S., Nees, D., Piatigorsky, J., and Ansari, N. H. (2005) Role of aldehyde dehydrogenase isozymes in the defense of rat lens and human lens epithelial cells against oxidative stress. *Invest. Ophthalmol. Vis. Sci. 46*, 259–267.
(35) Xiao, T., Shoeb, M., Siddiqui, M. S., Zhang, M., Ramana, K. V., Srivastava, S. K., Vasiliou, V., and Ansari, N. H. (2009) Molecular cloning and oxidative modification of human lens ALDH1A1: implication in impaired detoxification of lipid aldehydes. *J. Toxicol. Environ. Health, Part A 72*, 377–384.
(36) Lassen, N., Bateman, J. B., Estey, T., Kuszak, J. R., Nees, D. W., Piatigorsky, J., Duester, G., Day, B. J., Huang, J., Hines, L. M., and Vasiliou, V. (2009) Multiple and additive functions of ALDH3A1 and ALDH1A1: cataract phenotype and ocular oxidative damage in Aldh3a1(−/−)/Aldh1a1(−/−) knock-out mice. *J. Biol. Chem. 282*, 25668–25676.
(37) Estey, T., Piatigorsky, J., Lassen, N., and Vasiliou, V. (2007) ALDH3A1: a corneal Crystallin with diverse functions. *Exp. Eye Res. 84*, 3–12.
(38) Estey, T., Cantore, M., Weston, P. A., Carpenter, J. F., Petrash, J. M., and Vasiliou, V. (2007) Mechanisms involved in the protection of UV-induced protein inactivation by the corneal Crystallin ALDH3A1. *J. Biol. Chem. 282*, 4382–4392.
(39) Murphy, T. C., Amarnath, V., Gibson, K. M., and Picklo, M. J. (2003) Oxidation of 4-hydroxy-2-nonenal by succinic semialdehyde dehydrogenase (ALDH5A). *J. Neurochem. 86*, 298–305.
(40) Cadenas, E., Boveris, A., Ragan, C. I., and Stoppani, A. O. M. (1977) Production of superoxide radicals and hydrogen peroxide by NADH-ubiquinone reductase and ubiquinol-cytochrome *c* reductase from beef-heart mitochondria. *Arch. Biochem. Biophys. 180*, 248–257.
(41) Han, D., Williams, E., and Cadenas, E. (2001) Mitochondrial respiratory chain-dependent generation of superoxide anion and its release into the intermembrane space. *Biochem. J. 353*, 411–416.
(42) St-Pierre, J., Buckingham, J. A., Roebuck, S. J., and Brand, M. D. (2002) Topology of superoxide production from different sites in the mitochondrial electron transport chain. *J. Biol. Chem. 277*, 44784–44790.
(43) Muller, F. L., Liu, Y., and Van Remmen, H. (2004) Complex III releases superoxide to both sides of the inner mitochondrial membrane. *J. Biol. Chem. 279*, 49064–49073.
(44) Rodriguez-Zavala, J. S., and Weiner, H. (2002) Structural aspects of aldehyde dehydrogenase that influence dimer-tetramer formation. *Biochemistry 41*, 8229–8237.
(45) Rodriguez-Zavala, J. S. (2008) Enhancement of coenzyme binding by a single point mutation at the coenzyme binding domain of *E. coli* lactaldehyde dehydrogenase. *Protein Sci. 17*, 563–570.
(46) Laemmli, U. K. (1970) Cleavage of structural proteins during the assembly of the head of bacteriophage T4. *Nature 227*, 680–685.
(47) Velasco-García, R., González-Segura, L., and Muñoz-Clares, R. A. (2000) Steady-state kinetic mechanism of the $NADP^+$- and NAD^+-dependent reactions catalysed by betaine aldehyde dehydrogenase from *Pseudomonas aeruginosa*. *Biochem. J. 352*, 675–683.
(48) Lakowicz, J. R. (1983) *Principles of Fluorescence Spectroscopy*, p 44, Plenum Press, New York.
(49) Santisteban, I., Povey, S., West, L. F., Parrington, J. M., and Hopkinson, D. A. (1985) Chromosome assignment, biochemical and immunological studies on a human aldehyde dehydrogenase. ALDH3. *Ann. Hum. Genet. 49*, 87–100.
(50) Doorn, J. A., Hurley, T. D., and Petersen, D. R. (2006) Inhibition of human mitochondrial aldehyde dehydrogenase by 4-hydroxynon-2-enal and 4-oxonon-2-enal. *Chem. Res. Toxicol. 19*, 102–110.
(51) Nguyen, E., and Picklo, M.J.Sr. (2003) Inhibition of succinic semialdehyde dehydrogenase activity by alkenal products of lipid peroxidation. *Biochim. Biophys. Acta 1637*, 107–112.
(52) Doorn, J. A., and Petersen, D. R. (2002) Covalent modification of amino acid nucleophiles by the lipid peroxidation products 4-hydroxy-2-nonenal and 4-oxo-2-nonenal. *Chem. Res. Toxicol. 15*, 1445–50.
(53) Takahashi, K., and Weiner, H. (1980) Magnesium stimulation of catalytic activity of horse liver aldehyde dehydrogenase. Changes in molecular weight and catalytic sites. *J. Biol. Chem. 255*, 8206–8209.
(54) Zhou, J., and Weiner, H. (2000) Basis for half-of-the-site reactivity and the dominance of the E487 oriental subunit over the E487 Subunit in heterotetrameric human liver mitochondrial aldehyde dehydrogenase. *Biochemistry 39*, 12019–12024.
(55) Steinmetz, C. G., Xie, P., Weiner, H., and Hurley, T. D. (1997) Structure of mitochondrial aldehyde dehydrogenase: the genetic component of ethanol aversion. *Structure 5*, 701–11.

10.2 Participación del residuo R292 del sitio de unión del NAD^+ en ALDH3A1 en la protección frente a productos de la lipoperoxidación *(Datos no publicados)*.

La subfamilia de las ALDH3 está constituida por enzimas que tienen un rol específico en el metabolismo de los productos de la peroxidación de lípidos, tales como alquenales de cadena mediana e hidroxialquenales y se ha encontrado una alta actividad de ésta enzima en la cornea, el estomago, el hígado, el tracto urinario y en algunos tipos de cáncer [4]. En el artículo mostrado previamente, se reportó que el orden de susceptibilidad por aldehídos lipídicos en las ALDHs es ALDH2>>ALDH1>ALDH3 y se sugirió a la K292 como posible blanco de inactivación de las ALDHs tetraméricas por productos de la lipoperoxidación; pues al realizar un alineamiento de los aminoácidos involucrados en la unión y estabilización sitio de unión del NAD^+ entre las diferentes isoformas, se observó un residuo de arginina presente en la posición 292 en ALDH3A1 y no en ALDH1A1 y ALDH2; estas en la posición equivalente muestran un residuo de lisina. Por lo anterior y como continuación de ese trabajo, se decidió generar la mutante ALDH3-R292K con el fin de dilucidar la participación de este aminoácido en la protección o susceptibilidad a aldehídos tóxicos. Una vez generada esta mutante se clonó, sobre-expresó y purificó.

Los parámetros cinéticos de ALDH3A1-R292K fueron evaluados con el fin de detectar alguna diferencia con respecto a ALDH3A1 silvestre. Se determinó un incremento de 2 veces en la *Km* y una disminución de aproximadamente 6 veces en la *Kd* de la ALDH3A1-R292K por NAD^+. En cuanto al NADH, se encontró una

disminución en la afinidad por el producto de 5 veces para la mutante al ser comparada con la enzima nativa, contrario a lo que se esperaba, pues hubo un incremento en la afinidad por el NAD^+. Esto último indicaría que efectivamente hubo una modificación conformacional en el sitio de unión por el NAD^+ producto de la mutación realizada.

Lo siguiente fue determinar la participación y susceptibilidad de este sitio en la inactivación por acroleína. Pues se ha reportado que, los aldehídos como acroleína y 4-HNE reaccionan preferencialmente con residuos de cisteína, lisina e histidina y no reaccionan con residuos de arginina [Doorn], entonces se esperaba que la acroleína se uniera a la lisina de la proteína mutante y con ello afectara la unión del NAD^+ en su sitio, si es que este, participa en la inactivación an te este tipo de compuestos. Para este fin se formaron aductos enzima-acroleína, incubando 10 minutos a la enzima en presencia de acroleína (3mM), para posteriormente evaluar la *Kd* por NAD^+ en estas condiciones. Los resultados se pueden observar en la siguiente tabla:

Tabla 4. Efecto de la formación de aductos con acroleína sobre la afinidad de las enzimas por el NAD^+.

	Km NAD+	**Kd_{NAD+} en ausencia de acroleína**	**Kd_{NAD+} en presencia de acroleína**
ALDH3A1	29 ± 7	490	[1]25 [2]388
ALDH3-R292K	71 ± 10	[1]84 [2]689	[1]18 [2]338

Valores de Km y Kd en μM, 1 y 2 indican la presencia de dos componentes en el perfil cinético.

Al analizarse los resultados obtenidos a este respecto, se observó un incremento en el valor de *Kd* por NAD^+ para la enzima mutante al compararse con la enzima silvestre, contrario a lo que se esperaba (Tabla 4). Sin embargo, estos son datos preliminares. Por otro lado, se evidenciaron dos componentes en el perfil cinético tanto de la enzima silvestre como de la enzima mutante; para esta última los dos componentes se observaron tanto en ausencia como en presencia de acroleína. Estos datos, pueden ser una evidencia de que la ALDH3A1 trabaja de manera activa con sus dos sitios, aunque cada sitio posee diferente afinidad por el sustrato. De manera alterna, se evaluó la afinidad por el benzaldehído a pH 7.4 y 9.5 (Tabla 5 y 5.1) y no se encontró una diferencia significativa entre ALDH3A1 y ALDH3A1-R292K; lo cual se esperaba, puesto que la mutación fue realizada en el sitio de unión del NAD^+. Sin embargo; se observaron diferencias importantes en la afinidad por acroleína y por 4-HNE (Tabla 5 y 5.1), lo cual afirma que tanto el sitio de unión por NAD^+, así como el sitio de unión del aldehído, mantienen una importante comunicación y que al ser modificado uno solo de los aminoácidos involucrados en la unión de uno de los sustratos, este puede ser capaz de afectar el reacomodo de los demás residuos en el *"core"* catalítico y por ende modificar la especificidad por ambos sustratos.

Tabla 5. Especificidad de las enzimas por diferentes aldehídos.

	ALDH3			**H3R292K**		
	Benzaldehído	**Acroleína**	**HNE**	**Benzaldehído**	**Acroleína**	**HNE**
Km (mM)	0.2 ± 0.02	1.27±0.27	0.046±0.019	0.442 ± 0.085	1.2	0.068
Vmax	21.2 ± 6.2	1.3±0.25	2.34±0.093	1.2 ± 0.255	0.8	1.2

(μmol/min/mg)						
Vm/Km ***(ml*min^{-1}mg^{-1})***	105 ± 23	1.03 ± 0.14	50	3	0.66	17

****Experimentos realñizados a pH 7.4***

Tabla 5.1 Especificidad por diferentes aldehídos.

	ALDH3A1			**ALDH3R292K**		
	Benzaldehído	**Acroleína**	**4-HNE**	**Benzaldehído**	**Acroleína**	**4-HNE**
Km ***(mM)***	0.17 ± 0.04	2.47±0.21	0.035±0.015	0.489±0.137	a) 0.0025 b) 0.042	0.068
Vmax ***(μmol/min/mg)***	12 ± 1.3	2.1±0.4	1.5+0.15	5.77±0.24	a) 0.0113 b) 0.0508	1.6
Vm/Km ***(ml*min^{-1}mg^{-1})***	71 ± 13	0.84±0.09	42	13±4	a) 4.5 b) 1.2	23

****Experimentos realizados a pH 9.5. a y b indican la presencia de dos componentes en el perfil cinético.***

Como se puede observar en las tablas anteriores, a pH de 9.5 la afinidad por acroleína en el caso de ALDH3A1-R292K se incrementó prácticamente 60 veces con respecto a ALDH3A1 lo cual se ve reflejado en un incremento de la eficiencia catalítica por ese sustrato. En cuanto al 4-HNE, no se observaron cambios importantes en la afinidad,, incluso pareciera ser menos eficiente catalíticamente en presencia de este sustrato. Un hallazgo interesante a este respecto, es que, cuando se evaluó el comportamiento cinético de la mutante en presencia de la acroleína se observaron 2 componentes, uno con una *Km* de 2 μM y otro con *Km* de 30 μM, indicando con esto la presencia de ***dos sitios activos*** en la enzima con diferente afinidad, mientras que para ALDH3 se observa un solo componente con valor de *Km* de 2.4 mM (Tablas 5 y 5.1). Esto podría ser un indicio de que ALDH3

en realidad tiene reactividad de todos los sitios, pero quizá no se revelan dos componentes en su cinética pues ambos poseen la misma afinidad.

Una vez determinados los parámetros cinéticos por acroleína y 4-HNE para la enzima silvestre y la enzima mutante; se realizaron experimentos de inactivación. Este análisis se llevó a cabo en presencia y ausencia de los sustratos (NADH y benzaldehído). Como se puede observar, ALDH3-R292K (Figura 15B y Figura 15D) es menos resistente que ALDH3A1 (Figura 15A y Figura 15C) al efecto de estos aldehídos tóxicos. Aunado a estos datos, el NADH protege contra el efecto de inactivación de la acroleína en la mutante, resaltando la importancia del residuo de arginina 292 y del sitio de unión del NAD^+ en la protección de ALDH3A1. El efecto ejercido por el NADH no fue el mismo en presencia de 4-HNE, sugiriendo que este aldehído interactúa con otros residuos probablemente en el sitio de unión del aldehído.

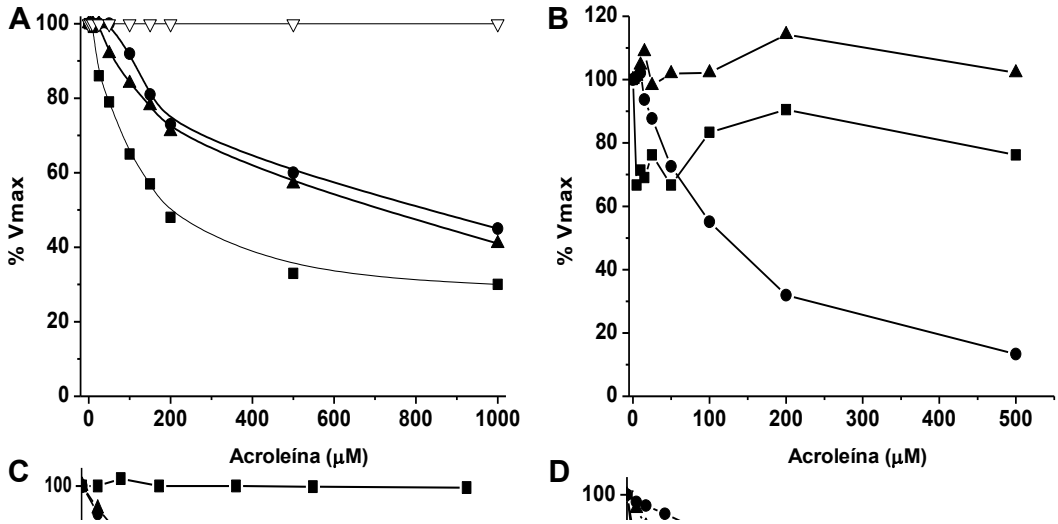

Figura 15. Inactivación por acroleína y HNE. A y C, ALDH3. B y D, ALDH3-R292K. ●, Control; ■, NADH (1 mM); ▲, Benzaldehído (1 mM); ▽, Benzaldehído (1 mM) + NADH (1 mM).

En resumen, estos resultados indican que el residuo R292 en ALDH3A1 es clave en el mecanismo de protección contra la inactivación por productos de la lipoperoxidación**.**

Con la finalidad de evaluar alguna modificación en el paso limitante de la reacción entre la enzima silvestre y la enzima mutante, se determinó el *"burst"* antes del estado estacionario. Al realizar dicha determinación, este fenómeno no fue observado en la mutante, tal y como ocurre en el caso de la enzima nativa. Para

completar este análisis, también se evaluó la actividad enzimática de ambas enzimas en presencia y ausencia de [^{2}H]-benzaldehído, pues al ser el paso limitante de la reacción la transferencia del hidruro en ALDH3A1, se espera que en presencia de [^{2}H]-benzaldehído la actividad enzimática disminuya por el efecto isotópico primario que ejerce dicho compuesto; pues el hecho de poseer el doble de la masa atómica en el hidrógeno hace que la reacción se lleve a cabo con mayor dificultad y ésta sea más lenta. Como se puede observar en la figura 16, no hubo diferencias significativas en los resultados de actividad obtenidos entre ALDH3A1 y ALDH3A1-R292K, lo cual nos llevó a concluir que no se modificó la etapa limitante de la reacción en la enzima mutante.

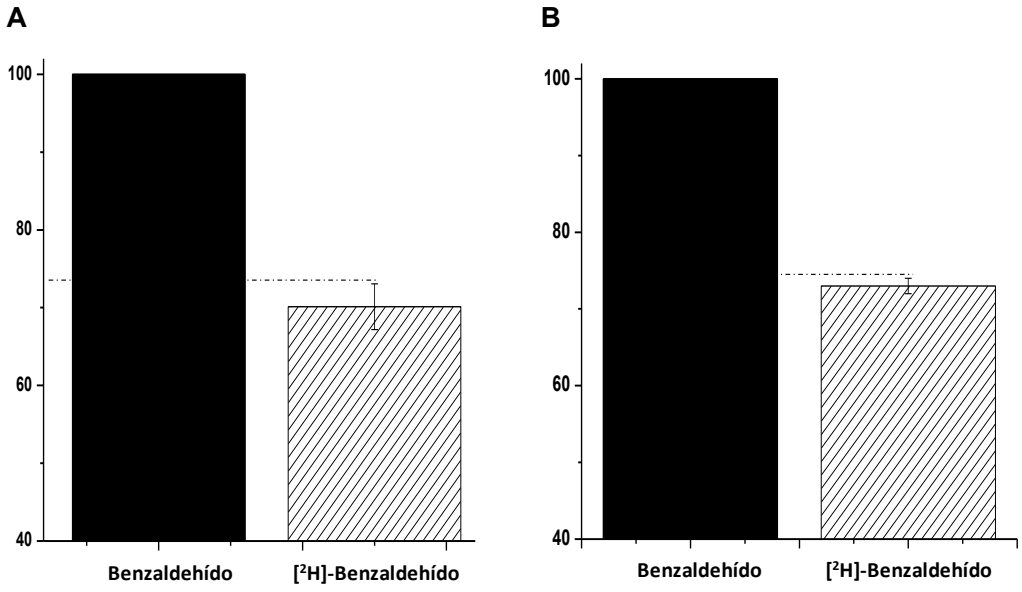

Figura 16. Efecto del [^{2}H]-Benzaldehído sobre la actividad de A) ALDH3 y B) ALDH3-R292K.

Capítulo 11. Otras publicaciones.

Las aldehído deshidrogenasas no sólo tienen un rol relevante en mamíferos, también son un importante mecanismo de detoxificación de aldehídos en diferentes organismos unicelulares; a continuación se presenta la relevancia y participación de estas enzimas en el protista de vida libre *Euglena gracilis* el cual ha sido estudiado ampliamente por su plasticidad metabólica y se ha propuesto como un posible biorremediador de aguas contaminadas por su capacidad de acumular diferentes metales pesados [Mendoza-Cózatl et al 2004, Rodríguez-Zavala et al. 2007]]. En el trabajo que se presenta a continuación, se muestra la caracterización y localización de diferentes enzimas involucradas con el metabolismo del etanol así como la repercusión de estas en dicho organismo.

J Bioenerg Biomembr (2011) 43:65–73
DOI 10.1007/s10863-011-9271-y

Novel mitochondrial alcohol metabolizing enzymes of *Euglena gracilis*

Helena Vivoli-Sánchez · Ricardo Jasso-Chávez · Elizabeth Lira-Silva · Rafael Moreno-Sánchez · José S. Rodríguez-Zavala

Received: 2 June 2011 / Accepted: 17 June 2011 / Published online: 28 July 2011

Abstract Ethanol is one of the most efficient carbon sources for *Euglena gracilis*. Thus, an in-depth investigation of the distribution of ethanol metabolizing enzymes in this organism was conducted. Cellular fractionation indicated localization of the ethanol metabolizing enzymes in both cytosol and mitochondria. Isolated mitochondria were able to generate a transmembrane electrical gradient ($\Delta\psi$) after the addition of ethanol. However, upon the addition of acetaldehyde no $\Delta\psi$ was formed. Furthermore, acetaldehyde (whereas $\Delta\psi$ generated by ethanol or malate but not by D-lactate. Pyrazole, a specific inhibitor of alcohol dehydrogenase (ADH), abolished the effect of acetaldehyde on $\Delta\psi$, suggesting that the mitochondrial ADH, by actively consuming NADH to reduce acetaldehyde to ethanol, was able to collapse $\Delta\psi$. When mitochondria were fractionated, 27% and 60% of ADH and aldehyde dehydrogenase (ALDH) activities were found in the inner membrane fraction. ADH activity showed two kinetic components, suggesting the presence of two isozymes in the membrane fraction, while ALDH kinetics was monotonic. The ADH K_m values were 0.64–6.3 mM for ethanol, and 0.16–0.88 mM for NAD^+, while the ALDH K_m values were 7–53 μM for acetaldehyde and 33–47 μM for NAD^+. These novel enzymes were also able to use aliphatic alcohols of different chain length and could be involved in the metabolism of fatty alcohol and aldehydes released from wax esters stored by this microorganism.

Keywords ALDH · ADH · Ethanol · Acetaldehyde · Mitochondria · Transmembrane electrical potential · *Euglena gracilis*

Abbreviations

ALD	Alcohol dehydrogenase
ALDH	Aldehyde dehydrogenase
SMPs	Submitochondrial particles
mtxALDH	Mitochondrial matrix aldehyde dehydrogenase
mmALDH	Inner mitochondrial membrane aldehyde dehydrogenase
mtxADH	Mitochondrial matrix alcohol dehydrogenase
mmADH	Inner mitochondrial membrane alcohol dehydrogenase
NAD^+-LDH	Pyridine nucleotides dependent lactate dehydrogenase
D-iLDH	Pyridine nucleotides independent lactate dehydrogenase
SSADH	Succinate semialdehyde dehydrogenase
SSA	Succinate semialdehyde
$\Delta\psi$	Transmembrane electrical gradient

Introduction

Euglena gracilis is a fresh water living protist with peculiar metabolism (Bégin-Heick 1972; Imai et al. 1982; Rotte et al. 2001; Shigeoka et al. 1988a; Tucci et al. 2010) and remarkable ability to resist and accumulate heavy metals

Electronic supplementary material The online version of this article (doi:10.1007/s10863-011-9271-y) contains supplementary material, which is available to authorized users.

H. Vivoli-Sánchez · R. Jasso-Chávez · E. Lira-Silva · R. Moreno-Sánchez · J. S. Rodríguez-Zavala (✉)
Departamento de Bioquímica, Instituto Nacional de Cardiología, Juan Badiano No. 1, Sección XVI, Tlalpan, México D.F. 14080, México
e-mail: rodriguezzavala@gmail.com

(Avilés et al. 2002; Cervantes et al. 2006; Devars et al. 1998, 2001; García-García et al. 2009; Navarro et al. 1997; Martínez-Cázal and Moreno-Sánchez 2005; Rodríguez-Zavala et al. 2007). Furthermore, this organism has the ability to produce significant amounts of different metabolites of potential biotechnological interest such as pamylon, a glucose polymer with immunostimulant and tumour-potentiator properties (Fruchauf et al. 1983; Kataoka et al. 2003; Sugawara and Ishizuka 1984); sterols/oils, vitamin A and terpenoid precursors (Schimmer and Krinsky 1966; Takeyama et al. 1997); and vitamin E (Fujita et al. 2008; Rodríguez-Zavala et al. 2010), an antioxidant used as a food complement, food preservative and in the cosmetic industry. Vitamin E produced by *E. gracilis* is composed by 97% alpha isomer (Shigeoka et al. 1986b), the isomer with highest biological activity (Kamal-Eldin and Appelqvist 1996), which represents an advantage with respect to other natural sources of vitamin E, composed of a mixture of several isomers. The use of carotenoids and vitamin E has become popular due to their protective role against oxidative stress (Dennis-Adem and Adams 2003; Li et al. 2010; Paiz et al. 2009; SanGiovanni et al. 2007; Vasil et al. 2010).

Our group recently reported that in the presence of ethanol *E. gracilis* produced high amounts of tyrosine (Rodríguez-Zavala et al. 2010), a vitamin E precursor, which reinforces the proposal that the *Euglena* whole cell might be used as a source of high quality protein (Takeyama et al. 1997).

This micro-organism can metabolize a wide variety of substrates as carbon source for growth and survival (Bernard et al. 2001; Fujita et al. 2008; Jasso-Chavez et al. 2005; Rodríguez-Zavala et al. 2006, 2010). This metabolic flexibility allows *Euglena* to populate different environments. Ethanol is one of the most efficient carbon sources for this micro-organism reaching maximal growth at an ethanol concentration of 177 mM. This is remarkable for an organism that, presumably, does not produce ethanol (Ono et al. 1995). Recently, it was shown that the combination of ethanol + glutamate + malate enhanced cell growth; the biomass yield reached was at least 5-fold higher than that obtained in the absence of ethanol (Rodríguez-Zavala et al. 2010). Increments in cell yield of this magnitude are of interest for the use of *Euglena* for biotechnological processes. Here, it appears relevant to understand the metabolism of ethanol in this micro-organism. Many alcohol dehydrogenases (ADHs) have been described in *Euglena* under different culture conditions (Mego and Faro 1974; Mann et al. 2002) and recently, one of these ADHs has been cloned and characterized (Talma-Gutiérrez et al. 2008). Furthermore, mitochondrial alcohol (Ono et al. 1995) and aldehyde (Rodríguez-Zavala et al. 2008) dehydrogenases from this organism have been purified to homogeneity and characterized.

In the present work a bleached mutant of *Euglena gracilis* Z grown on glutamate/malate *plus* ethanol, was used to perform an in-depth analysis of the subcellular distribution and kinetics of alcohol and aldehyde dehydrogenases in this microorganism.

Materials and methods

Chemicals

Acetaldehyde, ADP, β-mercaptoethanol, butyraldehyde, butanol, CCCP (carbonyl cyanide m-chloro phenyl hydrazone), cysteine, 2,6-dichlorophenolindophenol (DCPIP), DL-dithiothreitol, dodecyl aldehyde, ethylenediaminetetraacetic acid (EDTA), ethylene glycol bis(2-aminoethyl ether)-*N,N,N′,N′*-tetraacetic acid (EGTA), hexanal, 1-hexanol, MOPS (4-[*N*-morpholino] propanesulfonic acid), NAD$^+$, NADP$^+$, NADH, nonyl aldehyde, octanol, 2-oxoglutarate, phenazine methosulfate (PMS), phenylmethanesulfonyl fluoride (PMSF), propionaldehyde, pyruvate, rotenone, 1T5, rotenone, succinate-semialdehyde, tetradecanol and trypsin were from Sigma-Aldrich (St. Louis, MO, USA). 4-(2-hydroxyethyl)-1-piperazineethanesulfonic acid (HEPES) was from Research Organics (Cleveland, OH, USA). Ethanol was from MERCK (Whitehouse Station, NJ, USA). 2-Amino-2-hydroxymethyl-propane-1,3-diol (Tris) was from GibcoBRL (Grand Island, NY, USA). 5-Aminolevulinic acid (ALAA) was from Wakunaga Pharm. (Hiroshima, JP, USA).

Culture conditions

Euglena gracilis strain Z was grown for 6 day in 1 l of the medium described by Schiff et al. (1971), supplemented with 1% (v/v) ethanol (Rodríguez-Zavala et al. 2010), at 25 °C and pH 3.5. To determine the cell growth, 100 µl aliquots of culture were diluted 1:50 with double-distilled water (ddH$_2$O) and the cells were immobilized by adding 2% HCl and counted in a Neubauer chamber.

Cell fractionation

Cells were harvested by centrifugation at 3,000 *g* for 5 min at 4 °C, washed twice with sterile saline, and re-suspended in 1.5 ml of 100 mM Tris, pH 8.5 with 0.025% (v/v) β-mercaptoethanol. Cells (4.5×10^9/ml) were incubated in fresh 100 mM Tris, pH 8.5 with 0.025% (v/v) β-mercaptoethanol, in the presence of 1.5 mg trypsin (14,900 U/mg) at 35 °C for approximately 40 min, until about 25% of the cells were disrupted (which was determined by the uptake of 0.4% trypan blue). After incubation, the cells were diluted 10 times in ice-cold 100 mM Tris, pH 8.5 with 0.025% (v/v) β-mercaptoethanol, supplemented with 1 mM

EDTA and 1 mM PMSF to stop proteolysis, and centrifuged at 3,000 g and 4 °C for 5 min. The pellet was washed by re-suspending in the same buffer and centrifuging at 3,000 g for 5 min. Then, the pellet was re-suspended in 15 ml of 250 mM sucrose, 10 mM HEPES, 1 mM EGTA (SHE buffer), 0.025% β-mercaptoethanol, 1 mM PMSF, and disrupted by homogenization with a glass/teflon Potter-Elvehjem tissue grinder (10 strokes proposed this way were centrifuged at 270 g and 4 °C for 10 min. The resulting supernatant was called fraction S1, and contained cytosol, mitochondria, and microsomes. The fraction S1 was further centrifuged at 12,000 g and 4 °C for 10 min, to separate the mitochondrial fraction from the cytosol and microsomes (this second supernatant was fraction S2). The pellet (mitochondrial fraction) was re-suspended in 1 ml SHE buffer and supplemented with 1 mM ADP and 0.5% fatty acid-free bovine serum albumin, and incubated for 2 min at 4 °C. Then, the sample was diluted to 30 ml in SHE buffer and centrifuged again at 12,000 g at 4 °C for 10 min. The pellet was re-suspended in a small volume of SHE buffer and used for mitochondrial function and enzymic analysis. Fraction S1 was centrifuged at 100,000 g for 45 min to separate the cytosol from the microsomal fraction. The pellet from this last centrifugation containing the microsomal fraction was re-suspended in a small amount of SHE buffer. Rat liver and kidney mitochondria were isolated as previously described (Rodríguez-Zavala et al. 1997).

Protein determination

Aliquots of the samples were poured into glass tubes, mixed with 1% sodium deoxycholate, vortexed, diluted with dH_2O and mixed with Biuret reagent for protein determination (Gornall et al. 1949). Tubes were incubated for 15 min at room temperature and then centrifuged at 3,000 g for 20 min, to eliminate the turbidity caused by paramylon before reading the absorbance at 540 nm. Bovine serum albumin was used as standard.

Mitochondrial fractionation

Mitochondria were suspended in 10 ml of SHE buffer and disrupted by sonicating on ice, 10 cycles (10 s sonication/1 min rest), at 15% of the maximal output of the instrument (Branson sonifier model 450), using a tip probe of 1 cm diameter. The sonicated suspension was centrifuged at 100,000 g for 45 min at 4 °C. The supernatant was recovered and the pellet was re-suspended in 1 ml SHE buffer.

Enzyme activities

All the enzymatic determinations were carried out at 25 °C. Activities of all enzymes, except for D-LDH, were determined following the increase in the absorbance at 340 nm owing to the formation of $NAD(P)H$. ALDH activity was measured by mixing an aliquot of each fraction with 100 mM Na_2HPO_4, pH 7.4, 100 mM NaCl, 1 mM dithiothreitol, 0.1 mM pyrazole and 2 mM NAD^+; the reaction was started by adding the corresponding aldehyde. ADH activity was determined by mixing an aliquot of the supernatant from the mitochondrial fractionation with 100 mM HEPES, pH 8.5, 1 mM dithiothreitol, 2 mM NAD^+, 30 mM cysteine, and 2 mM Mg^{2+}; the reaction was started by adding 20 mM ethanol. The mtALDH activity was measured in a fluorimeter (Aminco Bowman Series 2), mixing an aliquot of the mitochondrial membrane fraction with 100 mM Na_2HPO_4, pH 7.4, 100 mM NaCl, 1 mM dithiothreitol, 0.1 mM pyrazole, 1 mM NAD^+ and starting the reaction by adding the corresponding aldehyde. Excitation and emission wavelengths were 340 and 460 nm, respectively. Activity of mtALDH was determined following the fluorescence of the NADH generated as described above. An aliquot of the membrane fraction was mixed with 100 mM HEPES, pH 8.5, 7 mM NAD^+, 30 mM cysteine, and 2 mM Mg^{2+}, the reaction was started by adding 2 to 30 mM of the corresponding alcohol.

Marker enzymes were used to determine cross-contamination of the cell fractions. NAD^+-LDH was used as cytosolic marker (Hogeboom 1955). Membrane-bound D-iLDH was used as mitochondrial membrane marker (Jasso-Chávez and Moreno-Sánchez 2003), whereas SSADH (Takenaga et al. 1975) and 2-oxoglutarate decarboxylase were used as mitochondrial matrix markers. NAD^+-LDH was assayed by mixing an aliquot of the indicated fraction with 100 mM MOPS, pH 7.5, and 0.1 mM NADH; the reaction was started by adding 5 mM pyruvate. SSADH was measured by adding an aliquot of a fraction to 100 mM HEPES, pH 8.0, and 1 mM $NADP^+$, the reaction was started by adding 2 mM succinate-semialdehyde. 2-oxoglutarate decarboxylase activity was determined by coupling the reaction with the $NADP^+$-dependent SSADH activity present in the sample (which was always in excess), adding 1 mM $NADP^+$ to saturate the coupling enzyme; the reaction was started by the addition of 1 mM 2-oxoglutarate. D-iLDH activity was determined by incubating a sample aliquot with 100 mM HEPES, pH 8.5, and 0.2 mM DCPIP and following the increase in the absorbance at 600 nm; the reaction was initiated by the addition of 20 mM D-lactate.

Mitochondrial permeability transition assay

Mitochondria (0.1–0.2 mg protein/ml) were added to 20 mM MOPS, pH 7.5, 0.5 mM EGTA and 120 mM KCl (KME buffer), in the presence of 2 mM phosphate, 2 mM $MgCl_2$ and 20–100 μM Ruthenium red, at 25 °C. The

excitation wavelength was 494 nm and the fluorescence recorded at 525 nm (Scaduto and Grotyohann 1999).

Synthesis of ethanol in isolated mitochondria

An aliquot of 50–60 µl of mitochondria (1–2 mg protein) was mixed with 40 µl of SHE buffer, pH 7.5 plus 10 mM $MgCl_2$ and 1 mM malate. Then the mixture was incubated 10 min in the presence or absence of 5 mM acetaldehyde and 0.1 mM pyrazole. Ethanol produced was determined using a gas chromatographic equipment (Shimadzu GC2010), equipped with a capillary column HP-PLOT/U of 30 m length, 0.32 mm I.D. and 10 µm film (Agilent, Santa Clara, CA, USA) and a flame ionization detector (Shimadzu, Columbia, MD, USA).

Submitochondrial particles preparation

Submitochondrial particles (SMPs) were prepared by sonicating mitochondrial suspensions as described by Jasso-Chávez et al. (2001). Briefly, 25 ml of mitochondrial suspension (18–25 mg protein/ml) were sonicated three times for 15 s at 15% of maximal output with 1 min rest in a Branson sonicator with a probe tip of 0.5 cm diameter on an ice bath. The sonicated mitochondrial suspension was centrifuged at 17,370 g for 10 min to remove unbroken mitochondria. Hence, the supernatant was centrifuged at 105,000 g for 45 min and 4 °C. Then, the pellet was re-suspended in 20 ml SHE buffer and centrifuged again at 105,000 g for 30 min and 4 °C to obtain submitochondrial particles.

Measurement of the ΔpH generation in submitochondrial particles (SMPs)

The generation of ΔpH was assayed in SMPs (0.3–0.5 mg protein/ml) incubated in KME medium in the presence of 0.5 µM ACMA, 5 mM Mg^{2+} and 1 mM NAD^+. The generation of ΔpH was started by the addition of 5 mM succinate/1 µM rotenone or 0.2 mM acetaldehyde/0.1 mM pyrazole. ACMA was excited at 415 nm and the fluorescence collected at 480 nm (Kaufmann and Moreno-Sánchez 1993).

Results

Distribution of ADH and ALDH activities in Euglena gracilis

To evaluate the subcellular distribution of alcohol dehydrogenase (ADH) and aldehyde dehydrogenase (ALDH) activities in *Euglena* grown in the presence of glutamate, malate and ethanol, cellular fractionation was carried out. Most of the ADH and ALDH activities were localized in mitochondria (68 and 57%, respectively, see Table 1) although still significant activity (25% for ADH, 24% for ALDH) was found in the cytosolic fraction. Robust validation of the subcellular enzyme distribution was provided by the low cross contamination of cytosol by the mitochondrial fraction as indicated by the marker enzymes (<4%; Table 1).

Effect of acetaldehyde on generation of transmembrane electric potential ($\Delta\psi$)

Considering that acetaldehyde might be generated in the cytosol as some of the ADH activity was found in this compartment, it was explored whether acetaldehyde could permeate into the mitochondria to be further metabolized. For this goal $\Delta\psi$ generated by several oxidizable substrates was determined in coupled *Euglena* mitochondria. Addition of either ethanol, succinate semialdehyde, or malate, substrates that generate NADH and feed the respiratory chain and promote $\Delta\psi$ generation (Fig. 1), but not of succinate, a substrate of an enzyme that feeds electrons to the respiratory chain at the ubiquinone pool level, in the presence of rotenone (Jasso-Chávez and Moreno-Sánchez

Table 1 Activities of ADH and ALDH in different fractions of *Euglena gracilis* grown in the presence of glutamate, malate and ethanol. Enzyme activities were assayed as indicated under the Materials and Methods section. The data shown are the mean ± SD of three independent preparations. Basal activities in the first experiment (mean ± sem) were: 2,300–4,000 for NAD$^+$-EtDH; 1,950–2,900 for DH-EtDH; 3,500–4,400 for SSADH; 1,900–2,300 for ADH and 400–650 for ALDH

	% NAD^+-EtDH	% D- EtDH	% 2-OGDC	% SSADH	% ADH	% ALDH
Fraction						
SI	100	100	100	100	100	100
Cytoplasmic	<1	9 ± 3	<1	5 ± 2	29 ± 6	32 ± 10
Cytosol	10 ± 6	<1	<1	3 ± 2	26 ± 3	21 ± 3
Microsomes	<1	7 ± 4	<1	<1	7 ± 0.6	<1
Mitochondria	<1	83 ± 9	98 ± 10	93 ± 8	68 ± 10	67 ± 6

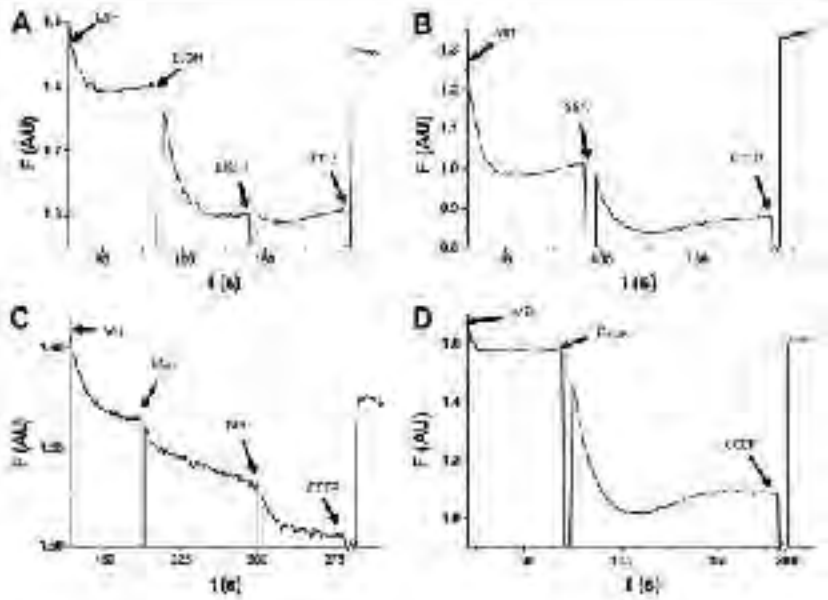

Fig. 1 Generation of mitochondrial transmembrane electrical potential by *Rhodococcus erythropolis*. Membrane potential was measured with Safranine (2.5 μM) as described under Materials and Methods. Figures are representative of at least 4–5 experiments with independent mitochondria preparations. Mit, mitochondria (0.05–0.1 mM Mitochondrial protein); CCCP, 2 μM carbonylcyanide-3-chlorophenylhydrazone; SSA, 0.25 mM succinate semialdehyde; Mal, 5 mM malate; D-Lac, 0.1 mM D-Lactate

2000), also promoted generation of a high $\Delta\psi$ (Fig. 1d). On the other hand, acetaldehyde did not generate $\Delta\psi$ and in fact collapsed that driven by endogenous substrates (Fig. 2a) and by added ethanol, 2-oxoglutarate or malate, but not that driven by SSA (Fig. 2c). In contrast, acetaldehyde did promote $\Delta\psi$ generation in rat liver and kidney mitochondria (Fig. 2b and c). When ethanol, 2-oxoglutarate or malate were added to *Euglena* mitochondria after the addition of acetaldehyde, no $\Delta\psi$ generation occurred (Fig. 2d), whereas D-lactate was still able to make a membrane $\Delta\psi$ (Fig. 2a and d). These observations suggested that acetaldehyde inhibited the respective

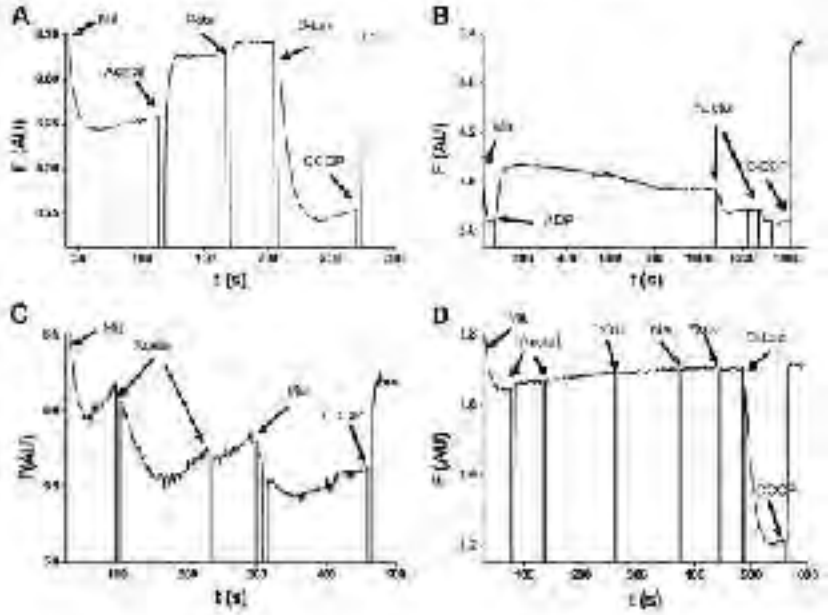

Fig. 2 Effect of acetaldehyde on the generation of transmembrane electrical potential ($\Delta\psi$) by mitochondria from different sources. Mitochondria were isolated from *Rhodococcus erythropolis* (A), *Euglena gracilis* (D), Rat liver mitochondria (B), Rat kidney mitochondria (C). Mit, mitochondria; Acetal, 0.2 mM acetaldehyde; Eth, 0.1 % ethanol; Rote, 2 μM rotenone; CCCP, 2 μM carbonylcyanide 3-chlorophenylhydrazone; NH4Cl, 25 mM ammonium chloride; SSA, 0.25 mM succinate semialdehyde; Mal, 5 mM malate; D-Lac, 0.1 mM D-Lactate. Results are representative of experiments with at least 3–4 independent mitochondria preparations

dehydrogenase activities in the respiratory chains in *Euglena* mitochondria

Effect of acetaldehyde on the activity of mitochondrial NAD$^+$-dependent enzymes

In rat liver, ethanol acetaldehyde was found a dehydrogenase inhibitor, the activities of some dehydrogenases were evaluated in detergent-permeabilized mitochondria. Acetaldehyde inhibited the NAD$^+$-dependent SSADH (Fig. 3A) and malate dehydrogenase activities (data not shown), whereas NADP$^+$-dependent SSADH was insensitive (Fig. 3B). The addition of pyruvate, a specific inhibitor of ADH (Lees and Trimell, 1985), prevented the recovery of the NAD$^+$-dependent SSADH (Fig. 3a) and malate dehydrogenase activities (data not shown). But ADH activity was also inhibited by acetaldehyde (Fig. 3c). Remarkably, pyruvate revealed a pronounced mitochondrial ALDH activity (Fig. 3d). Furthermore, generation of $\Delta\psi$ in isolated mitochondria by acetaldehyde was achieved in the presence of pyruvate (Fig. 4).

Ethanol synthesis by isolated *Euglena* mitochondria

Euglena mitochondria synthesized 37±15 nmol of ethanol (n=7) after 10 min following the addition of 5 mM acetaldehyde (ref. to the presence of malate as the

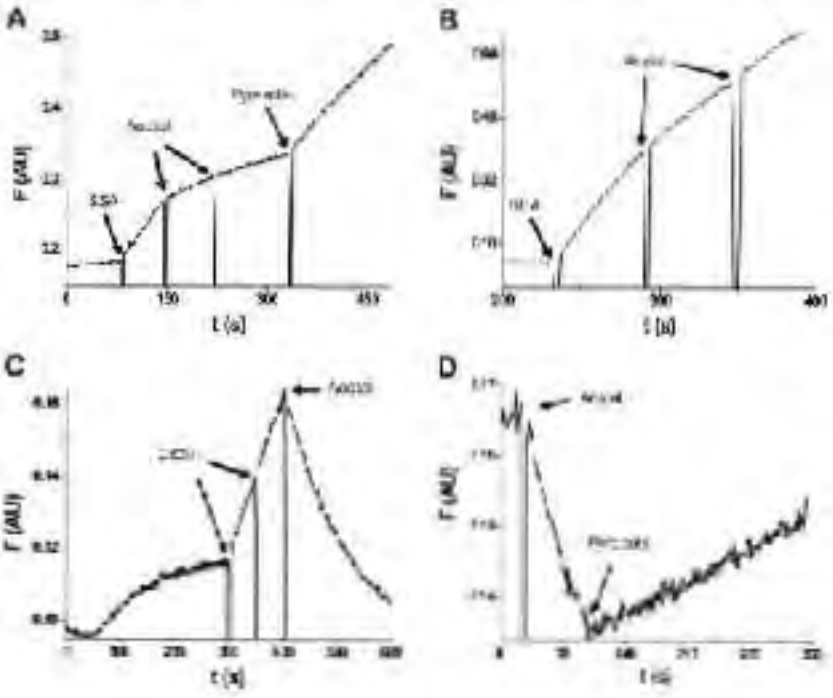

Fig. 3. Effect of acetaldehyde on the mitochondrial SSADH activities. Enzyme activities were determined with 0.3 mM NAD^+ (a) or 0.5 mM $NADP^+$ (b) in permeabilized cells (Material and Methods). Acetal, 0.2 mM acetaldehyde; Pyruvate, 0.1 mM pyruvate; NADH, 1 mM (from) SSA, 0.25 mM succinic semialdehyde. Results are representative of experiments with at least 3 independent mitochondrial isolates.

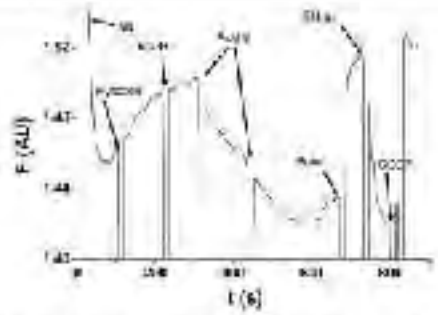

Fig. 4 Restoration of acetaldehyde-dissipated $\Delta\psi$ by pyrazole. Acetal, 0.2 mM acetaldehyde; Pyrazole, 0.1 mM pyrazole; Rot, 5 μM rotenone; D Lac, 0.1 mM D Lactate; CCCP, 2 μM carbonylcyanide 3 chlorophenylhydrazone. Results are representative of experiments with at least 3 independent mitochondrial preparations

activity of mmADH exhibited two well-defined kinetic components (Fig. 3C), showing high and low affinities for both substrates, whereas mtADH kinetics was similar to that of the membrane high affinity component (Table 3). The three ADH isoforms also showed significant activity with alcohols of different chain length but not with aromatic alcohols. These ADHs were fully sensitive to the inhibitor pyrazole (data not shown).

Generation of ΔpH by submitochondrial particles

Submitochondrial sealed particles were prepared to further assess the presence of ALDH in the inner mitochondrial membrane. Generation of ΔpH by succinate in the presence of rotenone was used as control (Fig. 3SA). Acetaldehyde in the presence of NAD^+ and pyrazole, prompted the generation of ΔpH, which was collapsed by the uncoupler CCCP (Fig. 3SB).

Orientation of the active sites of mmALDH and mmADH

Sealed mitochondria were incubated in the presence of 1 mM NAD^+ plus 1 mM acetaldehyde, or 10 mM ethanol, to elucidate whether the active sites of mmALDH or mmADH were orientated towards the cytosolic side or the membrane. No activity was observed in these assays until 0.01% of the detergent triton x-100 was used to permeabilize the membranes, indicating that the active sites of these enzymes were not exposed to the cytosolic compartment.

Discussion

Effect of acetaldehyde on $\Delta\psi$ generation

Several ADHs have been reported for *Euglena*, some localized in the cytosol (Mego and Parb 1974; Munir et al. 2002; Palma-Gutiérrez et al. 2008) and one in the mitochondria (Ono et al. 1995), while only a mitochondrial ALDH has been described (Rodríguez-Zavala et al. 2006) for this microorganism. When culturing *Euglena* in the presence of ethanol, the cytosolic ADH can be oxidized by cytosolic ADH to form acetaldehyde. The toxicity of acetaldehyde makes necessary its rapid oxidation and/or transport into the mitochondria to be detoxified to avoid cellular damage. In this regard, significant ALDH activity was found in the cytosol as it also occurs in other organisms (Crow et al. 1974; Hurdman et al. 1985; Kirch et al. 2004; Tottmar et al. 1973; Wang et al. 1998; Wood and Duff 2009), which supports the requirement for this specific cellular defense mechanism.

However, some of the acetaldehyde produced in the cytosol might permeate into the mitochondria. Acetaldehyde readily collapsed the ethanol-induced transmembrane electrical potential. Initially it was thought that acetaldehyde was altering the integrity of the membranes at first it was considered as a K+ ionophore. The generation of $\Delta\psi$ induced by D-lactate in the presence of acetaldehyde, discarded the first possibility, whereas the pyrazole reversing effect on $\Delta\psi$ and on ADH and NAD^+-SSADH activities indicated that site I was active. The explanation of the acetaldehyde effect was that the ADH activity, in the presence of added acetaldehyde, was responsible for the diminution of $\Delta\psi$ by sequestering the NADH produced by the other enzymes and thus masking their activities. This explanation was supported by the restoring pyrazole effect on $\Delta\psi$ and on the activity of the mitochondrial matrix NAD^+-dependent enzymes, both inhibited by acetaldehyde

Table 2 Activities of ADH and ALDH in the different mitochondrial fractions. Enzyme activities were assayed as described under Materials and Methods. Results are the mean ± SD of three independent mitochondrial preparations. Total activities in mitochondrial extract (nmol/min) were: 7.6(C–4.6)/0 for D-LDH; 7.6(C–3.8)/0 for NAD^+-SSADH; 600 ± 200 for ADH and 300 ± 85 for ALDH

Fraction	% SSADH	% D-LDH	% ADH	% ALDH
Mitochondrial extract	100	100	100	100
Mitochondrial matrix	38 ± 3	93 ± 3	81 ± 10	87 ± 7
Mitochondrial matrix	58 ± 9	~3	92 ± 6	91 ± 3
Mitochondrial membrane	5 ± 2	8 ± 8	27 ± 8	61 ± 11

Table 3 Kinetic parameters of mitochondrial ALDHs and ADHs

	mALDH		mALDH	
Substrate	K_m (μM)	V_m (%) of the Acetaldehyde	K_m (μM)	V_m (%) of the acetaldehyde
NAD$^+$	47±19 (n=3)	100	71±11 (n=3)	100
Acetaldehyde	5.1±1.4 (n=3)	100	4.9±1.1 (n=3)	100
Butanal	1.8±0.8 (n=3)	130±10	7.7±0.7 (n=3)	175±18
Hexanal	5.3±1.5 (n=3)	95±15	7.4±0.5 (n=3)	80±9
Octanal	1.1±0.1 (n=3)	110±12.5	6.4±1.1 (n=3)	105±15
Dodecanal	5.6±2 (n=3)	15.5±1.5	8±1.8 (n=3)	48.3±6.5
	cADH		cNADH			
	K_m (mM)	V_m	K_m (mM)	V_m (% of Et$^+$ DDH)	K_m (mM)	V_m (% of Et$^+$ DDH)
NAD$^+$	0.88±0.71 (n=3)	100	0.15±0.05 (n=3)	82±8.5	0.66±0.25 (n=3)	100
Ethanol	0.64±0.52 (n=3)	100	1.12±0.82 (n=3)	94±10	0.5±0.3 (n=3)	100
Butanol	0.77 (n=2)	97	0.9 (n=2)	77	4.2 (n=2)	103
Octanol	0.15±0.13 (n=3)	89±14	0.16 (n=2)	90	0.6 (n=2)	116
Myristic alcohol	0.05 (n=3)	15	0.1 (n=2)	170	0.9 (n=2)	144

For mtALDH = 12–20 nmol·min^{-1}·mg; for mmALDH = 5–9 nmol/min*mg. For mtADH = 0.27 nmol·min^{-1}·mg; for mmADH = 0.30 nmol·min^{-1}·mg, as in ethanol oxidation, respectively. Where indicated, results are the mean ± SD of the number of experiments shown in parentheses

Acetaldehyde did not affect the generation of $\Delta\psi$ by SSA, or the activity of NADP$^+$-dependent SSADH, but it did inhibit NAD$^+$-SSADH. As the I of the respiratory chain cannot oxidize NADPH, one explanation of the last results was that an efficient transhydrogenase catalyzed a fast NADPH/NADH exchange. A second possibility was that the synthesis of succinate by NADP$^+$-SSADH, a substrate that feeds the pool of quinones of the respiratory chain, bypassed acetaldehyde inhibition. However, generation of $\Delta\psi$ by SSA in the presence of 2 mM malonate (this concentration of malonate completely inhibited the activity of *Euglena* succinate dehydrogenase; data not shown) was only 15% inhibited.

Like in yeast, metabolism of acetaldehyde is displaced to ethanol synthesis in *Euglena* mitochondria (see Figs. 2 and 3). However, in yeast ethanol synthesis takes place in the cytosol under anaerobic conditions. In higher organisms, acetaldehyde metabolism is shifted to oxidation, which occurs mainly in the mitochondrial matrix (Symons and Beevers 1955).

Thermodynamics of ethanol oxidation

The standard ΔG of the reaction for acetaldehyde reduction at pH 7.0 is −5.5 kcal/mol and hence the K_{eq} value at 25 °C is $1.6 \cdot 10^4$, indicating that acetaldehyde reduction is thermodynamically favored (scheme 1). However, at ethanol/acetaldehyde and NAD$^+$/NADH ratios values higher than 100, the direction of the reaction can be changed. On the other hand, $\Delta G^{\circ\prime}$ for acetaldehyde oxidation is −12.9 kcal/mol and K_{eq} $2.6 \cdot 10^9$, indicating that the reaction of acetaldehyde oxidation is practically irreversible under near-physiological conditions.

Possible role of membrane-bound ethanol metabolizing enzymes

Different membrane-bound ADHs and ALDHs have been reported for several Gram-negative bacteria (Fukaya et al. 1989; Gómez-Manzo et al. 2010; Goodwin and Anthony 1998; Kay et al. 2004; Wu et al. 2011), which use pyrroloquinoline quinone (PQQ) as the redox prosthetic group. A NAD(P)$^+$-dependent ALDH has also been found in the mouse liver microsomal membrane (Masaki et al. 1989; Vasiliou et al. 1999) and this enzyme has been related to the detoxification of medium chain aldehydes produced during lipid peroxidation (Lindahl and Petersen 1991; Mitchell and Petersen 1989).

Under anaerobic conditions, *Euglena* produces and accumulates wax esters (Kobayashi et al. 1971), synthesized at the expense of paramylon storage (Imai et al. 1982,

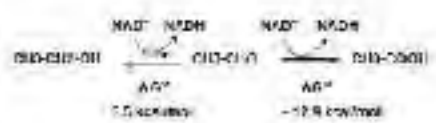

Scheme 1 Reactions of ethanol and acetaldehyde oxidation

1992). Wax esters form water insoluble aggregates of high molecular weight that are accumulated in the cytosol (Inui et al. 1982a). Under aerobic conditions, aliphatic alcohols and aldehydes are produced from the degradation of wax esters in the cytosol (Inui et al. 1986). Thus, it is possible that the different ADHs and ALDHs expressed by *Euglena* might be involved in the metabolism of the aliphatic alcohols produced during wax esters degradation. Fatty alcohols and aldehydes are partly soluble in water and therefore preferentially interact with the membranes. The presence of ADH and ALDH at the outer mitochondrial membrane may favor the diffusion of ethanol and acetaldehyde in the vicinity of the internal mitochondrial membrane, thus preventing the toxic effects of these compounds on respiratory chain and mitochondrial matrix enzymes.

Euglena does not possess an active pyruvate dehydrogenase complex (Inui et al. 1984; Shigeoka et al. 1985a). Thus, pyruvate can only be used to transfer redox equivalents at the mitochondria through the lactate shuttle (Jasso-Chávez and Moreno-Sánchez 2006). However, carbon equivalents from pyruvate have to be used by other pathways to avoid its accumulation. The results shown in the present work permit to visualize a model (Fig. 5) in which acetaldehyde can be synthesized in the cytosol from pyruvate by pyruvate decarboxylase (Hurlbert and Rittenberg 1962), in the cytosol, acetaldehyde could be used by cytosolic alcohol dehydrogenase (ADHc) to produce ethanol. Alternatively, acetaldehyde can also be produced by ADHc when cells are cultivated in the presence of ethanol. Then, acetaldehyde can be oxidized to acetate by cytosolic aldehyde dehydrogenase (ALDHc). Acetate can enter into the mitochondria to be metabolized by acetate thiokinase that produces acetyl CoA to feed the Krebs cycle. A fraction of the cytosolic acetaldehyde might permeate the mitochondrial membrane to be oxidized by ALDHm or reduced by ADHm. Ethanol can also permeate into the mitochondria where it is oxidized to acetaldehyde by mtcADH (Ono et al. 1995) or by the mtrADHs with production of NADH. In turn, acetaldehyde is oxidized to acetate by mtrALDH (Inui et al. 1984) or mtcALDH, also with the generation of NADH. Acetate can then be used by acetate thiokinase to synthesize acetyl CoA to feed the Krebs cycle (Fig. 5).

The presence of different ADHs and ALDHs in cytosol and mitochondria of *Euglena gracilis* raises the possibility that in this microorganism an ethanol-acetaldehyde shuttle such as that described for yeast (Dekker et al. 2000;

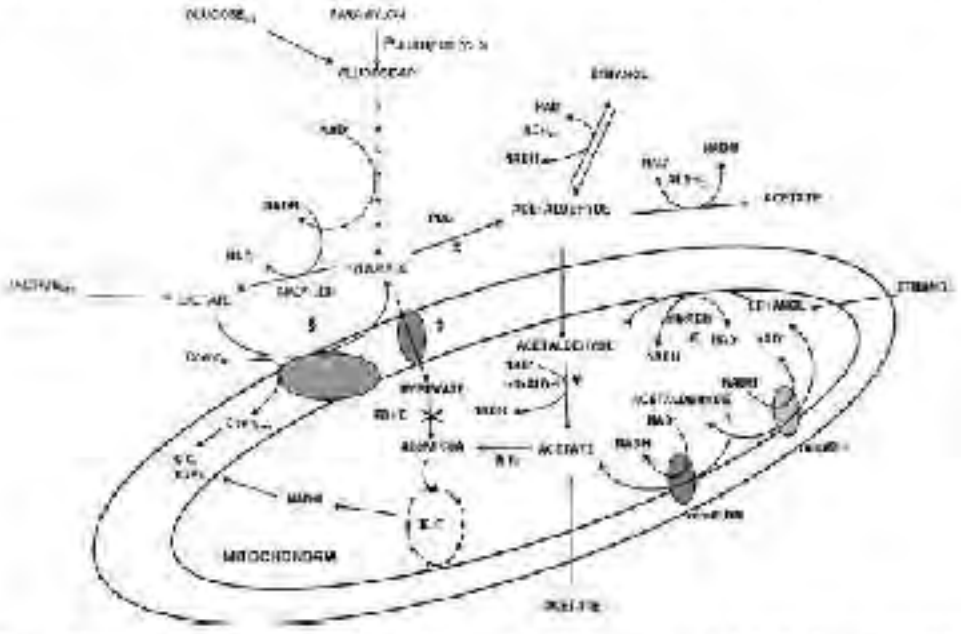

Fig. 5 Scheme of the ethanol metabolism in *Euglena gracilis*. PDC pyruvate decarboxylase, ADHc cytosolic alcohol dehydrogenase, cLDH, NAD$^+$ dependent lactate dehydrogenase, rLDH, RAD$^+$ independent lactate dehydrogenase, ALDHc cytosolic aldehyde dehydrogenase, mtcADH, mitochondrial matrix alcohol dehydrogenase, mtcALDH, mitochondrial matrix aldehyde dehydrogenase, mtrADH, mitochondrial membrane alcohol dehydrogenase, mtrALDH, mitochondrial membrane aldehyde dehydrogenase, PDHC pyruvate dehydrogenase complex, ACT, Acetate thiokinase, KC, Krebs cycle, RC, respiratory chain. 1, Reported by Hurlbert and Rittenberg 1962; 2, Described by Jasso-Chávez and Moreno-Sánchez 2006; 3, Characterized by Inui et al. 1982a, b; 4, Reported by Ono et al. 1995

Lertwattanasakul et al. 2009) might be operating. It has been suggested that this shuttle is important for the transference of reduced equivalents from mitochondria to cytosol under anaerobic or microaerophilic conditions, in which generation of NADH still occurs (Bakker et al. 2000). It is worth noting that *Euglena* is a facultative organism and can switch its metabolism from aerobic to anaerobic and vice versa depending on the environmental conditions (Coleman et al. 1988; Inui et al. 1984; Tucci et al. 2010). In order to clarify this possibility, the purification and in-depth characterization of these novel membrane bound ADH and ALDH of *Euglena gracilis* is necessary and it is currently under progress in our laboratory.

In conclusion, *Euglena gracilis* possesses several alcohol metabolizing enzymes distributed in cytosol and mitochondria; those new isozymes of this pathway were found bound to the inner mitochondrial membrane. These enzymes can use aliphatic aldehydes and alcohols of different chain size. mmALDH and mmADHs could be part of the antioxidant defense mechanism and could also participate in the metabolism of complex alcohols and aldehydes, produced as part of the metabolism of wax esters, accumulated by this organism in anaerobic conditions.

Acknowledgments This work was supported in part by CONACyT grants No. 78775, 80534, 80412, 102/20 and ICyTDF grant PICSA [illegible].

References

Avilés C, Loza-Tavera H, Terry N, Moreno-Sánchez R (2003) Mercury pretreatment selects an enhanced cadmium-accumulating phenotype in *Euglena gracilis*. Arch Microbiol 180:1–10

Bakker BM, Bro C, Kötter P, Luttik MAH, Van Dijken JP, Pronk JT (2000) The mitochondrial alcohol dehydrogenase Adh3p is involved in a redox shuttle in *Saccharomyces cerevisiae*. J Bacteriol 182:4730–4737

Barsanti L, Vismara R, Passarelli V, Gualtieri P (2001) Paramylon (β-1,3-glucan) content in wild type and WZSL mutant of *Euglena gracilis*. Effects of growth conditions. J Appl Phycol 13:59–65

Bégin-Heick N (1973) The localization of enzymes of intermediary metabolism in *Astasia* and *Euglena*. Biochem J 134:607–616

Bergmeyer HU (1983) In: Bergmeyer HU (ed) Methods of enzymatic analysis, vols 3–9. Weinheim Verlag Chemie, Germany

Cervantes C, Espino-Saldaña AE, Acevedo-Aguilar F, León-Rodríguez IL, Rivera-Cano ME, Ávila-Rodríguez M, Wrobel-Kaczmarczyk K, Wrobel-Zasada K, Gutiérrez-Corona JF, Rodríguez-Zavala JS, Moreno-Sánchez R (2006) Microbial interactions with heavy metals. Rev Latinoam Microbiol 48:203–210

Coleman LW, Rosen BH, Schwartzbach SD (1988) Environmental control of carbohydrate and lipid synthesis in *Euglena*. Plant Cell Physiol 29:423–432

Crow KE, Kitson TM, MacGibbon AKH, Batt RD (1974) Intracellular localisation and properties of aldehyde dehydrogenases from sheep liver. Biochim Biophys Acta 350:121–128

Demmig-Adams B, Adams WW 3rd (2002) Antioxidants in photosynthesis and human nutrition. Science 298:2149–2153

Devars S, Hernández R, Moreno-Sánchez R (1998) Enhanced heavy metal tolerance in *Euglena gracilis* by preexposure to mercury or cadmium. Arch Environ Contam Toxicol 34:128–135

Devars S, Rodríguez-Zavala JS, Moreno-Sánchez R (2011) Enhanced tolerance to cadmium in an [illegible] strain of *Euglena gracilis*. Water Air Soil Pollut 218:51–57

Frasciani JJ, Burnand GD, Herberman RB (1982) The effect of lectins on production of interleukin-1 by human monocytes. Immunopharmacology 5:17–24

Fujita T, Aoyagi H, Ogbonna JC, Tanaka H (2008) Effect of mixed organic substrate on α-tocopherol production by *Euglena gracilis* in photoheterotrophic culture. Appl Microbiol Biotechnol 79:371–378

Fukaya M, Tayama K, Tamaki T, Tagami H, Okumura H, Kawamura Y, Beppu T (1989) Cloning of the membrane-bound aldehyde dehydrogenase gene of *Acetobacter polyoxogenes* and improvement of acetic acid production by use of the cloned gene. Appl Environ Microbiol 55:171–176

García-García JD, Rodríguez-Zavala JS, Jasso-Chávez R, Mendoza-Cózatl D, Moreno-Sánchez R (2009) Chromium uptake, retention and reduction in photosynthetic *Euglena gracilis*. Arch Microbiol 191:431–440

Gómez-Manzo S, Chavez-Pacheco JL, Contreras-Zentella M, Sosa-Torres ME, Arreguín-Espinosa R, Pérez de la Mora M, Membrillo-Hernández J, Escamilla JE (2010) Molecular and catalytic properties of the aldehyde dehydrogenase of *Gluconacetobacter diazotrophicus*, a quinoheme protein containing pyrroloquinoline quinone, cytochrome b, and cytochrome c. J Bacteriol 192:5718–5724

Goodwin PM, Anthony C (1998) The biochemistry, physiology and genetics of PQQ and PQQ-containing enzymes. Adv Microb Physiol 40:1–80

Gornall AG, Bardawill CJ, David MM (1949) Determination of serum proteins by means of the biuret reaction. J Biol Chem 177:751–766

Hempel JD, Ward K, Kennedy NP, Weiner DH, Lipsky RP (1985) Subcellular distribution of aldehyde dehydrogenase activities in human liver. Alcohol 2:103–110

Hurlbert RE, Rosenberg SH (1962) Glucose metabolism of *Euglena gracilis* var. *bacillaris*; growth and enzymes of aerobic [illegible]. J Protozool 9:170–182

Inui H, Miyatake K, Nakano Y, Kitaoka S (1982) Wax ester fermentation in *Euglena gracilis*. FEBS Lett 150:89–93

Inui H, Miyatake K, Nakano Y, Kitaoka S (1984) Occurrence of oxygen-sensitive NADP+-dependent pyruvate dehydrogenase in mitochondria of *Euglena gracilis*. J Biochem 96:931–934

Inui H, Ohya O, Miyatake K, Nakano Y, Kitaoka S (1985) Assimilation and metabolism of fatty alcohols in *Euglena gracilis*. Biochim Biophys Acta 875:543–548

Inui H, Miyatake K, Nakano Y, Kitaoka S (1992) Synthesis of reserved polysaccharide from wax esters accumulated as the result of anaerobic energy generation in *Euglena gracilis* returned from anaerobic to aerobic conditions. Int J Biochem 24:799–803

Jasso-Chávez R, Moreno-Sánchez R (2003) Cytosol–mitochondria transfer of reducing equivalents by a lactate shuttle in heterotrophic *Euglena*. Eur J Biochem 270:4942–4951

Jasso-Chávez R, Torres-Márquez ME, Moreno-Sánchez R (2001) The membrane-bound L- and D-lactate dehydrogenase activities in mitochondria from *Euglena gracilis*. Arch Biochem Biophys 390:295–303

Jasso-Chávez R, García-Cano I, Marín-Hernández A, Mendoza-Cózatl D, Rendón JL, Moreno-Sánchez R (2005) The bacterial-like

...aldehyde dehydrogenase from halotolerant *Euglena gracilis*. Biochim Biophys Acta 1729(2):81–89.

...Wang Y, Zhang X, Xu N, Cong X, ... (2013) Tumor preventive activities of saponins and sapogenins. Carcinogenesis 34(8):1745–1754.

Kamal-Eldin A, Appelqvist LÅ (1996) The chemistry and antioxidant properties of tocopherols and tocotrienols. Lipids 31(7):671–701.

Kaleuki K, Muta T, Yamazaki S, Iwashima K (2002) Acyclides, ... from *Dugong dugon*. II. Structures of acyclides. Tetrahedron 58(3):...

Kato T, Wu M, Morisaga H, Ohmiya H, Hirai R (2011) Characterization of the PhLJ isozyme excised in *Zymomonas mobilis*. J Mol Microbiol Biotechnol 20(4):...

Kim HH, Hurtado D, Wu X, Salcedo PS, Wood AJ (2004) The ALDH gene superfamily of *Arabidopsis*. Trends Plant Sci 9:271–277.

Kusakabe PE (1970) Reduction of fatty acids to aldehydes by cell-free preparations of *Euglena gracilis*. Biochemistry 9:1055–1062.

Lapenna D, Salvatorelli E, Ciofani G, Emma F, Duni L, Pennelli A, Di Ilio C, Cuccurullo F, Mezzetti A (2008) The effects of the aldehyde dehydrogenase inhibitor nitroglycerin on endothelial function and oxidative stress. Toxicol Appl Pharmacol 230:...

Lee CK, Cantrell H (1969) Human liver microsomal dehydrogenase: inhibition by pyruvate and pyruvate analogs. Acta Chem Scand 23:882–902.

Lindahl R, Petersen DR (1991) Lipid aldehyde inhibition of aldehyde dehydrogenases. II. Aldehyde dehydrogenases. Biochem Pharmacol 41:1583–1587.

Mitsuda H, Yamamoto A, Sakurai Y (1964) Oxidation of aldehydic compounds by rat liver tissue slices. Jpn J Nutr 22:...

Moyo EL, Fan RH (1984) Aldehyde dehydrogenases of *Euglena gracilis*, strain Z. Biochim Biophys Acta 800:237–243.

Murakawa-Cassall E, Moreno-Sánchez R (2005) Cd2+ transport and storage in the chloroplast of *Euglena gracilis*. Biochim Biophys Acta 1706:88–97.

Mitchell DG, Petersen DR (1989) Mechanism of aldehydic products of lipid peroxidation by the liver 9-mitochondrial aldehyde dehydrogenase. Arch Biochem Biophys 269:...

Muniz E, Nakamura M, Hattori K, Yamaji R, Inui H, Miyatake K, Nakano Y (2000) Occurrence of a novel NAD(P)(+)-linked aldehyde dehydrogenase in *Euglena gracilis*. Comp Biochem Physiol B Biochem Mol Biol 126(4):535–540.

Navarro L, Torres-Márquez ME, González-Murcia S, Devars S, Hernández R, Moreno-Sánchez R (1987) Comparison of growth-dependent changes in *Euglena gracilis* among strains of different origin: heterotrophic and photoheterotrophic cells. Comp Biochem Physiol 116:269–277.

Ono K, Kawamoto Y, Inoue Y, Ito R, Miyatake K, Uchida S, Nakano Y (1995) Mitochondrial aldehyde dehydrogenase from marine-green *Pylaiella littoralis*. J Biochem 117:1176–1182.

Palacios-Ballesteros RS, Rosa-Barcelo JS, Lazo-Cabrales R, Moreno-Sánchez R, Saavedra E (2008) Gene cloning and biochemical characterization of an aldehyde dehydrogenase from *Euglena gracilis*. J Eukaryot Microbiol 55:251–261.

Park S, Kim AL, Lee M (2000) Synergic effects of alpha-tocopherol and ascorbate on very early nephrogenesis in murine. Biochem Biophys Res Commun 270:...

Rodríguez-Zavala JS, Saavedra-Molina A, Moreno-Sánchez R (1997) Effect of uncoupled cadmium on Mg2+ on citric-line synthesis in rat liver mitochondria. Biochem Mol Biol Int 41:175–187.

Rodríguez-Zavala JS, Díaz-Cruz MA, Moreno-Sánchez R (2000) Characterization of an aldehyde dehydrogenase from *Euglena gracilis*. J Eukaryot Microbiol 47:...

Rodríguez-Zavala JS, García-Torres IB, Díaz-Cruz MA, Moreno-Sánchez R (2003) Molecular mechanisms of resistance to heavy metals in the protist *Euglena gracilis*. J Environ Sci Health A 42:1565–1578.

Rodríguez-Zavala JS, Ochoa-Leyva MA, Mendoza-Hernández G, Moreno-Sánchez R (2010) Expression, synthesis of a novel aldehyde dehydrogenase and proteomic analysis by *Euglena gracilis* under conditions of high heavy metal content. J Appl Microbiol 109:2062–2072.

Rotruck JT, Swapkal R, Ahrens C, Knuth S, Morris W (1981) Pyruvate NADP...-associated cytochrome reductase in *Euglena gracilis* and liver: an enzyme-locus *Cryptococcus neoformans* a biochemical role. Linking pyruvate metabolism in mitochondrial and mitochondrial redox. Mol Biol Evol 18:715–720.

Rozanowska M, Morand...Sarna T (1993) The pyruvate-supported activity of H...Pases in isolated Euglena cells. Biochim Biophys Acta 1143:161–170.

Sánchez-Antonio JE, Chávez AY, Carmona CB, Ortiz JG, Gonzalez-Moreno...Martínez JE, Sánchez-Ibarra M, Sánchez RJ (2007) The relationship of dietary tocopherol and ascorbic A, E and C acids with age-related macular degeneration in a case-control study. ARMD Report No. 22. Arch Oftalmol 125:1225–1232.

Scanlan RS, Lee Chang-Jeon LW (1969) Microbiological nitrosoalkyl metabolite potential using fluorescent Escherichia coli. Appl Microbiol Biotechnol J 76:815–827.

Schiff JA, Lyman H, Russell GK (1957) Isolation of mutants from *Euglena gracilis*. Mich Enzymol 73:153–162.

Schirmer RH, Kennedy SI (1988) The structure of a soluble and the mitochondrial form of aldehyde dehydrogenase from *Euglena gracilis*. Biochemistry 27:1814–1820.

Shigenaga S, Ohnishi T, Hatada K, Nakano T, Kimura S (1986a) Characterization of human pyridine-dependent 2-oxoglutarate dehydrogenase in mitochondria of *Euglena gracilis*. Hoppe Seyler Biol Chem 367:...17.

Shigenaga S, Ohnishi T, Nakano Y, Kimura S (1986b) The metabolism of cellular distribution of D-lactate in *Euglena gracilis*. Agric Biol Chem 50:1965–1965.

Shigenaga T (Ohnishi T (1987) Polyoxyanions with sulfite group on serum from *Euglena* and marine polychaete II cell activators (PBSs). II. Cellulose sulfate and dextran sulfate with two different serum molecular weights. Mitochondrial Enzymes 24:831–839.

Swamy GN, Weiss B (1982) Aldehyde oxidation activity in the rat Ehrlich ascites tumor mitochondria: role in alcohol metabolism. Arch Biochem Biophys 239:36–45.

Taniguchi H, Kawamura A, Yoshida S, Kikuchi H, Kawamura Y, Matsunaga T (1997) Production of antioxidant vitamins, E, carotene, vitamin C, and vitamin B2 by two-step culture of *Euglena gracilis* Z. Fermentec Tissue Eng 83:165–171.

Takenaga M, Nakano Y, Kimura S (1976) Separation and properties of the NAD-linked and NADP-linked enzymes of succinic semialdehyde dehydrogenase in *Euglena gracilis*. Biochim Biophys Acta 429:52–62.

Tolbert NE, Petersen H, Sarachan RH (1973) The intracellular distribution of 2 properties of aldehyde dehydrogenase in rat liver. Biochem J 135:777–786.

Tsuzuki S, Suzuki A, Kawamoto J, Prakash P, Matsuo A (2011) Characterization of aldehyde dehydrogenase in marine and freshwater *Euglena gracilis* strains sensitive to oxygen and the electron inhibitor fadecanol. J Eukaryot Microbiol 57:63–69.

Ward, R., Parkinson, H., Cuzin, A., Delagoutte, A., Peters, W. (1998) Protective effects of β-carotene on methylmercuric chloride-induced oxidative damage. Toxicol Pathol. 18:97–99.

Vasiliou, V., Kozak, C.A., Lindahl, R., Nebert, D.W. (1996) Mouse mitochondrial class 3 aldehyde dehydrogenase: ALDH3 cDNA sequence, inducibility by chlorin and chromosomal and genomic mapping. DNA Cell Biol. 15:255–265.

Wang, X., Mann, C., Bai, S.A., L., Wenner, B. (1998) Molecular characterization and potential roles of cytosolic and mitochondrial aldehyde dehydrogenases in ethanol-oxidizing rat tissues. Biochem Cell Biol. 76:322–333.

Wood, A., Duff, H., Johnston, J. (1999) The aldehyde dehydrogenase (ALDH) gene superfamily of the mouse *Peromyscus polionotus* and the cDNA sequence of the mouse *Peromyscus maniculatus* and *Peromyscus leucopus*. Biochem Biophys Acta. 1:1–11.

Wu, G., Mill, J., Jin, R., Wu, D.Z. (2001) Highly selective oxidation of benzyl alcohol using engineered *Gluconobacter oxydans* in biphasic system. Appl Microbiol. 67:1213–1217.

11. Referencias.

[1]. Yoshida, A.; Rzhetsky, A.; Hsu, L. C.; Chang, C. (1998). Human aldehyde dehydrogenase gene family. Eur. J. Biochem. 251:549-557.

[2]. Lindahl, R.; (1992) Aldehyde dehydrogenases and their role in carcinogenesis, Crit. Rev. Biochem. Mol. Biol. 27:283–335.

[3]. Marchetti, S. A.; Brocker, C.; Stagos, D.; Vasiliou, V. (2008) Non-P450 aldehyde oxidizing enzymes: the aldehyde dehydrogenase superfamily, Expert Opin. Drug Metab. Toxicol. 4:697–720.

[4]. Liu, Z. J.; Sun, Y. J.; Rose, J.; Chung, Y. J.; Hsiao, C. D.; Chang, W. R.; Kuo, I.; Perozich, J.; Lindhal, R.; Hempel, J. and Wang, B. C.. (1997). The first structure of an aldehyde dehydrogenase reveals novel interactions between NAD and the Rossmann fold, Nat. Struct. Biol. 4:317-326.

[5] Steinmetz, C. G.; Peiguang, X.; Weiner, H. and Hurley, T. D. (1997) Structure of mitochondrial aldehyde dehydrogenase: the genetic component of ethanol aversion, Structure 5:701–711.

[6] Moore, S. A.; Baker, H. M.; Blythe, T. J.; Kitson, K. E.; Kitson, T. M. and Baker, E. N. (1998) Sheep liver cytosolic aldehyde dehydrogenase: the structure reveals the basis for the retinal specificity of class 1 aldehyde dehydrogenases, Structure 6:1541–1551.

[7]. Ni, L., Zhou, J., Hurley, T. D., and Weiner, H. (1999) Human liver mitochondrial aldehyde dehydrogenase: Three-dimensional structure and the restoration of solubility and activity of chimeric forms Protein Sci. 8:2784-2790.

[8]. Zhou, J., and Weiner, H. (2001) The N-terminal portion of mature aldehyde dehydrogenase affects protein folding and assembly. Protein Sci. 10:1490-1497.

[9]. Rodríguez-Zavala J.S. and Weiner H. (2002) Structural aspects of Aldehyde dehydrogenase that influence dimer-tetramer formation. Biochemistry 41:8229-8237.

[12]. Wang, X., Sheikh, S., Saigal, D., Robinson, L., and Weiner, H. (1996) Heterotetramers of human liver mitochondrial (class 2) aldehyde dehydrogenase expressed in Escherichia coli. A model to study the heterotetramers expected to be found in Oriental people. J. Biol. Chem. 271:31172-31178.

[13]. Mann, C. J.; and Weiner, H. (1999) Differences in the roles of conserved glutamic acid residues in the active site of human class 3 and class 2 aldehyde dehydrogenases, Protein Sci. 8:1922–1929.

[14]. Allali-Hassani, A. and Weiner, H. (2001) Interaction of human aldehyde dehydrogenase with aromatic substrates and ligands, Chem.Biol. Interac. 130:125-133.

[15]. Wang, X.P. and Weiner, H. (1995) Involvement of glutamate 268 in the active site of human liver mitochondrial (class 2) aldehyde dehydrogenase as probed by site-directed mutagenesis. Biochemistry 34:237–243.

[16]. MacGibbon, A.K., Buckley, P. D. and Blackwell L. F. (1977) Evidence for two-step binding of reduced nicotinamide-adenine dinucleotide to aldehyde dehydrogenase. Biochem. J. 165:455–462.

[18]. Rodriguez-Zavala J.S., Allali-Hassani A. and Weiner H. (2006) Characterization of *E. coli* tetrameric aldehyde dehydrogenases with atypical properties compared to other aldehyde dehydrogenases Protein Sci. 15:1387-1396.

[19]. Rodriguez-Zavala J.S. (2007) Enhancement of coenzyme binding by a single point mutation at the coenzyme binding domain of *E. coli* lactaldehyde dehydrogenase Protein Sci. 17:563-70.

[20]. Lamb, A. L. and Newcomer, M. E. (1999) The structure of retinal dehydrogenase type II at 2.7 A, resolution: implications for retinal specificity, Biochemistry 38:6003–6011.

[21]. Weiner, H.; Wei, B. and Zhou, J. (2001) Subunit communication in tetrameric class 2 human liver aldehyde dehydrogenase as the basis for half-of-the-site reactivity and the dominance of the oriental subunit in a heterotetramer, Chem Biol Interact 130-132(1-3):47-56.

[22]. Zhou, J. and Weiner, H. (2000) Basis for half-of-the-sites reactivity and the dominance of the K487 oriental subunit over the E487 subunit in heterotetrameric human liver mitochondrial aldehyde dehydrogenase, Biochemistry 39 (39):12019-24.

[23]. Hurley, T. D.; Perez-Miller, S. and Breen, H. (2001) Order and disorder in mitochondrial aldehyde dehydrogenase. Chem Biol Interact. 130-132 (1-3):3-14.

[26]. Johansson, K.; El-Ahmad, M.; Ramaswamy, S.; Hjelmqvist, L.; Jornvall, H. and Eklund, H. (1998) Structure of betaine aldehyde dehydrogenase at 2.1 A, resolution, Protein Sci. 7:2106–2117.

[31]. Perez-Miller, S. J., and Hurley, T. D. (2003) Coenzyme isomerization is integral to catalysis in aldehyde dehydrogenase, Biochemistry 42:7100-7109.

[32]. Blackwell, L. F., Motion, R. L., MacGibbon, A. K., Hardman, M. J., and Buckley, P. D. (1987) Evidence that the slow conformation change controlling NADH release from the enzyme is rate-limiting during the oxidation of propionaldehyde by aldehyde dehydrogenase, Biochem. J. 242:803-808.

[33]. Weiner, H., Hu, J. H., and Sanny, C. G. (1976) Rate-limiting steps for the esterase and dehydrogenase reaction catalyzed by horse liver aldehyde dehydrogenase, J. Biol. Chem. 251:3853-3855.

[34]. Feldman, R. I., and Weiner, H. (1972) Horse liver aldehyde dehydrogenase. II. Kinetics and mechanistic implications of the dehydrogenase and esterase activity, J. Biol. Chem. 247:267-272.

[35]. Ho, K. K., Allali-Hassani, A., Hurley, T. D., and Weiner, H. (2005) Differential effects of Mg2+ ions on the individual kinetic steps of human cytosolic and mitochondrial aldehyde dehydrogenases, Biochemistry 44:8022-8029.

[40]. Conklin, D.J.; Barski, O.A.; Lesgards, J.F.; Juvan, P.; Rezen, T.; Rozman, D.; Prough, R.A.; Vladykovskaya, E.; Liu, S.; Srivastava, S. and Bhatnagar, A. (2010). Acrolein consumption induces systemic dyslipidemia and lipoprotein modification, Toxicol. Appl. Pharmacol. 243:1–12

[41]. Wang, G.W.; Guo, Y.; Vondriska, T.M.; Zhang, J.; Zhang, S.; Tsai, L. L.; Zong, N.C.; Bolli, R.; Bhatnagar, A. and Prabhu, S.D. (2008). Acrolein consumption exacerbates myocardial ischemic injury and blocks nitric oxide-induced PKCepsilon signaling and Cardioprotection. J. Mol. Cell. Cardiol. 44:1016–1022.

[42]. Esterbauer, H.; Schaur, R. and Zollner, H. (1991). Chemistry and biochemistry of 4-hidroxynonenal, malondialdehyde and related aldehydes. Free Radic. Biol Med. 11:81-128.

[43]. Subramaniam, R.; Roediger, F.; Jordan, B.; Mattson, M. P.; Keller, J. N.; Waeg, G. and Butterfield, D. A. (1997) The lipid peroxidation product, 4-hydroxy-2-trans-nonenal, alters the conformation of cortical synaptosomal membrane proteins. J. Neurochem. 69: 1161-1169.

[44]. Uchida, H. and Stadtman, E. R. (1992) Modification of histidine residues in proteins by reaction with 4-hydroxynonenal. Proc. Natl. Acad. Sci. USA 89:4544-4589.

[45]. Uchida, K. (2000) Role of reactive aldehyde in cardiovascular diseases. Free Radic. Biol. Med. 28, 1685-1696.

[46]. Destaillats, H.; Spaulding, R. S. and Charles, M. J. (2002) Ambient air measurement of acrolein and other carbonyls at the Oakland-San Francisco Bay Bridge toll plaza. Environ Sci Technol. 36:2227-2235.

[47]. Rickert, W. S.; Robinson, J. C. and Young, J. C. (1980) Estimating the hazards of less hazardous cigarettes. I. Tar, nicotine, carbon monoxide, acrolein,

hydrogen cyanide, and total aldehyde deliveries of Canadian cigarettes. J. Toxicol. Environ. Health 6:351-365.

[48]. O´brien, P. J.; Siraki, A.G. and Shangari, N. (2005) Aldehyde sources, metabolism, molecular toxicity mechanisms, and possible effects on human health. Crit Rev Toxicol. 35: 609-662.

[50]. Schauenstein, E.; Esterbauer, H. and Zollner, H. (1977) Aldehydes in biological systems: their natural occurrence and biological activities. Pion, London.

[51]. Esterbauer, H. (1993) Cytotoxicity and genotoxicity of lipid-oxidation products. American J. Clin. Nutr. 57(suppl): 779S-86S.

[52]. Yokoyama, A.; Muramatsu, T.; Ohmori, T.; Makuuchi, H.; Higuchi, S.; Matsushita, S.; Yoshino, K.; Maruyama, K.; Nakano, M. and Ishii, H. (1996) Multiple primary esophageal and concurrent upper aerodigestive tract cancer and the aldehyde dehydrogenase-2- genotype of Japanese alcoholics. Cancer. 77:1986-1990.

[53]. Burcham, P.C. and Fontaine, F. (2001). Extensive protein carbonylation precedes acroleinmediated cell death in mouse hepatocytes, J. Biochem.Mol. Toxicol.15:309–316.

[54]. Stevens, J.F. and Maier, C.S. (2008). Acrolein: sources, metabolism, and biomolecular interactions relevant to human health and disease. Mol. Nutr. Food Res. 52:7–25.

[55]. Tanel, A. and Averill-Bates, D.A. (2007). Inhibition of acrolein-induced apoptosis by the antioxidant N-acetylcysteine. J. Pharmacol. Exp. Ther. 321:73–83.

[56]. Cheng, J. Z.; Singhal, S.S.; Sharma, A.; Saini, M.; Yang, Y.; Awasthi, S.; Zimniak, P. and Awasthi, Y. C. (2001). Transfection of mGSTA4 in HL-60 cells protects against 4-hydroxynonenal-induced apoptosis by inhibiting JNK-mediated signaling. Arch. Biochem. Biophys. 392:197-207.

[57]. Thornberry, N. A. and Lazebnik, Y. (1998). Caspases: enemies within. Science. 281: 1312-1316.

[58]. Stadtman, E.R. (1986) Oxidation of proteins by mixed-function oxidation systems: implication in protein turnover, ageing and neutrophil function.Trends Biochem. Sci. 11:11-12.

[59]. Stadtman, E. R. (1990) Metal ion-catalyzed oxidation of proteins: Biochemical mechanism and biological consequences. Free Radic. Biol. Med. 9, 315-325.

[60]. Stadtman, E. R. and Oliver, C.N. (1991). Metal-catalyzed oxidation of proteins. Physiological consequences. J. Biol. Chem. 266, 2005-2008.

[61]. Stadtman, E. R. (1992) Protein oxidation and aging. Science 257, 1220-1224.

[62]. Hempel, J.; Bahr-Lindstrom, H. and Jornvall, H., (1984) Aldehyde dehydrogenase from human liver. Primary structure of the cytoplasmic isoenzyme. Eur. J. Biochem. 141, 21-35.

[63]. Zhai Y.; Sperkova Z. and Napoli, J. L. (2001) Cellular expression of retinaldehydrogenase types 1 and 2: effects of vitamin A status on testis mRNA. J. Cell. Physiol. 186, 220-232.

[64]. Picklo, M. J.; Olson, S. J.; Markesbery, W. R. and Montine, T. J. (2001) Expression and activities of aldo-keto oxidoreductases in Alzheimer disease. J. Neuropathol. Exp. Neurology. 60(7): 686-695.

[65]. Patel, M.; Lu, L.; Zander, D.S.; Sreerama, L.; Coco, D. and Moreb, J.S. (2008) ALDH1A1 and ALDH3A1 expression in lung cancers: Correlation with histologic type and potential precursors. Lung Cancer. 59, 340-349.

[66]. Lassen, N.; Bateman, B. B.; Estey, T.; Kuszak, J.R.; Nees, D.W.; Piatigorsky, J.; Duester, G.; Day, B.J.; Huang, J.; Hines, L.M. and Vasiliou, V. (2007) Multiple and additive functions of ALDH3A1 and ALDHA1. Cataract phenotype and ocular oxidative damage in Aldh3a1 (-/-)/ Aldh1a1 (-/-) knock-out mice. J. Biol. Chem. 282, 25668-25676.

[67]. King, C. T. and Holmes, R. S. (1997) Human corneal and lens aldehyde dehydrogenase: purification and properties of human lens ALDH1 and differential expression as major soluble proteins in human lens (ALDH1) and cornea (ALDH3). Adv. Exp. Med. Biol. 414: 19-27.

[68]. Hilton, J. (1984) Role of aldehyde dehydrogenase in cyclophosphamide-resistant L1210 leukemia. Cancer Res. 44: 5156-5160.

[69]. Sladek, N. E. and Landkamer, G. L. (1985) Restoration of sensitivity to oxazaphosphorines by inhibitors of aldehyde dehydrogenase activity in cultured oxazaphosphorine-resistant L1210 and cross-linking agent-resistant P388 cell lines. Cancer Res. 45:1549-1555.

[70]. Jiang, F.; Qiu, Q.; Khanna, A.; Todd, N. W.; Deepak, J.; Xing, L.; Wang, H.; Liu, Z.; Su, Y.; Stass, S. A. and Katz, R. L. (2009) Aldehyde dehydrogeanse 1 is a tumor stem cell-associated marker in lung cancer. Mol. Cancer Res. 7:330-338.

[71]. Lovell, M. A.; Xie, C. and Markesbery, W. R. (2001) Acrolein is increased in Alzheimer´s disease brain and is toxic toprimary hippocampal cultures. Neurobiol. Aging 22: 187-194.

[72]. Yoshida, A.; Davé, V.; Han, H. and Scanlon, K. J. (1993) Enhanced transcription of the cytosolic ALDH gene in cyclophosphamide resistant human carcinoma cells. Adv. Exp. Med. Biol. 328: 63-72.

[73]. Li, Z.; Srivastava, S.; Yang, X.; Mittal, S.; Norton, P.; Resau, J.; Haab, B. and Chan, Ch. (2007). A hierarchical approach employing metabolic and gene

expression profiles to identify the pathways that confer cytotoxicity in HepG2 cells. BMC Systems Biology. 1:21.

[74]. Galter, D.; Buervenich, S.; Carmine, A.; Anvret, M. and Olson, L. (2003) ALDH1 mRNA: presence in human dopamine neurons and decreases in substantia nigra in Parkinson´s disease and in the ventral tegmental area in schizophrenia. Neurobiol. Dis. 14: 637-647.

[75]. Chung, S.; Hedlund, E.; Hwang, M.; Kim, D. W.; Shin, B. S.; Hwang, D. Y.; Jung Kang, U.; Isacson, O. and Kim, K. S. (2005). The homeodomain transcription factor Pitx3 facilitates differentiation of mouse embryonic stem cells into AHD2-expressing dopaminergic neurons. Mol. Cell. Neurosci. 28:241-252.

[76]. Jacobs, F. M.; Smits, S. M.; Noorlander, C. W.; von Oerthel, L.; van der Linden, A. J.; Burbach, J. P. and Smidt, M. P. (2007). Retinoic acid counteracts developmental defects in the substantia nigra caused by Pitx3 deficiency. Development. 134: 2673-2684.

[77]. Marchitti, S. A.; Deitrich, R. A. and Vasiliou, V. (2007). Neurotoxicity and metabolism of the catecholamine-derived 3,4-dihydroxiphenylacetaldehyde and 3,4-dihydroxyphenylglycolaldehyde: the role of aldehyde dehydrogenase. Pharmacol. Rev. 59: 125-150.

[78]. Mark, M.; Ghyselinck, N.B.; Wedling, O.; Dupe, V.; Mascrez, B.; Kastner, P. and Chambon, A. (1999). A genetic dissection of the retinoid signaling pathway in the mouse. Proc. Nutr. Soc. 58:609-613

[79]. Yoshida, A.; Hsu, L. C. and Davé, V. (1992) Retinal oxidation activity and biological role of human cytosolic aldehyde dehydrogenase. Enzyme 46, 239-244.

[80]. Yoshida, A. (1992) Molecular genetics of human aldehyde dehydrogenase. Pharmacogenetics. 2:139–147.

[81]. Sladek, N.E. (1999). Aldehyde dehydrogenase-mediated cellular relative insensitivity to the oxazaphosphorines. Curr. Pharm. Des. 5:607–625.

[82] Yoval-Sánchez, B. and Rodríguez-Zavala, J. S. (2012). Differences in Susceptibility to Inactivation of Human Aldehyde Dehydrogenases by Lipid Peroxidation Byproducts. Chem. Res. Toxicol. 25:722-729

[83]. Rodríguez-Zavala, J. S. and Weiner, H. 2001. Role of the C- terminal tail on the quaternary structure of aldehyde dehydrogenases. Chem. Biol. Interact. 130: 151-160.

[85]. Ducci, F., Goldman, D. (2008) Genetic approaches to addiction: genes and alcohol. Addiction. 103: 1414-1428.

[86]. Yoshida, A. (1994) Genetic polymorphisms of alcohol metabolizing enzymes related to alcohol sensivity and alcoholic diseases. Alcohol Alcohol. 29: 693-696

[87]. Li, S. Y.; Gomelsky, M.; Duan, J.; Zhang, Z.; Gomelsky, L.; Zhang, X.; Epstein, P. N. and Ren, Jun. (2004) Overexpression of aldehyde dehydrogenase-2 (ALDH2) transgene prevents acetaldehyde-induced cell injury in human umbilical vein endothelial cells. J. Biol. Chem.. 279: 11244-11252.

[88]. Katzman, R. and Saitoh, T. (1991) Advances in alzheimer´s disease. FASEB J. 5:278-286.

[89]. Markesbery, W. R. (1997) Oxidative stress hypothesis in Alzheimer´s disease. Free Radic. Biol. Med. 23:134-147.

[90]. Avdulov, N.; Chochina, S.; Igbavboa, U.; O´Hare, E. O.; Schroeder, F.; Cleary, J. P. and Wood, W. G. (1997) Amiloid beta-peptides increase annular and bulk fluidity and induce lipid peroxidation in brain synaptic plasma membranes. J. Neorochem. 68: 2086-2091.

[91]. Bruce-Keller, A. J.; Begley, J. G.; Fu, W.; Butterfield, D. A.; Bredesen, D. E.; Hutchins, J. B.; Hensley, K. and Mattson, M. P. (1998) Bcl-2 protects isolated plasma and mitochondrial membranes against lipid peroxidation induced by hydrogen peroxide and amyloid beta-peptide. J. Neurochem. 70:31-39.

[92]. Butterfield, D. A.; Hensley, K.; Harris, M.; Mattson, M. and Carney, J. (1994) Beta-amyloid peptide free radical fragments initiate synaptosomal lipoperoxidation in a sequence-specific fashion: implications to Alzheimer´s disease. Biochem. Biophys. Res. Commun. 200: 710-715.

[93]. Daniels, W. M.; van Rensburg, S. J.; van Zyl, J. M. and Taljaard, J. J.(1998) Melatonin prevents beta-amyloid-induced lipid peroxidation. J. Pineal Res. 24:78-82.

[94]. Gridley, K. E.; Green, P. S. and Simpkins, J. W. (1997) Low concentrations of stradiol reduce beta-amyloid (20-35)-induced toxicity, lipid peroxidation and glucose utilization in human SK-N-SH neuroblastoma cells. Brain Res. 778:158-165.

[95]. Mark, R. J.; Lovell, M. A.; Markesbery, W. R.; Uchida, K. and Mattson, M. P. (1997) A role for 4-hydroxynonenal, an aldehyde product of lipid peroxidation, in disruption of ion homeostasis and neuronal death induced by amyloid □-peptide. J. Neurochem. 68:255-264.

[96]. Mark, R. J.; Fuson, K. S. and May, P. C. (1999) Characterization of 8-epiprostaglandin F2a as a marker of amyloid □-peptide-induced oxidative damage. J. Neurochem. 72:1146-1153.

[97]. Pocernich, C. B.; Cardin, A.; Racine, C.; Lauderback, C. M. and Butterfield, D. A. (2001) Glutathione elevation and its protective role in acrolein-induced protein damage in synaptosomal membranes: relevance to brain lipid peroxidation in neurodegenerative disease. Neurochem. Int. 39: 141-149.

[98]. Markesbery, W. R. and Lovell, M. A. (1998) 4-hydroxynonenal, a product of lipid peroxidation, is increased in the brain in alzheimer´s disease. Neurobiol. Aging 19:33-36.

[99]. Sayre, L. M.; Zelasko, D. A.; Harris, P. L.; Perry, G.; Salomon, R. G. and Smith, M. A. (1997) 4-hydroxynonenal-derived advanced lipid peroxidation products are increased in alzheimer´s disease. J. Neurochem. 68:2092-2097

[100]. Mark, R. J.; Pang, Z.; Lovell, M. A.; Uchida, K. and Mattson, M. P. (1997) Amyloid b-peptide impairs glucose transport in hippocampal and cortical neurons: involvement of membrane lipid peroxidation. J. Neurosci. 17:1046-1054.

[101]. Cheng, C.H.; Budas, G. R.; Churchill, E. N.; Disatnik, M. H.; Hurley, T.D. and Mochly-Rosen D. (2008) Activation of aldehyde dehydrogenase-2 reduces ischemic damage to the heart. Science 321(5895):1493–5.

[102]. Eaton, P.; Li, M.; Hearse, D. J. and Shattock, M. (1999) Formation of 4-hydroxy-2-nonenal-modified proteins in ischemic rat heart. Am. J. Physiol. Heart Circ. Physiol. 276:H935-H943.

[103]. Wenzl, M.V.; Beretta, M.; Gorren, A.C.; Zeller, A.; Baral, P.K.; Gruber, K.; Russwurm, M.; Koesling, D.; Schmidt, K. and Mayer, B. (2009) Role of the general base glu-268 in nitroglycerin bioactivation and superoxide formation by aldehyde dehydrogenase-2. J. Biol. Chem. 284 (30):19878-19886.

[104]. Sun, L.; Batista Ferreira, J. C. and Mochly-Rosen, D. (2011) ALDH2 activator inhibits increased myocardial infarction injury by nitroglycerin tolerance. Sci. Transl. Med. 3(107):1-7.

[105]. Kawasaki, T.; Igarashi, T.; Koeda, T.; Sugimoto, K.; Nakagawa, K.; Hayashi, S.; Yamahi, R.; Inui, H.; Fukusato, T. and Kawasaki, T. Y. (2009) Rats fed fructose-enriched diets have characteristics of nonalcoholic hepatic steatosis. J. Nutr. 139(11): 2067-2071.

[106]. Harada, S.; Agarwal, D. P. and Goedde, H.W. (1985) Aldehyde dehydrogenase polymorphism and alcohol metabolism in alcoholics. Alcohol 2:391–392.

[107]. Peng, G. S.; Wang, M. F.; Chen, C. Y.; Luu, S. U.; Chou, H. C.; Li, T. K. and Yin, S. J. (1999) Involvement of acetaldehyde for full protection against alcoholism by homozygosity of the variant allele of mitochondrial aldehyde dehydrogenase gene in Asians, Pharmacogenetics 9:463–476.

[108]. Ni, L.; Sheikh, S. and Weiner H. (1997) Involvement of glutamate 399 and lysine 192 in the mechanism of human liver mitochondrial aldehyde dehydrogenase. J. Biol. Chem. 272:18823-18826.

[109]. Holmes, R. S. and Hempel, J. (2011) Comparative studies of vertebrate aldehyde dehydrogenase 3: sequences, structures, phylogeny and evolution. Evidence for a mammalian origin for the ALDH3A1 gene. Chem. Biol. Interact. 191:113-121

[110]. Canuto, R. A.; Muzio, G.; Ferro, M.; Maggiora, M.; Federa, R.; Bassi, A. M.; Lindhal, R. and Dianzani, M. U. (1999) Inhibition of class-3 aldehyde dehydrogenase and cell growth by restored lipid peroxidation in hepatoma cell lines. Free Radic. Biol. Med. 26: 333-340.

[111]. Muzio, G.; Trombetta, A.; Martinasso, G.; Canuto, R. A. and Maggiora, M. (2003) Antisense oligonucleotide against aldehyde dehydrogenase 3 inhibit hepatoma cell proliferation by affecting MAP kinases. Chem. Biol. Interact. 143-144:37-43.

[112]. Pappa, A.; Brown, D.; Koutalos, Y.; DeGregori, J.; White, C. and Vasiliou V. (2005) Human aldehyde dehydrogenase 3A1 inhibits proliferation and promotes survival of human corneal epithelial cells. J. Biol. Chem. 280: 27998-28006.

[113]. Lassen, N.; Pappa, A.; Black, W. J.; Jester, J. V.; Day, B. J.; Min, E. and Vasiliou V. (2006) Antioxidant function of corneal ALDH3A1 in cultured stromal fibroblasts. Free Radic. Biol. Med. 41: 1459-1469.

[114]. Piatigorsky, J. (1998) Gene sharing in lens and cornea: facts and implications. Prog. Retin. Eye Res. 17:145-174.

[115]. Moreb, J. S.; Baker, H. V.; Chang, L.; Amaya, M.; Lopez, M. C.; Ostmark, B. and Chou, W. (2008) ALDH isozymes downregulation affects cell growth, cell motility and gene expression in lung cancer cells. Mol. Cancer. 7:87.

[116]. Ruzinova, M. B. and Benezra, R. (2003) Id proteins in development, cell cycle and cancer. Trends Cell Biol. 13:410-418.

[117]. Sarhadi, V. K.; Wikman, H.; Salmenkivi, K.; Kuosma, E.; Sioris, T.; Salo, J.; Karjalainen, A.; Knuutila, S. and Anttila, S. (2006). Increased expression of high mobility group A proteins in lung cancer. J. Pathol. 209: 206-212.

[118]. Esterbauer, H.; Zollner, H. and Schaur, R. J. (1988). Hydroxyalkenals: Cytotoxic products of lipid peroxidation. ISI Atlas Sci. Biochem. 1: 311-317.

[119]. Marchitti, S.A.; Chen, Y.; Thompson, D.C. and Vasiliou, V. (2011) Ultraviolet radiation: cellular antioxidant response and role ocular aldehyde dehydrogenase enzymes. Eye Contact Lens. 37: 206-213

[120]. Benedetti, A.; Comporti, M. and Esterbauer, H. (1980) Identificaton of 4-hydroxynonenal as a citotoxic product originating from the peroxidation of liver microsomal lipids. Biochem. Biophys. Acta 620: 281-296

[121]. Cadenas, E.; Muller, A.; Brigelius, R.; Esterbauer, H. and Sies, H. (1983) Effects of 4-hydroxynonenal on isolated hepatocytes: studies on chemiluminiscence response, alkane production and glutathione status. Biochem. J. 214: 479-487

[122]. Poot, M.; Verkerk, A.; Koster, J. F.; Esterbauer, H. and Jongkind, J. (1988) Reversible inhibition of DNA and proteins synthesis by cumene hydroperoxide and 4-hydroxynonenal. Mech. Ageing Dev. 43:1-9

[123]. Canuto, R. A.; Biocca, M.E.; Muzio, G.; Garcea, R. and Dianzani, M. U. (1985) The effect of various aldehydes on the respiration of rat liver and hepatoma AH-130 cells. Cell Biochem. Funct. 3:3-8

[124]. Gadoni, E.; Olivero, A.; Miglieta, A.; Bocca, C. and Gabriel, L. (1993) Cytoeskeletal modifications induced by 4-hydroxinonenal. Cytotechnology 11:62-64.

[125]. Canuto, R. A.; Ferro, M.; Muzio, G.; Bassi, A. M.; Leonarduzzi, G.; Maggiora, M.; Adamo, D.; Poli, G. and Lindahl, R. (1994). Role of aldehyde metabolizing enzymes in mediating effects of aldehyde products of lipid peroxidation in liver cells. Carcinogenesis. 15: 1359-1364.

[126]. Muzio, G.; Trombetta, A.; Maggiora, M.; Martinasso, G.; Vasiliou, V.; Lassen, N. and Canuto, R. A. (2006) Arachidonic acid suppresses growth of human lung tumour A549 cells through down regulation of ALDH3A1 expression. Free Radic. Biol. Med. 40: 1929-1938.

[[127]. Piatigorsky, J. (1998) Multifunctional lens crystallins and corneal enzymes. More than meets the eye. Ann. N. Y. Acad. Sci. 842: 7-15

[128]. Pappa, A.; Sophos, N. A. and Vasiliou, V. (2001) Corneal and stomach expression of aldehyde dehydrogenases: from fish to mammals. Chem. Biol. Interact. 130-132:181-191.

[129]. Pappa, A.; Chen, C.; Koutalos, Y.; Townsend, A. J. and Vasiliou, V. (2003) ALDH3A1 protects human corneal epithelial cells from ultraviolet and 4-hydroxi-2-nonenal-induced oxidative damage. Free Radic. Biol. Med. 34:1178-1189.

[130]. Sreerma, L. and Sladek N.E. (1997) Class 1 and class 3 aldehyde dehydrogenase levels in the human tumor cell lines currently used by the National Center Institute to screen for potentially useful antitumor agents. Adv. Exp. Med. Biol. 414, 81-94.

[131]. Stephanou, P.; Pappas, P.; Vasiliou, V. and Marselos, M. (1999). Prepubertal regulation of the rat dioxin-inducible aldehyde dehydrogenase (ALDH3). Adv. Exp. Med. Biol. 463:143-150.

[132]. Reisdorph, R. and Lindahl, R. (2007) Constitutive and 3-methylcholanthrene-induced rat ALDH3A1 expression is mediated by multiple xenobiotic response elements. Drug. Metab. Dispos. 35:386-393.

[133]. Vasiliou, V.; Reuter, S. F.; Kosak, C. A. and Nebert, D. W. (1993) Mouse dioxin-inducible cytosolic aldehyde dehydrogenase-3: AHD4 cDNA sequence, genetic mapping, and differences in mRNA levels. Pharmacogenetics. 3:281-290.

[134]. Perozich, J.; Kuo, I.; Wang, B. C.; Boesch, J. S.; Lindahl, R. and Hempel, J. (2000).Shifting the NAD/NADP preference in class 3 aldehyde dehydrogenase. Eur. J. Biochem. 267:6197-6203.

[136]. Klyosov, A. A. (1996) Kinetics and specificity of human liver aldehyde dehydrogenase toward aliphatic, aromatic, and fused polycyclic aldehydes. Biochemistry. 35:4457-4467.

[137]. Ho, K. K.; Hurley, T. D. and Weiner, H. (2006) Selective alteration of the rate limiting step in cytosolic aldehyde dehydrogenase through random mutagenesis. Biochemistry. 45:9445-9453.

[138]. Rashkovetsky, L. G.; Maret, W. and Klyosov, A. A. (1994) Human liver aldehyde dehydrogenases: new method of purification of the major mitochondrial and cytosolic enzymes and re-evaluation of their kinetic properties. Biochimica et Biophysica Acta. 1205(2):301-307.

[139]. Yoshida, A.; Hsu, L. C. and Yasunami, M. (1991) Genetics of human alcohol-metabolizing enzymes. Progress in Nucleic Acid Research and Molecular Biology. 40:255-287.

[140]. Yang, K.; Feng, C.; Lip, H.; Bruce, W. R. and O´Brien, P. J. (2011) Cytotoxic molecular mechanisms and cytoprotection by enzymic metabolism for glyceraldehydes, hydroxypyruvate and glycolaldehyde. Chemico-Biological Interactions. 191:315-321.

[141]. Boesch, J. S.; Lee, C. and Lindahl, R. G. (1996) Constitutive expression of class 3 aldehyde dehydrogenase in cultured rat corneal epithelium. J. Biol. Chem. 271:5150-5157.

[142]. Jones, D. E.; Brennan, M. D.; Hempel, J. and Lindahl, R. (1988) Cloning and complete nucleotide sequence of a full-length Cdna encoding a catalytically functional tumour-associated aldehyde dehydrogenase. Proc. Natl. Acad. Sci. U. S. A. 85:1782-1786.

[145]. Lam, J. P.; Mays, D. C. and Lipsky, J. J. (1997). Inhibition of recombinant human mitochondrial and cytosolic aldehyde dehydrogenases by two candidates for the active metabolites of disulfiram. Biochemistry. 36: 13748-13754.

[146]. Lakowicz JR. (2006) Principles of fluorescence spectroscopy. 3rd ed. New York: Springer.

[147]. Vasiliou V, Bairoch A, Tipton KF, Nebert DW.(1999). Eukaryotic aldehyde dehydrogenase (ALDH) genes: human polymorphisms, and recommended nomenclature based on divergent evolution and chromosomal mapping. Pharmacogenetics. 9:4, 421-434.

[148]. Larson, H. N.; Zhou, J.; Chen, Z.; Stamler, J. S.; Weiner, H. and Hurley, T. D. (2007) Structural and functional consequences of coenzyme binding to the inactive asian variant of mitochondrial aldehyde dehydrogenase. Roles of residues 475 and 487. J. Biol. Chem. 282:17, 12940-12950.